OPTIMAL ENERGY MANAGEMENT OF A HYBRID SOLAR WATER HEATING SYSTEM WITH GRID CONNECTION UNDER TIME-BASED PRICING

By

PERCY ANDREW HOHNE

Dissertation submitted in fulfilment of the requirements for the degree:

Master of Engineering in Electrical Engineering

In the Department of Electrical, Electronic and Computer Engineering

Faculty of Engineering and Information Technology

Central University of Technology, Free State

Supervisor: Prof. K. Kusakana

Co-Supervisor: Dr. B.P. Numbi

December 2017

DECLARATION

I, PERCY ANDREW HOHNE, student number , do hereby declare that this research project, which has been submitted to the Central University of Technology Free State, for the degree : Master of Engineering in Electrical Engineering, is my own independent work and complies with the Code of Academic Integrity, as well as other relevant policies, procedures, rules and regulations of the Central University of Technology, Free State. This project has not been submitted before by any person in fulfilment (or partial fulfilment) of the requirements for the attainment of any qualification.

_____

P.A. Hohne Date: **1st December 2018**

DEDICATION

To my late father, Percy Andrew Hohne Snr, and my Lord, my Saviour Jesus Christ; for the many blessings bestowed upon me.

ACKNOWLEDGMENTS

The realization of this work was possible due to the following people to whom I wish to express my utter gratefulness.

To my supervisors, Professor Kanzumba Kusakana and Doctor Bubele Papy Numbi, I am grateful for the trust in my work and for the motivation demonstrated during this challenging course. Their support was without a doubt crucial to my dedication for this research.

I would like to acknowledge the inspirational instruction, guidance and the initial driving force to study optimal operation control from Dr. Bubele Papy Numbi, who has given me a deep appreciation and love for the beauty and detail of this subject.

I would also like to acknowledge the support and assistance given to me by the Central University of Technology, Free State (CUT). CUT has been very generous in supporting my academic pursuits and many of my colleagues have contributed with ideas, feedback and advice.

I would like to thank my late father, Mr. Percy Hohne Snr., for always believing that I was capable of achieving my dreams and goals, however difficult.

My mother, Mrs. Sonja Hohne and sister, Miranda Hohne, for their support and reassurance.

Dr. Frikkie Kruger and Ms. Erna Vlok for their continuous care and encouragement through the years.

Finally, I would like to thank in a special way, my partner and her father, Andrea Walle and Mr. Erich Walter Walle, for their support, prayers and good wishes. I could not have completed this effort without their assistance, tolerance and enthusiasm.

Thank you.

LIST OF ABBREVIATIONS

BEP	Break-even point
EE	Energy efficiency
ESTWH	Electric storage tank water heater
ETC	Evacuated tube collector
FPC	Flat plate collector
GFTWH	Gas-fired tankless water heater
GSHPWH	Geothermal source heat pump water heater
HPWH	Heat pump water heater
HSWH	Hybrid solar water heater
LCC	Life cycle cost
LM	Load management
MINLP	Mixed integer linear programming
NERSA	National Energy Regulator of South Africa
PBP	Payback period
PDC	Parabolic dish collector
PTC	Parabolic trough collector
PV	Photovoltaic
PVT	Photovoltaic thermal collector
SCIP	Solving constraint integer programs
SWH	Solar water heater
TOU	Time-of-Use (electricity tariff)

ABSTRACT

In South Africa, 40 to 60% of the total energy of a normal residential building can be allocated to the heating of water. Traditionally, a standard electric storage tank-water heater (ESTWH) has been the main device for residential water heating within the country. However, as a result of the increase in the South African population, economy and living standards have led to an energy shortage, which has resulted in a steadily increasing electricity price. As an attempt to solve this electricity crisis, Eskom, the main electricity supplier, has recently introduced energy management activities such as energy efficiency (EE) and the use of renewable energy (RE) systems.

On the one hand, the EE activities consist of reducing the total (overall) energy consumption during all the time periods, while load management (LM) activities aim to reduce the energy consumption during given time periods, such as peak times, when the Eskom grid cannot meet the demand. During peak times, the electricity consumption is charged at higher rates to encourage customers to shift their loads to off-peak and standard periods when the electricity is at a lower cost. This type of tariff is referred to as time-of-use (TOU) electricity tariff. With TOU, customers can therefore reduce their electricity bills by shifting load demands away from the peak time periods.

On the other hand, in order to reduce the larger amount of residential peak load demand, renewable energy systems, such as the solar water heater (SWH), was recently introduced and implemented in South Africa as a replacement to the ESTWH. However, it has been observed that SWHs was not continuously meeting the thermal comfort of the users, under certain weather conditions. During winter, for instance, the amount of thermal energy required is greater than that of summer due to the temperature difference of the water that needs to be heated, while the solar radiation in winter is considerably less due to shorter days and the position of the sun with reference to the earth's location.

As a solution to this, the coupling of the SWH with the ESTWH, referred to as hybrid solar water heating (HSWH) system, is nowadays seen as technical and economic feasible option for water heating in South Africa. The system is composed of a solar collector that

uses solar radiation to increase the temperature of water and the ESTWH, which stores the hot water. In the case of poor solar radiation, the SWH fails to increase the temperature of water to the comfortable level; therefore, the required temperature is maintained by the ESTWH.

However, implementing optimal energy management of the HSWH can help to meet the required thermal comfort level while reducing the electricity cost, even more so when the TOU tariff is implemented.

With this in mind, the aim of this work is to develop an optimal energy management model that will improve the operation efficiency of the HSWH. The main objective is to minimize the water heating energy cost from the grid by taking advantage of the TOU electricity tariff, meanwhile maximizing the thermal comfort level of hot water users.

Simulations are performed using Matlab software, and the results demonstrate that operating the proposed hybrid system under the developed optimal energy management model reduced the operation cost when compared to a traditional ESTWH. In addition, the comparisons made in lifecycle costs of these systems shows that in the long run, the hybrid system will be the less costly option with a 49 % saving over a project lifetime of 20 years.

Keywords:

Cost minimization; Flat plate solar collector; Hot water storage tank; Hybrid solar/electric storage tank water heater modelling; Optimal scheduling; Water heating technologies.

CONTENTS

LIST OF FIGURES

LIST OF TABLES

CHAPTER I: INTRODUCTION

1.1 BACKGROUND

Water heating for hygienic purposes such as showering and bathing is one of the most energy consuming processes in residential areas. For instance, in South Africa about 40 to 60% of the total energy of a normal residential building can be allocated to the heating of water [1]. Water needs to be heated from a lower temperature to the user's specific comfortable thermal temperature level. Traditionally, a standard electric storage tank-water heater (ESTWH), also known as a geyser in South Africa, has been the main device for residential water heating within the country. However, the increase in the South African population, economy and living standard has led to an energy shortage that has resulted in a steadily increasing electricity price. As an attempt to solve this, the main electricity supplier, Eskom, has recently introduced energy management activities, such as energy efficiency (EE) activities, and the use of renewable energy (RE) systems [2].

On the one hand, the EE activities consist of reducing the overall energy consumption during all time periods, while load management activities aim to reduce the energy consumption during given time periods such as peak times when the Eskom grid cannot meet the demand.

During peak times, the electricity consumption is charged at higher rates to encourage customers to shift their loads to off-peak and standard periods when the electricity is at lower cost. This type of tariff is referred to as time-of-use (TOU) electricity tariff. With TOU, customers can therefore reduce their electricity bills by shifting load demands away from the peak time periods [3]. Some EE activities on ESTWH have been suggested to reduce the corresponding overall energy consumption.

The first method is the use of insulation material on the tank for standby loss reduction. This solution showed significant savings in energy costs. The second method, which is the most cost-effective, is to reduce the temperature to which the water needs to be heated. This is accomplished by simply changing the setting of the thermostat to a lower value. The

temperature can be reduced to suit the consumers' needs and thermal comfort level [4]. However, by reducing the temperature, a risk of bacterial infection arises and this is an important factor that needs to be considered when assessing thermal comfort level of the hot water users. This can potentially result in the production of the Legionella pnuemphilla, which is a hot water bacterium growing at water temperatures ranging from 20 ºC to 45 ºC. In its most virulent form, it can cause Legionnaire's Disease, however studies have shown that only 1-5% of people exposed to the bacteria were infected [5].

With South Africa's populations ever decreasing health condition and increase in immune virus infections, the probability of contracting this form of disease is of higher possibility. The World Health Organization (WHO) has therefore determined that a temperature of 60 ºC can eliminate these bacteria in hot water. It has been determined that the hot water supply should reach a temperature of 60 ºC once daily to prevent the formation of bacteria [6].

In order to reduce a greater amount of residential peak-load demand, renewable energy systems such as solar water heaters (SWHs) were recently introduced and implemented in South Africa to serve as a replacement to the ESTWH. However, observations revealed that SWH was not continuously meeting the thermal comfort of the users under certain weather conditions. During winter, for instance, the amount of thermal energy required is greater than that of summer. This is mainly due to the temperature difference between the water that needs to be heated and the desired hot water. In addition, the solar radiation in winter is considerably less than in summer, due to shorter days and the position of the earth with reference to the sun [7]. As a solution to this, the coupling of the SWH with the ESTWH, referred to as a hybrid solar water heater (HSWH) system is seen today as a technical and economically feasible option for water heating in South Africa.

The system is composed of a solar collector that uses solar radiation to increase the temperature of water, and the ESTWH used to store the hot water. In the case of poor solar radiation when the SWH fails to increase the temperature of water to the comfortable level (usually 60 °C), the required temperature is maintained by the ESTWH [8]. However, the periods in which the ESTWH system switches on typically falls in the high electricity cost regions of the TOU tariff. A popular control method implemented by consumers is the use

of a timer system in order to schedule the switch-on periods of the ESTWH. This type of method provides cost savings in terms of the times that hot water is required, so that unnecessary energy usage is limited. The drawback of this control technique is the lack of sensitivity to the TOU tariff regions. In retrospect, implementing an optimal thermal and electrical management scheme for the HSWH can assist in meeting the required thermal comfort level while reducing the electricity cost, specifically with the TOU tariff taken into consideration.

With this in mind, the aim of this work is to develop an optimal energy management model that will improve the operation efficiency of the HSWH. The objective is to minimize the water heating energy cost from the grid by taking advantage of the TOU electricity tariff, while maximizing the thermal comfort level of hot water users.

1.2 PROBLEM STATEMENT

Several studies have concentrated on optimization and efficiency of the different types of solar water heating schemes. However, not many have considered the hybrid solar water heating (HSWH) system in conjunction with energy management factors such as the time-of-use (TOU) electricity tariff.

The main problem arises from the fact that the solar radiation in a 24-hour day is at times insufficient to maintain the necessary temperature of the water. This can mainly be accredited to insufficient solar irradiance from the sun in the event of overcast skies or lack of radiation during the night. Thus, the ESTWH is essential in providing the additional energy in order to compensate for the periods where solar radiation is poor or absent. Taking advantage of TOU tariff, an optimal energy management strategy can help reduce the total cost associated with the energy consumption of the HSWH system, while maintaining the thermal comfort level of the hot water users.

1.3 OBJECTIVES

The objective of this work was the development of an optimal energy management model for HSWH by taking advantage of the TOU electricity tariff to achieve both minimal energy cost and maximum thermal comfort level. The model was developed with input variables such as hot water demand, solar radiation and inlet water temperatures, as well as the ambient air temperatures. An economic analysis was performed which included the life cycle costs and break-even point evaluation.

1.4 EXPECTED OUTCOME OF THE STUDY

- Scientific outcomes:
  - The development of a mathematical model for optimal control of a hybrid solar water heating system that takes into account both physical and operational constraints such as the desired temperature and the switching boundaries.
  - To achieve minimal operation and life cycle costs as compared to the traditional storage tank water heater, based on time-of-use tariff.
  - To publish and document the research results in a master's dissertation as well as conference and journal publications.
- Social impact:
  - Increase awareness towards energy saving in South Africa.

1.5 RESEARCH METHODOLOGY

To achieve the objectives of the study, the methodology is as follows:

- Literature Review: A thorough survey of literatures related to water heating systems, hybrid solar water heating systems design and operation and the control of grid-connected hybrid solar water heating systems have been reviewed.

- System Modelling: After studying the operation of the hybrid solar water heating system, not only an optimal energy management model to minimize the electricity cost based on TOU tariff, but also to maximize the thermal comfort of the hot water users was developed. The proposed optimal energy management model considered solar radiation availability throughout the year and the possibility for bacterial infection if water temperature is too low. Both physical and operational system constraints have been taken into account in the model.
- System variables: Fig. 1.1 illustrates the block diagram of the research modelling process with the defined variables.

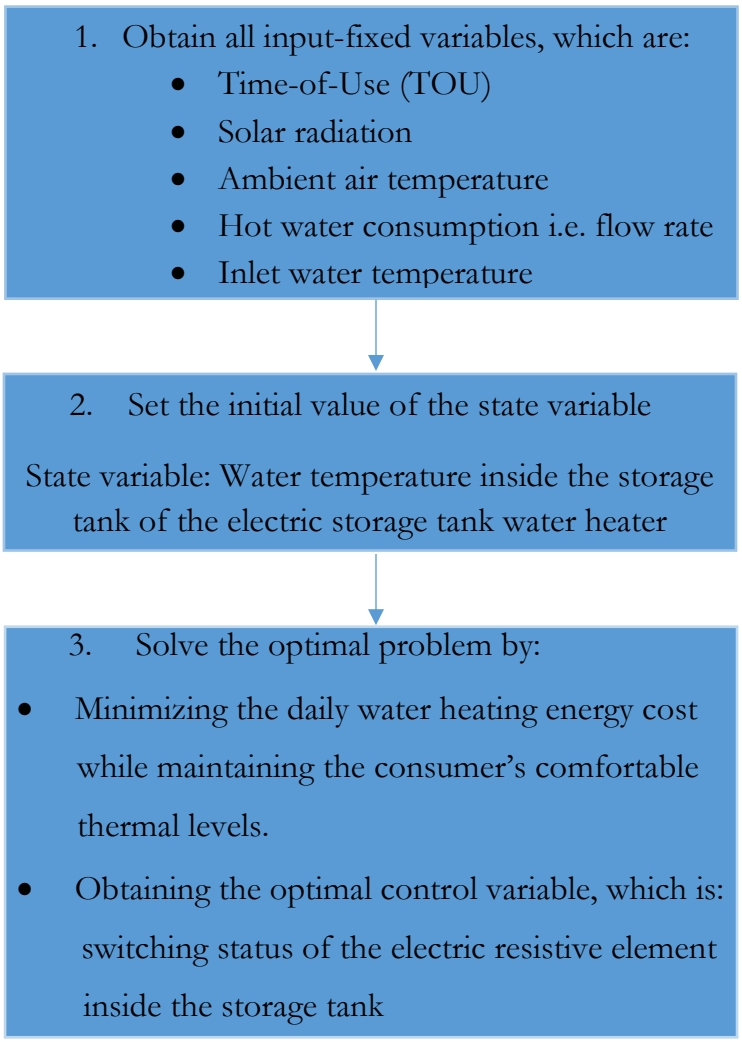

Figure 1.1: Block diagram of methodology and research design

- Independent variables which are all input variables are classified as below:
- Control variable i.e. manipulated variable (Switching status of the water heating system) and input-fixed variables i.e. exogenous variables (TOU, solar radiation, ambient air temperature, hot water consumption and input water temperature)
- Dependent variables: all variables that are affected by any change or variation in the input variables. In this case, it is the hot water temperature inside the tank considered as "state variable".

- Data collection: The real input data used in the developed optimal energy management model was:
  - TOU tariff structure retrieved from Electricity supplier approval letter.
  - Hot water consumption profile measured for a specific medium density household in Bloemfontein.
  - Inlet water temperatures obtained from a water quality analysis done on the water supply networks in Bloemfontein.
  - Ambient air temperatures and solar irradiance data retrieved from a weather station located at the University of the Free State.
- Solving the optimization problem:
  - The optimization problem was identified as a mixed integer non-linear problem.
  - The universal Solving Constraint Integer Programs (SCIP) solver in Matlab OPTI-Toolbox was used for this problem due to its high speed solving capabilities.
- Simulation:
  - The simulated results include the optimal switching function of the electric resistive element, the temperature of the water inside the storage tank and the daily cumulative costs incurred with respect to the TOU tariff structure for a Summer and winter case.

1.6 HYPOTHESIS

- Electricity costs will be reduced significantly compared to the traditional electric storage tank water heater and this will be achieved with TOU tariffs as the core consideration.
- The HSWH will have a lower lifecycle cost compared to the ESTWH.
- The HSWH will be best suited for domestic water heating purposes compared to the ESTWH for the South African climate, due to the abundance in solar irradiance in the region.

1.7 DELIMITATION

The study was conducted with the following limitations:

- Only open-loop optimal energy management was considered
- Only Homeflex Eskom Tariff was used since this applies to customers that consume energy from Eskom for the heating of water.
- Only weekdays TOU tariff were used, since the peak demand does not take place on Saturdays and Sundays.
- Only model developments and simulations were considered.
- Electrical energy consumption of the pump (forced circulation) in the hybrid system was not considered, as it only operates when the HSWH is switched on and forms an integral part of the system to function sufficiently.
- Only the indirect flat plate collector was considered, as it was found to be suitable for the case study.

1.8 PUBLICATIONS DURING THE STUDY

Conference papers:

- P.A. Hohne, K. Kusakana "A review of water heating technologies". South African Universities Power Engineering Conference (SAUPEC 2017), pp. 159-163, Cape Town, South Africa, 30 January – 1 February, 2017.
- P.A. Hohne, K. Kusakana, B.P. Numbi "Optimal Energy Management of a Hybrid Solar Water Heating System with Grid Connection Under Time-Based Pricing". Submitted to the International Conference on Domestic Use of Energy (DUE 2018).

Journal papers:

- P.A. Hohne, K. Kusakana, B.P. Numbi "Operation cost minimization and energy usage optimization modelling of hybrid solar/electric water heating system". (Accepted to be published in advanced science letters).

Journal papers submitted:

- P.A. Hohne, K. Kusakana, B.P. Numbi "A review of water heating technologies: An application to the Southern Africa context" (Submitted to renewable and sustainable energy reviews).
- P.A. Hohne, K. Kusakana, B.P. Numbi "Optimal Energy Management and Economic analysis of a grid-connected Hybrid Solar Water Heating System in Bloemfontein". (Submitted to Applied Energy).
- P.A. Hohne, K. Kusakana, B.P. Numbi "Scheduling Hybrid Solar Water Heating System Demand based on timer and optimal control". (Submitted to Energy Conversion and Management).

1.9 DISSERTATION LAYOUT

This dissertation has been divided into six Chapters, with the main research results being presented in Chapter IV and Chapter V.

Chapter I presents the background of the work, underlines the problems and provides the objectives and methodology.

Chapter II reports the thorough review of advancements in water heating technologies and comparing the limitations, advantages, efficiency, and cost effectiveness of the different methods of heating water. The chapter concludes with a recommended hybrid water heating system for the case study.

Chapter III describes the optimal control model formulation of a hybrid solar/electric water heating system and gives a general overview of the optimization problem. The choice of a suitable optimization algorithm is presented and discussed. The constraints of operation which includes the desired temperature range of the water inside the storage tank and switching function variable of the electric resistive element is defined.

Chapter IV presents and discusses all the input fixed variable data as well as the comparison of a baseline system to the optimized proposed system simulation results.

Chapter V evaluates the economic feasibility and presents the break-even point and life cycle cost analysis of the hybrid water heating system compared to a baseline water heating system.

Chapter VI concludes the work of this dissertation and sets the stage for future studies.

CHAPTER II: REVIEW OF DIFFERENT WATER HEATING TECHNOLOGIES

2.1 INTRODUCTION

In this chapter, the most common water heating systems in South Africa in terms of water heating efficacy and operation are discussed. In addition, some existing alternative methods of water heating are mentioned that might have relevance in the near future. The operation of water heating systems discussed in sections 2.1.1 - 2.1.8 include standalone renewable energy systems, electrical/gas input devices and hybrid systems that might exist in different configurations.

These configurations can consist of either hybrid renewable systems or a hybrid renewable system coupled with an electrical input device. The most relevant publications related to water heating technologies have been reviewed and categorized in terms of technology used and contributions made in section 2.2. Advantages and drawbacks of each of these systems have been discussed and summarized in section 2.3. The conclusion in section 2.4 recommends a HSWH for the specific case of South Africa.

2.1.1 Electric storage tank water heater (ESTWH)

The electric storage tank water heater has two functions, to heat water using electrical energy and to store the hot water until such a time as to when it is required. Electrical energy is supplied to electrical resistive elements inside the storage tank. Current flows through the elements in order to create heat which is exchanged to the surrounding water. The process gradually increases the thermal level of the entire water mass inside the storage tank water heater. A thermostat maintains a certain thermal level set by its user and the electric element is switched on when the temperature of the water falls below a certain value therefore increasing hot water availability. Some electric storage tanks have two electric elements each

controlled by an independent thermostat. One element located at the bottom of the storage tank as illustrated in Fig. 2.1, assists in replacing lost energy due to the temperature gradient between the ambient air and the water [9]. The upper element provides thermal energy to the water when the demand is high, making the dual element storage tank more efficient than that of conventional single element systems [10, 11].

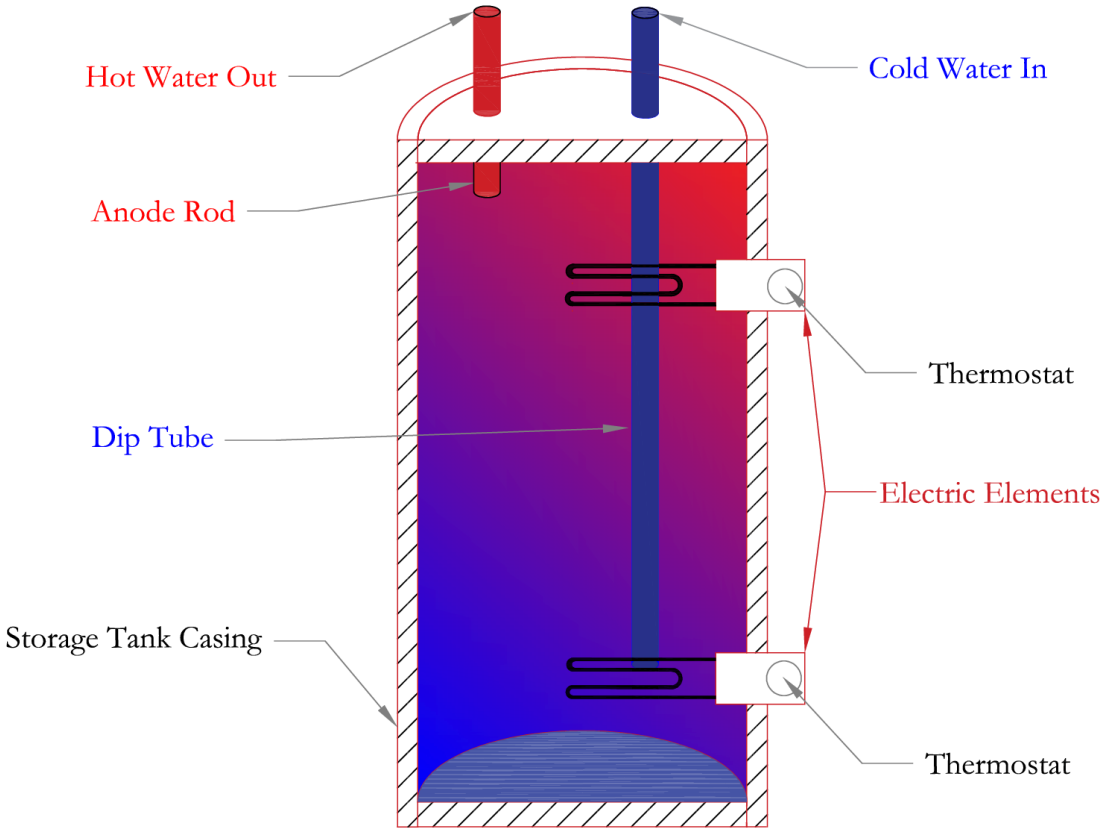

Figure 2.1: Electric storage tank water heater (ESTWH)

2.1.2 Electric tankless water heater (ETWH)

This water heater works on the same principle as the ESTWH; multiple elements heat water to ensure instantaneous hot water access. This system is a demand type water heater, which means that water is heated only when it is required. No hot water is stored assisting in the prevention of standby losses [12].

However, due to the immense amounts of hot water needed at a specific time, the instantaneous heating of the water consumes a substantial amount of electricity. Referring to Fig. 2.2, when hot water is needed, cold water flows into the heater where it is heated by three separate electrical resistive elements. The water temperature increases while it passes through each heating segment so that the final desired temperature is reached at the third and final element.

The microprocessor control board regulates the amount of energy needed to heat the water to the temperature set by the user. Inlet cold water temperature, outlet hot water temperature and the flow of the water is monitored and the power is adjusted accordingly. Due to the absence of a storage tank, the heater requires less space so that it can be placed near the hot water demand location. This, in turn reduces heat losses [12].

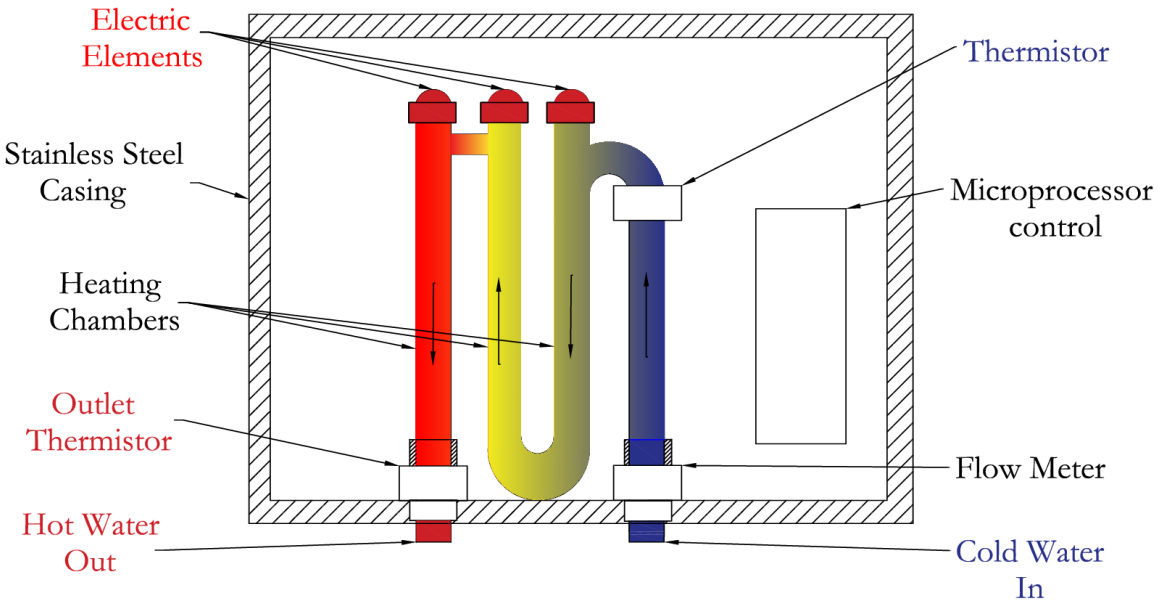

Figure 2.2: Electric tankless water heater

2.1.3 Solar Water Heater (SWH)

Only a few countries in the world receive high concentrations of solar irradiation, South Africa is fortunate in being one of these countries. Fig. 2.3 presents the average annual direct normal solar radiation per square meter in kWh/m^2 received from the sun. The Northern

Cape Province receives the most radiation annually, which can be described on average as more than 3 kWh/m², other provinces, for example, KwaZulu-Natal and Mpumalanga, receive less than this average radiation (< 2 kWh/m²) [13]. All provinces in South Africa receives an adequate amount of solar energy for water heating purposes. It is evident that a solar technology, such as solar water heaters, can thrive in the South African climate, thus its growing popularity throughout the country.

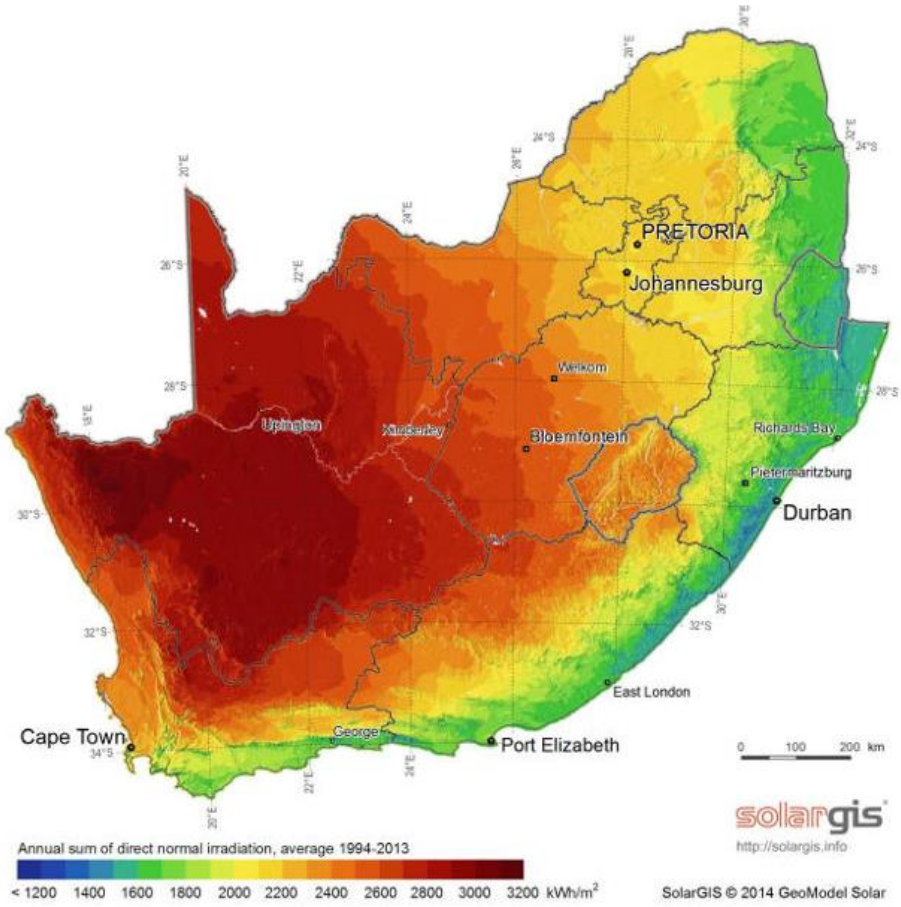

Figure 2.3: Annual solar irradiation in South-Africa (MAP form Solargis) [13]

Solar water heaters absorb thermal energy from the sun and transfers it to water. This method of water heating is beneficial due to the fact that the energy used is costless, abundant and indefinitely renewable. The solar collector placement and tilt angle plays a significant role in the amount of energy it can absorb. It has been established that when a collector facing north is tilted at an angle of approximately 30°, it will reach near optimal annual energy absorption rates [14]. It should also be mentioned that the collector should not at any time of

the day be obscured from the sun; this means that most solar collectors are mounted on the rooftops of buildings. Most solar water heaters have thermal storage tanks fixed at a position higher than that of the collector itself. This is done so that circulation can take place naturally through thermosiphon [15]. Thermosiphon is a phenomenon whereby higher density cold water displaces less dense hot water through natural convection. The water circulates through the collector and tank in order to continuously maintain a high water temperature [16].

Active and passive solar water heating systems are categorized in Fig. 2.4. The Active system uses forced circulation to induce a flow of the fluid in the system. This means the fluid is pumped to achieve the required circulation. Furthermore, active systems can have an open loop (direct heating of residential water supply) or closed loop (indirect heating of the water by means of a heat transfer fluid) [17]. The passive system uses a natural method for inducing circulation through the thermosiphon phenomena. The Integrated collector storage (ICS) system is an example of the passive system where natural circulation takes place.

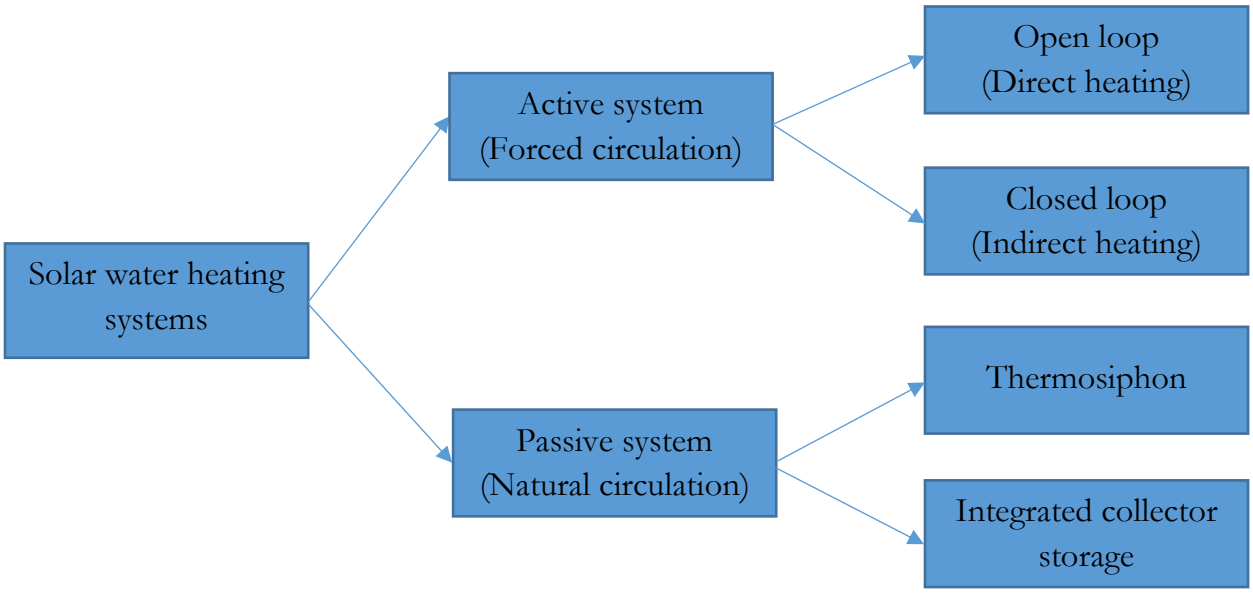

Figure 2.4: Solar water heating systems

Four types of collectors are currently available in solar water heating technologies. The Flat plate collector as shown in Fig. 2.5, evacuated tube collector as illustrated in Fig. 2.6 and concentrated solar collectors (parabolic collectors as presented in Figs. 2.7 and 2.8). The

integrated storage collector system is a solar collector (flat plate type) coupled with a thermal storage tank. The ICS system will not be discussed due to the low frequency of usage by consumers.

2.1.3.1 Flat plate solar collector (FPC)

Referring to Fig. 2.5, solar radiation penetrates the collector through the glazed cover. The heat absorbers receive thermal energy and transfer the heat radiation to the liquid substance flowing through it to increase the temperature of the substance. The heated liquid is then transported to fluid tubes, usually fitted with heat fins to increase the surface area for maximum absorption, where it flows to storage [18]. A temperature and pressure relief valve protects the system from overheating, the valve is located at the top part of the storage tank. Fig. 2.5 demonstrates how the cold water flows from the storage tank to the collector where it is heated and, through thermosiphon action, flows back to the tank. This process repeats itself to maintain a high water temperature in the storage tank.

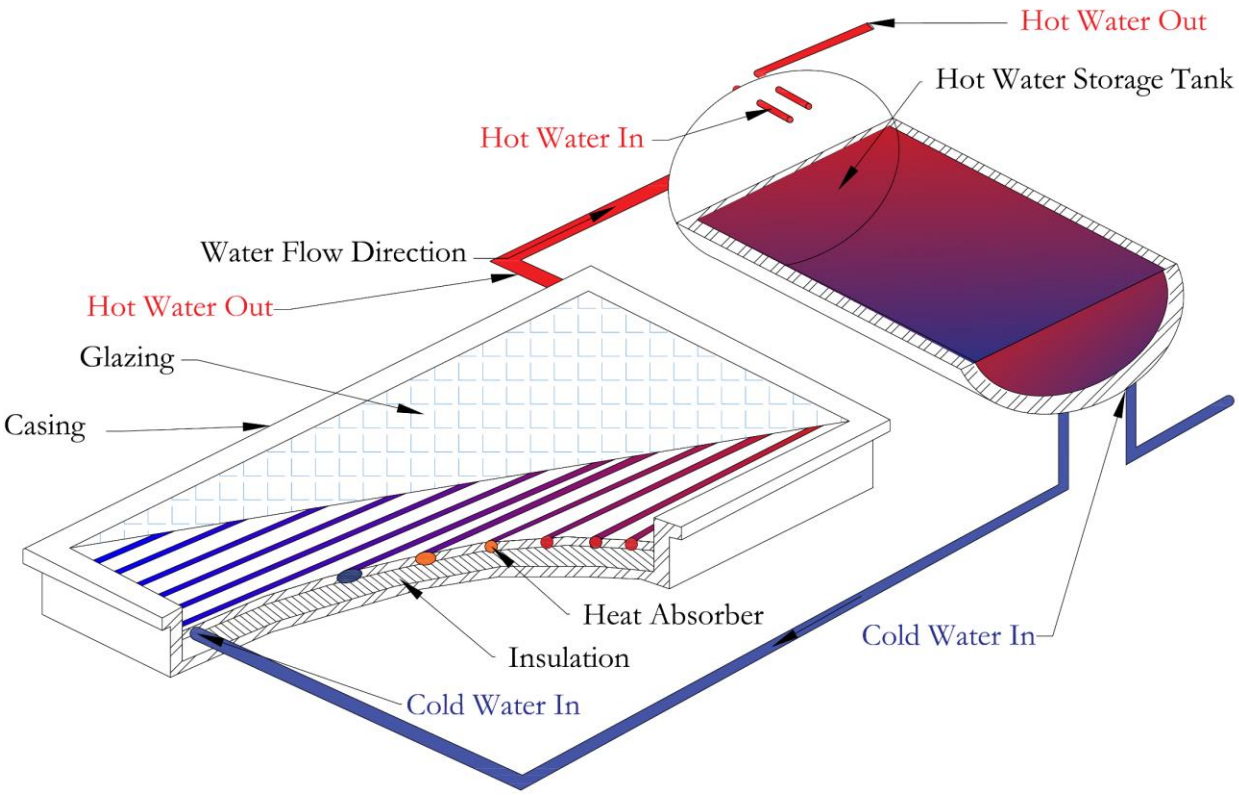

Figure 2.5: Flat plate collector components and operation principle

2.1.3.2 Evacuated tube collector (ETC)

The top layer of the evacuated tube collector, the first transfer layer, consists of a glass tube casing designed to protect the heat absorbing components inside the collector. Heat radiation passes through the top layer of the evacuated tube and is absorbed by a cylindrical collector pipe (fluid tube). This cylindrical collector is covered in a black coating for maximum heat absorption. A transfer fluid inside the tube absorbs the thermal radiation which then rises to the heat exchanger head. The heat exchanger heads terminate inside an insulated manifold. Water flows past the heat exchanger heads in the manifold of the collector and gains thermal energy. Through this action, the transfer fluid is cooled down and returns back to the bottom part to be heated again as illustrated in Fig. 2.6. The water then travels from the manifold to the storage tank through the pipes due to natural convection. The transfer fluid inside the evacuated tubes have anti freezing properties which makes it an excellent solar water heater for countries that frequently experience freezing temperatures [19].

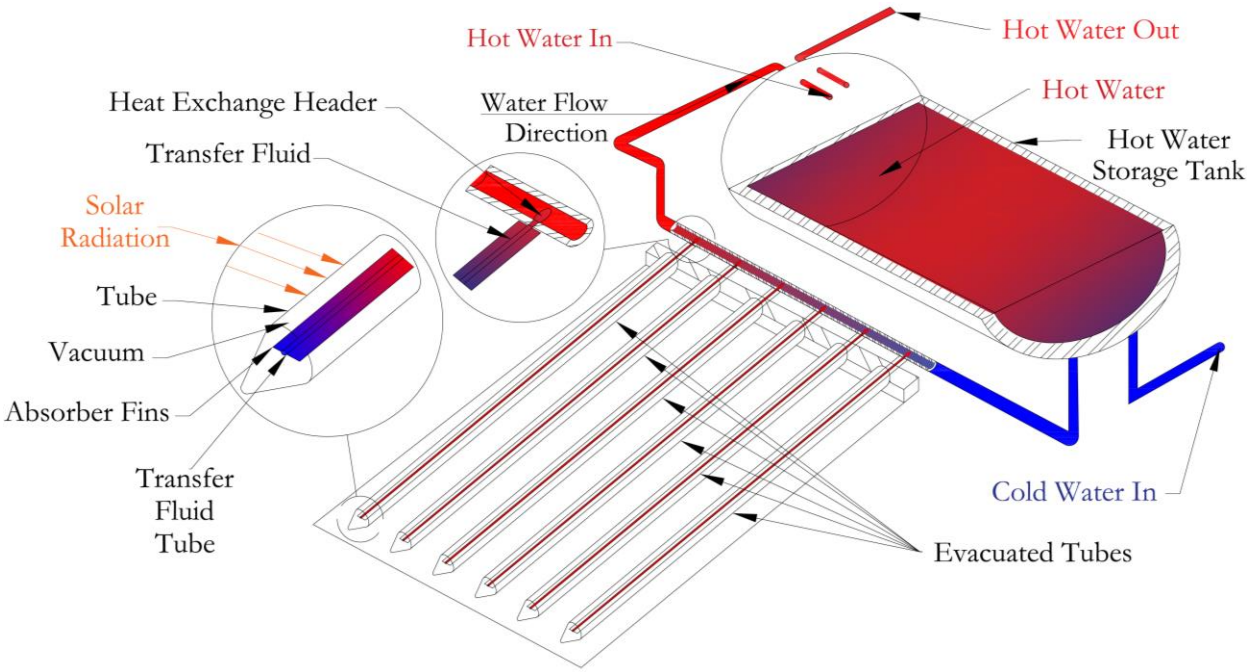

Figure 2.6: Evacuated tube collector components and operation

2.1.3.3 Parabolic dish collector (PDC)

The parabolic dish collector in Fig. 2.7 uses concentrated solar energy to heat a water heating receiver at the focal point of the dish. The collector dish tracks the movement of the sun on both the vertical and horizontal axis, in order to maximize the absorption of solar energy throughout the day. The tracking system requires electrical energy to operate the solar tracking mechanism. The receiver absorbs the focused solar energy and transfers it to the circulating fluid within. The circulating fluid can be a refrigerant or water. The water then flows to the storage tank for recirculation. This type of collector can either generate electricity through thermal generator action or directly heat a circulating fluid [20].

The parabolic dish collector is less common in the South African case due to the complexity of the solar tracking system. However, the efficiency of the system has increased in recent years and looks to be a competitive alternative for some regions.

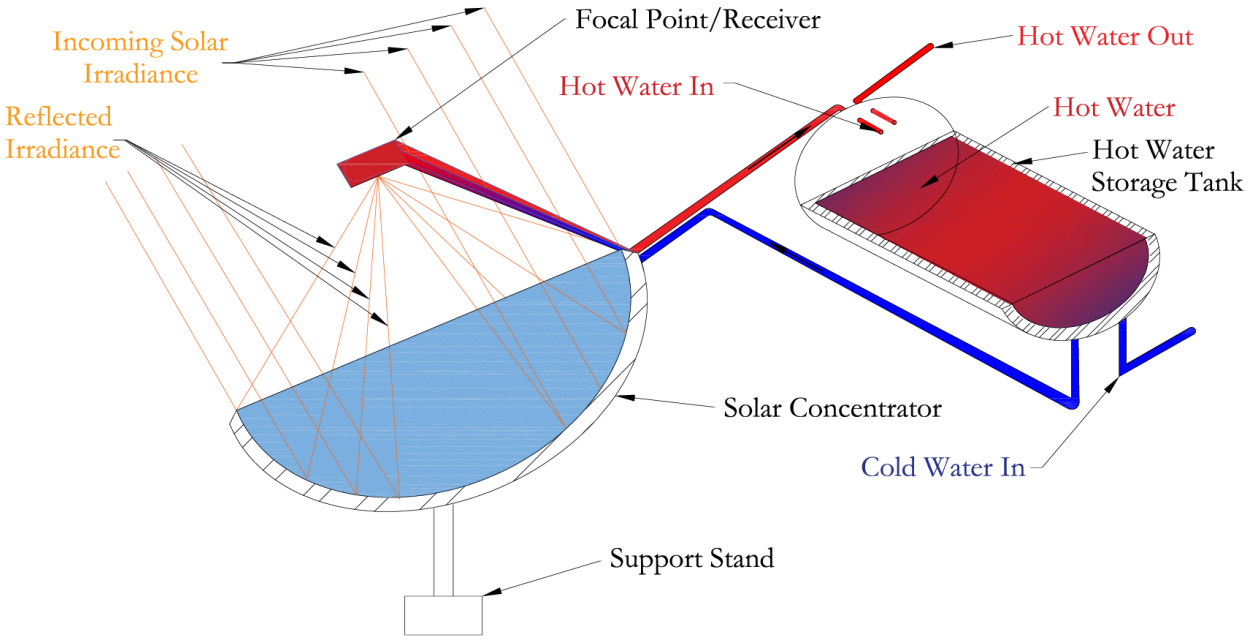

Figure 2.7: Parabolic dish collector components and operation

2.1.3.4 Parabolic trough collector (PTC)

The parabolic trough collector works on the same principle as the PDC. This system, however, employs single axis solar tracking where the solar tracking only takes place on the horizontal axis. This system has a focal line rather than a receiving point. The concentrator consists of a semi-circular reflective metal which focuses solar energy onto the focal line. A tube is fitted inside the focal line with the water or transfer fluid that needs to be heated flowing through it. The tube is encased in glass with a black coating [21]. Circulation takes place through thermosiphon or with the assistance of a circulating pump. It is usually recommended to place the collector facing North so that maximum absorption can take place in winter. Fig. 2.8 presents the system setup and operation of the parabolic trough collector [22].

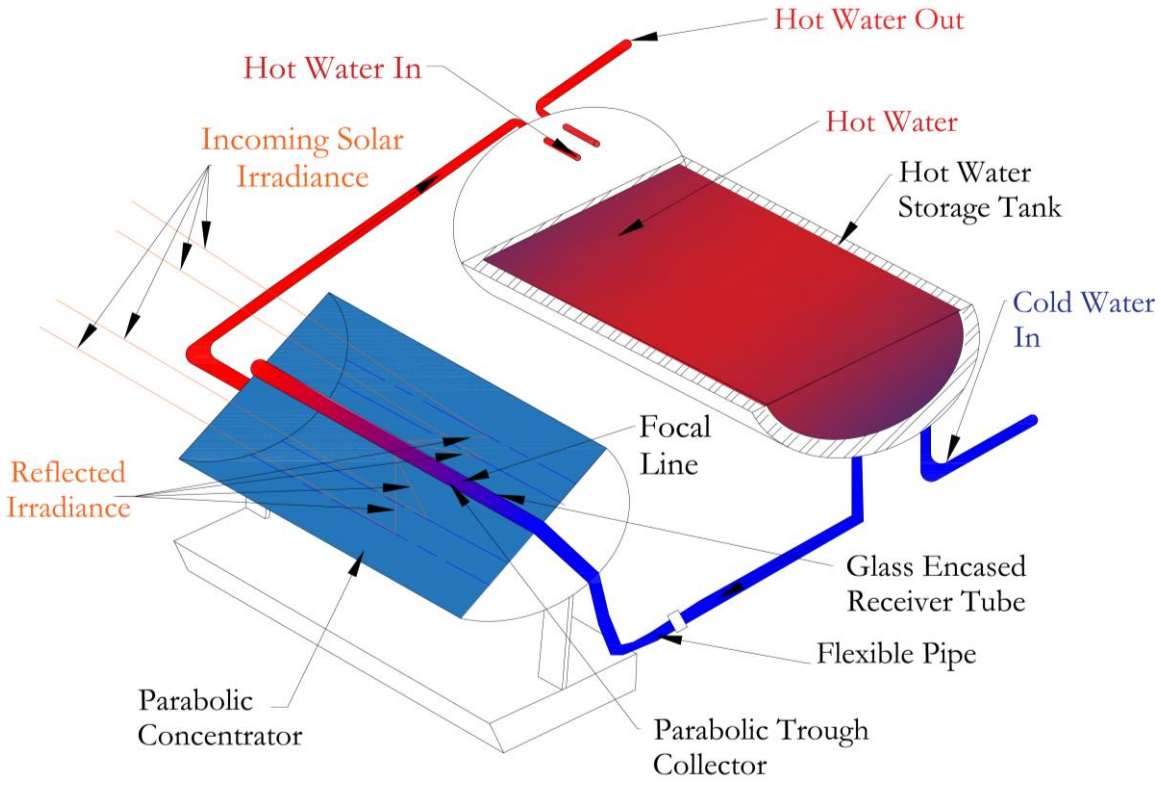

Figure 2.8: Parabolic trough collector components and operation

2.1.3.4 Hybrid solar/electric storage tank water heater (SWH/ESTWH)

Standalone solar water heaters can sometimes prove insufficient in heating water. Solar radiation is only available during the day and poses a substantial problem in meeting hot water demands. When hot water is required at all times of the day, the SWH discussed in Section 2.1.3 can be fitted to an existing ESTWH (described in Section 2.1.1), to form a hybrid solar water heater (HSWH) so that water can be heated when the solar radiation is inadequate.

Referring to Fig. 2.9, the electric element inside the storage tank increases the temperature of the water when the thermal level of the water falls below the desired value [23]. This hybrid system incorporates a circulation pump due to the matter that most existing electric storage tanks are fitted beneath the roof of a residential building. The solar collector is fitted at an optimal absorption angle on the rooftop of the building. While the storage tanks' position is lower than the collector, natural convection (thermosiphon) cannot take place to circulate the fluid, hence the circulation pump is required to assist in circulation.

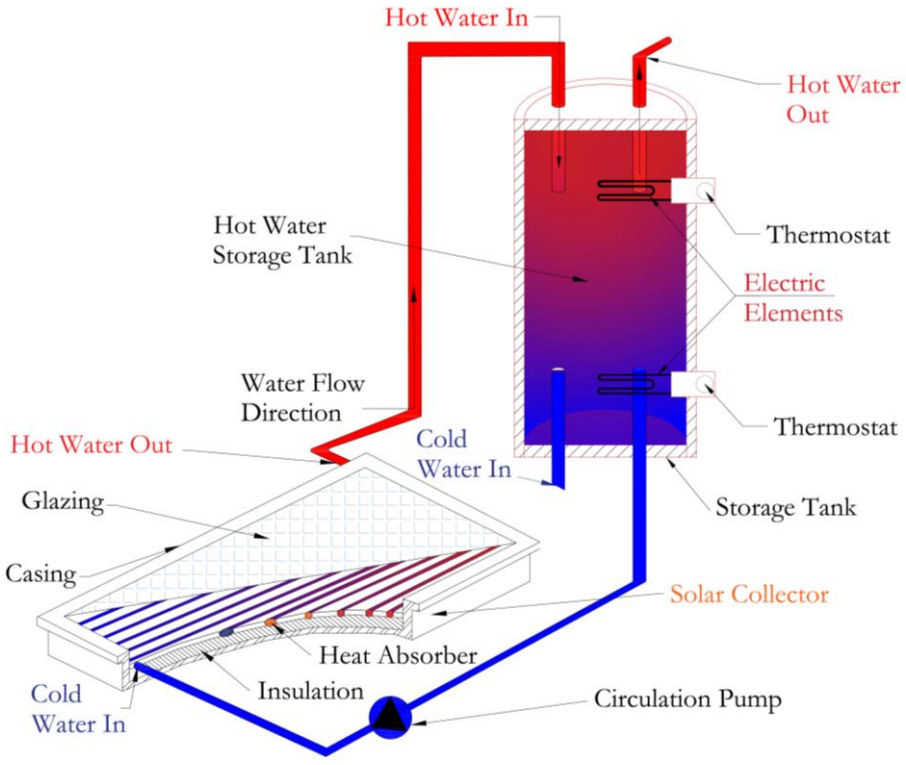

Figure 2.9: Hybrid solar water heating system components and operation

2.1.4 Heat pump water heater (HPWH)

The heat pump water heater extracts ambient energy from the surrounding air in order to heat water. This method of water heating is superior to any other electrical source water heater. Other electricity based water heaters convert electrical energy into thermal energy, where it can be said that the heat pump water heater only transfers the thermal energy from one place to another. The major parts of the heat pump water heater are the compressor, evaporator, expansion valve and the condenser. Refrigerant is contained within a closed loop where it absorbs the heat from the ambient air. The same refrigerant is then compressed in order to exchange heat with water as illustrated in Fig. 2.10; condensed while the heat is exchanged and then expanded in order to return back to the evaporator for reabsorption of ambient energy. The component that consumes the most energy is the compressor, and this is a modest amount in contrast to the electrical energy used by conventional electric water heaters [24].

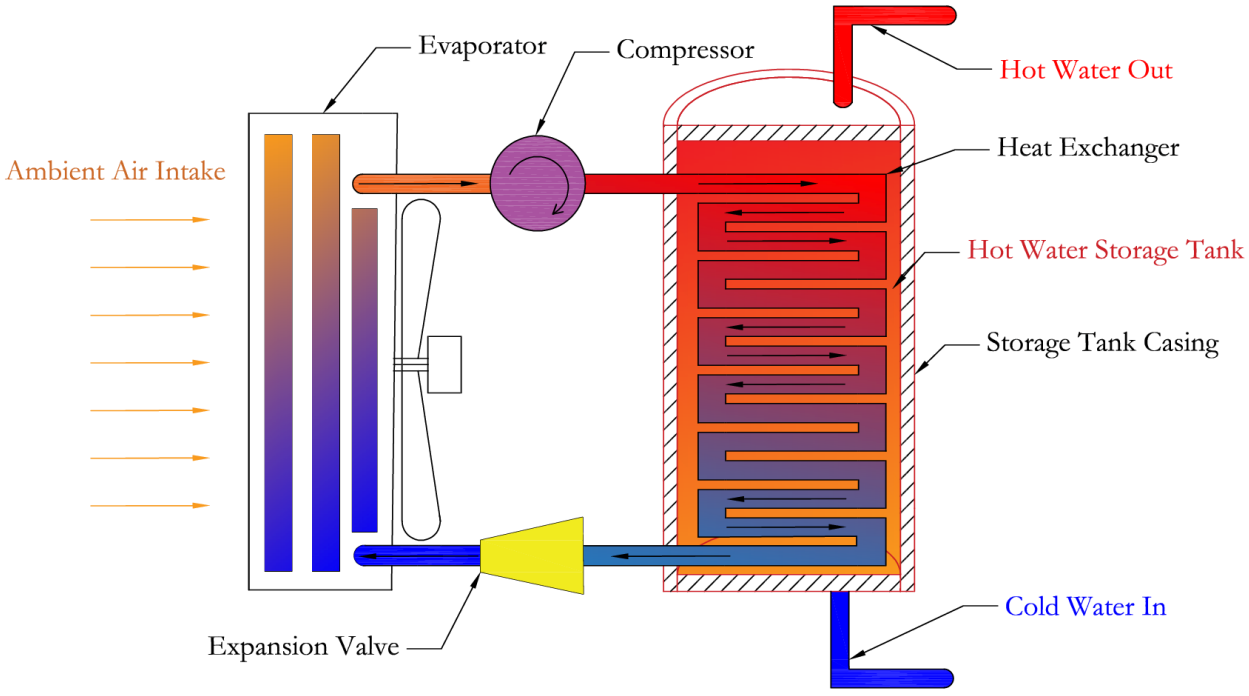

Figure 2.10: Heat pump operation refrigerant loop cycle

2.1.5 Gas fired tankless water heater (GFTWH)

This water heater instantaneously heats water when a demand for hot water presents itself. The water heater is switched on by igniting liquefied petroleum gas (LPG) supplied to the heater. After ignition, the regulator control valve maintains a constant flame. The constant flame produces thermal energy captured by heating fins. These heating fins transfer the energy to the water flowing through conductive pipes as shown in Fig. 2.11. Sensors located at the cold water inlet valve and hot water outlet valve sends data to the microprocessor, where decisions are made to decrease or increase the gas flowing to the burner [25]. The gas supplied will be increased within operating limits if the temperature at the hot water outlet side is below the desired temperature set by the user. Similarly, the gas will be decreased if the water temperature exceeds the desired temperature.

The water flow rate can be adjusted to suit the users need, but an increase in flow rate will require an increase in gas supplied to the burner. This heater offers the same advantages as the electric tankless water heater, the only difference is the source of energy supplied [26].

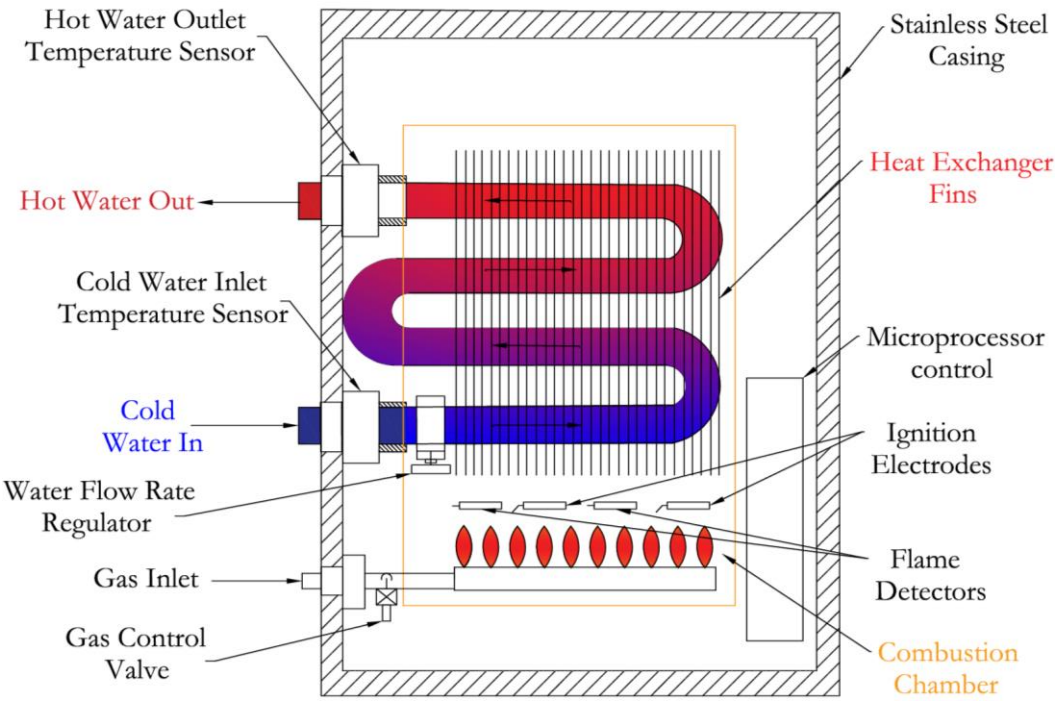

Figure 2.11: Gas fired tankless water heater components and operation

2.1.6 Hybrid heat pump coupled with gas fired water heater (HPWH/GFWH)

The following setup uses a conventional heat pump water heater described in section 2.1.4 and gas fired tankless water heater (section 2.1.5), that acts as a gas booster system. This hybrid system offers increased reliability due to the ability of the two systems to operate independently if one system should fail. Refrigerant is heated by the heat pump through the process described in section 2.4. The heat from the refrigerant cycle is exchanged with a secondary closed loop heat exchanger system [27] as shown in Fig. 2.12. The transfer fluid inside the secondary closed loop system has its thermal level increased further by means of the gas fired water heater [28]. The secondary exchanger loop has a higher thermal level due to this process and heat is again exchanged with water that will be used by the consumer.

In case of colder climates, when thermal energy in the ambient air is insufficient to heat water to the desired temperature levels, the gas fired tankless water heater can then increase the temperature independently. Standby losses and inadequate ambient energy will increase gas consumption which in turn will increase the operating costs in colder climates.

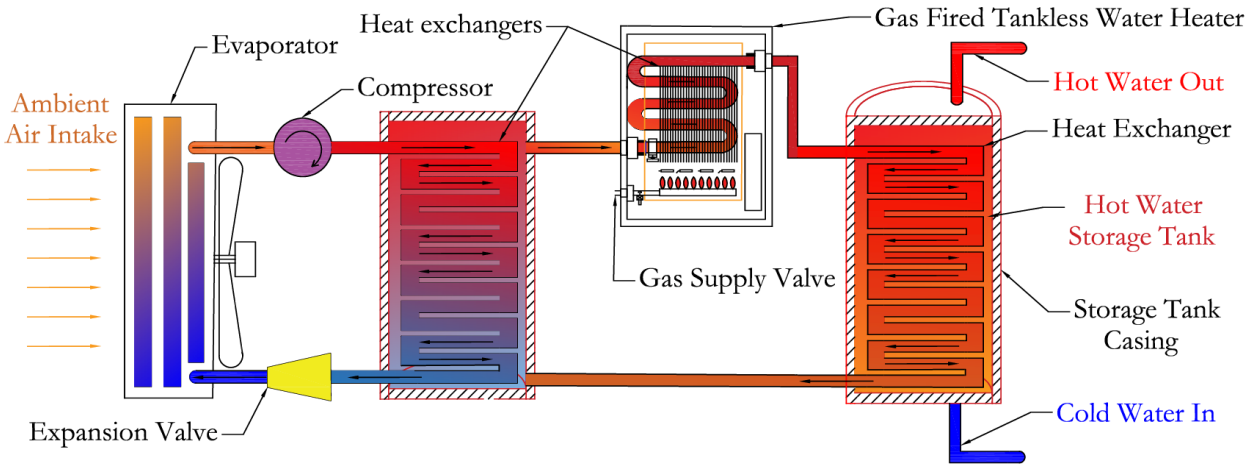

Figure 2.12: Schematic diagram of the heat pump gas fired water heater hybrid

2.1.7 Geothermal water heating systems

Geothermal water heating systems can be divided into two types of systems: geothermal hot spring water extraction and geothermal (ground-source) energy extraction.

2.1.7.1 Geothermal hot spring water extraction (GHSWE)

Geothermal energy heats groundwater, which in turn emerges from the crust of the Earth. The heated water at Earth's surface level forms a hot spring. The geothermally heated water occurs naturally and hot spring locations can be found in many locations across the world. Some locations have hot springs where the water temperature can be safe for bathing. Only hot springs with water temperatures not exceeding safe bathing limits can be used as a hot water source. Similarly, some hot springs have unacceptably low thermal levels, thus they are not suitable for bathing purposes. When a hot spring with a suitable thermal level is found, the hot water from the spring can be pumped to residential areas, as long as these areas are in the vicinity of the hot spring. The close proximity will minimize heat losses.

This water needs to be treated or filtered to avoid bacterial infection. The hot spring water can be used for hygienic purposes. Referring to Fig. 2.13, eight thermal springs in South Africa have thermal levels deemed appropriate for household use (exceeding 50°C) [29].

Figure 2.13: Distribution of thermal springs in South Africa [33]

2.1.7.2 Geothermal heat pump water heater (GTHPWH)

Geothermal heat pumps extract thermal energy beneath ground level. High thermal levels beneath the ground can be attributed to the radio-active decay of minerals and solar radiation absorbed by the surface of the earth. A conventional heat pump system is used, but in this arrangement, heat is extracted from the ground. This type of heat pump is also called a ground-source heat pump water heater. The system consists of a primary and secondary heat exchange system. The primary heat exchanger has a transfer fluid flowing within it and the second has a refrigerant. Part of the primary heat exchanger is buried underground [30]. The depth at which it is buried is at approximately 10 metres below the earth's surface. Fig. 2.14 shows that at about 10 metres below ground level, the temperature ranges between 10 °C and 12 °C. The temperature remains constant throughout the year even during winter months, where the air temperature is known to fluctuate significantly.

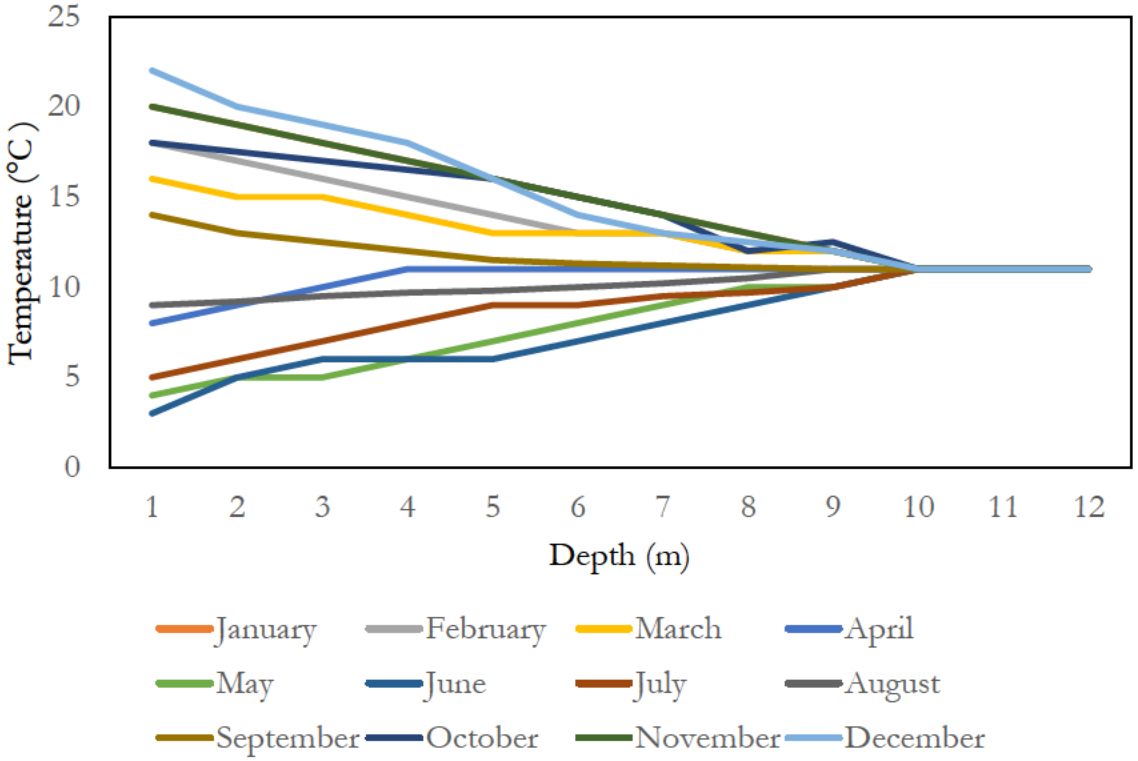

Figure 2.14: Ground temperature at each depth level (adjusted approximation for Southern hemisphere).

Referring to Fig. 2.15, after energy extraction from the earth, the heat is exchanged with the secondary heat exchanger where it is compressed, condensed (process of secondary heat exchange with water) and then expanded in order to start the cycle again. The result is hot water for consumption by the user. This system is recommended for winter months, during summer months the heat pump can be retrofitted for normal operation with the air-source evaporator. The energy in the ambient air is much higher in hotter months when compared to the energy in the ground [31].

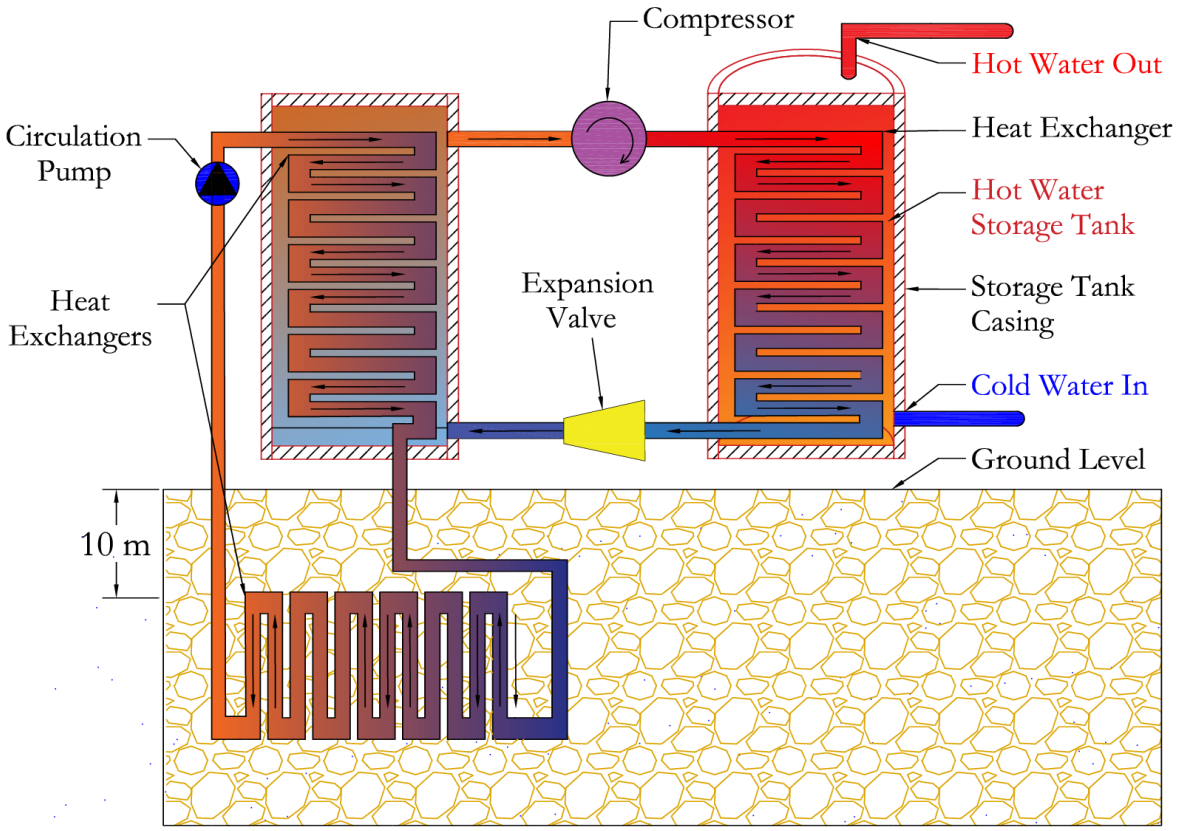

Figure 2.15: Ground source heat pump and thermal loop.

2.1.8 Photovoltaic-thermal water heater (PV/TWH)

The photovoltaic-thermal (PV/T) collector is the combination of a SWH and a PV cell. A PV cell's efficiency is highly dependent on temperature. If the temperature of the cell is too high, the efficiency drops significantly. This efficiency drop can be mitigated by adding a solar collector [32]. The solar collector acts as a heat sink while it uses the thermal energy gained to heat water. Any PV module can easily and cheaply be retrofitted to become a water heater.

Referring to Fig. 2.16, the PV cell is surrounded by water flow ducts protected by a metal casing. The top and bottom layer of the upper collector is made up of glass, so that solar radiation can be transferred to the PV panel [33]. The lower collector is enclosed and forms part of the collector casing. Small circular channel cut-outs form part of the circulation path and evens out heat distribution. Cold water is supplied to the collector system and heated,

while thermosiphon assists in the circulation of the water through the entire system. This ensures continuous heating of the water so that the water can be used by the consumer [34].

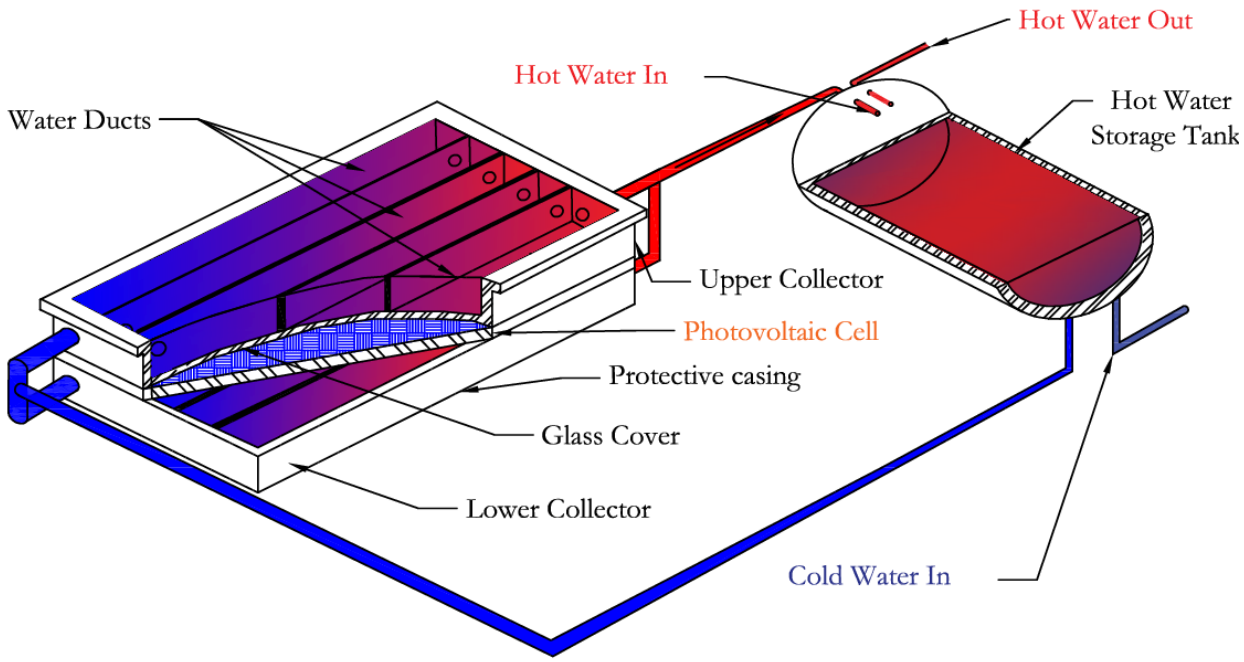

Figure 2.16: Photovoltaic-thermal collector with dual absorber channels

2.2 REVIEW OF RELEVANT LITERATURE

Numerous authors have done energy efficiency, load management and optimal parameter design studies with the decrease in energy consumption of water heating systems in mind. Table 2.1 summarizes different papers by the different authors in which attempts have been made to increase the efficiency of the water heating systems by using the different methods and procedures as explained thus far. This table provides the source authors, the contributions made by the respective authors and a summary of the findings/results of each water heater system.

Table 2.1: Review of papers linked to optimization and improving efficiency of different water heating configurations

Authors	Highlights/Contribution	Technology
Abbas N., Nawaz R., Khan N. [35]	• Refrigerant Parametric Quantification method was developed for optimal thermosiphon operation for SWHs. • CO_2 has a high quality factor when compared to other refrigerants while R-1234yf showed superior characteristics for commercial heating applications.	SWH
Aguilar F.J., Aledo S., Quiles P.V. [36]	• Feasibility study done on PV energy supplying heat pump water heaters. • Results denoted a performance factor of 8.92 with a solar input energy compared to non-renewable input was 61.7%	HPWH
Alberto P. and Ferrer F. [37]	• Feasibility evaluation of solar water heater systems for low density residential areas with estimated water consumer profiles. • Results show that the payback time is onwards of eight years and exceeds the life cycle warranty period by three years.	SWH
Atikol U. and Aldabbagh L.B.Y. [38]	• Development and experimental analysis of exergy clearance and stand by time between discharging periods, tested for altering initial volume discharges. • More exergy efficient storage tank designs and strategies of operation can be of result when evaluating correlations.	ESTWH

Bagarella G., Lazzarin R., Noro M. [39]	• Model was simulated with summer and winter temperatures in order to evaluate the average efficiency of the setup throughout the year. • Small size HPWH connected in a parallel arrangement can increase energy savings by setting the cut-off temperature below the boiler temperature, whereas larger systems have no advantages applying this method.	HPWH
Benrejeb R., Helal O., Chaouachi B. [40]	• Parabolic dish concentrator coupled to an integrated collector storage system was designed in order to increase energy absorbed from solar irradiance. • Results showed higher temperatures obtained.	SWH
Benrejeb R., Helal O., Chaouachi B. [41]	• Truncated parabolic dish reflectors coupled to an integrated collector storage system was designed in order to increase energy absorbed from solar irradiance that could operate while insulation periods are low at acceptable thermal comfort levels. • Manufacturing costs will decrease with the proposed truncation. • Optimal thermal performance has been found.	SWH
Benrejeb R., Helal O., Chaouachi B. [42]	• Effect on optical and thermal performance of full parabolic concentrators was investigated when adding truncation. • Optical and thermal performances remained acceptable for domestic use.	SWH

Bleicher A. and Gross M. [43]	• Geothermal energy harvesting technologies caused reservations concerning environmental impacts and technical viability. • Decentralized geothermal energy sources are not ready-made and need to be modified in order to improve compatibility to the situation.	GTHPWH
Bourke G. and Bansal P. [44]	• Experimental analysis of the performance of in line gas boosters coupled to solar water heating systems. • Condensing gas booster has higher performance when used in conjunction with solar water heaters, however non-condensing gas boosters was found to lag behind.	Hybrid GFTWH/SWH
Bourke G. and Bansal P., Robert R. [45]	• Gas-fired tankless water heater was tested with regard to efficiency against several standards. • Results shows that there is significant difference between the different standards tested.	GFTWH
Bovand M. and Rashidi S., Esfahani J.A. [46]	• Porous solar water heater numerically investigated with focus on heat transfer and fluid flow. • Results show an increased Nusselt number when increasing the radiation parameters.	SWH
Browne M.C. and	• Performance of a photovoltaic thermal water heating system coupled with a phase-change material arrangement experimentally analysed.	Hybrid PVT/PCM

Norton B., McCormack S.J. [47]	• Temperature increase was observed with the phase change material in place rather than without.	
Calise F., d'Accadia M.D., Figaj R.D., Vanoli L. [48]	• Modelling of HPWH and absorption chiller mainly for air conditioning purposes supplied by PVT collectors and grid input. • Thermo-economic evaluation of a poly-generation system. • With incentive, the calculated system payback period is approximately eight years.	Hybrid PVT/HPWH
Carnevale E., Lombardi L., Zanchi L. [49]	• Life cycles of PV cells and SWH compared and evaluated. • Evaluation show that SWH scheme has longer life cycles than PV modules, these modules can have an improved life cycle score if recycled at the end of their respective life cycle.	SWH
Das D. and Basak T. [50]	• Modelling and optimization in discrete solar water heaters in favour of increased heating efficiency. • Triangular-type 2 enclosure casing has increased internal thermal mixing.	SWH
Del Col D., Azzolin M., Benassi G., Mantovan M. [51]	• Investigation of ground source heat pump water heater field data. • Maximized seasonal coefficient of performance of the HPWH is predicted.	GTHPWH

Deng W. and Yu J. [52]	• Investigation of performance of a hybrid solar and air source heat pump water heater. • Results show that higher performance is obtained when the amount incoming solar irradiance is low.	Hybrid SWH/HPWH
Deng Y., Zhao Y., Quan Z., Zhu T. [53]	• Experimental testing of a flat plate collector solar water heater with micro heat pipe arrangement packed closely for maximum solar irradiance absorption and surface area maximization. • Tested collector showed excellent thermal operation and heat absorption.	SWH
Der J.P., Kostiuk L.W., McDonald A.G. [54]	• Tankless water heater hybrid performance evaluated. • Results show that for thermal levels set at between 38°C and 60°C, efficiencies of approximately 90% for water demand of 7.6 litres/min. • Efficiency decreases with higher water demand.	ETWH
Devanaravan K. and Kalidasa Murugavel K. [55]	• Review of integrated solar collector storage water heater systems with the use of compound parabolic reflector developments. • Latest designs in the integrated solar collector storage water heaters shows good operating possibilities with the added benefit reliability for longer periods of time.	SWH

Gong J. and Sumathy K. [56]	• Evaluation and review of solar energy supplied water heaters and market their market potential. • Review indicates that solar water heaters have gained popularity across the world with a high market potential.	SWH
Zou D., Ma X., Liu X., Zheng P., Cai B., Huang J., Guo J. [57]	• Grey system theory used to predict energy consumed by a domestic heat pump water heater. • Investigation shows positive results from using the evaluated theory with high accuracy heat detection.	HPWH
Hafez A.Z., Attia A.M., Eltwab H.S., Elkousy .O., Afifi A.A., AbdElhamid A.G., [58]	• Survey of mathematical methods, design parameters and simulated models of the parabolic trough collector in several countries. • Results indicates that optical efficiency values are close to 63% and possible maximum optical efficiency can be at 75%	PTC
Hepbasli A. and Kalinci Y. [59]	• Review of HPWH, focusing on energetic and exergetic aspects was done. • Review showed that GEHP systems have gained efficiency in both space heating and water heating applications.	HPWH

Higgins A., McNamara C., Foliente G. [60]	• Forecast model was developed to predict the uptake of PV's and solar water heaters. • Considerable differences in the efficacy of different policy scenarios to increase the uptake of PV systems and solar water heaters was observed.	PV/TWH
Huang B.J., Wang J.H., Wu J.H., Yang P.E. [61]	• Fast response heat pump water heater with isolated dual storage tanks developed and experimentally analysed. • Acceptable for domestic operation, 50 litres of water with a temperature increase of 30 °C in 40 minutes was observed.	HPWH
Ibrahim O., Fardoun F., Younes R., Hasna L-G. [62]	• Model of a wind turbine, solar collector and battery storage system all serving as an energy supply to the heat pump water heater. • The model evaluation shows that the setup is feasible with savings incurred annually.	HPWH
Ibrahim O., Fardoun F., Younes R., Hasna L-G. [63]	• Review of most commonly used water heating setups. • Solar water heating systems and heat pump water heaters was observed to be most economically feasible.	WH
Johnson G. and Beausoleil Morrison I. [64]	• Modelling and verification of a gas fired water heating system. • Model predictions of energy consumption correlates with field data.	GTWH

Kato T. and Suzuoki Y. [65]	• Automatic heat pump switching control in order mitigate voltage spikes due to voltage generated from photovoltaic systems. • Controlled switching was successful in mitigation of voltage rises in the system.	HPWH
Keinath C.M. and Garimella S. [66]	• Cost and energy comparison regarding three different domestic water heating technologies. • Gas-fired heat pump water heaters have a payback period of around four years when compared to electric storage tank water heater. • Electric heat pump water heaters have a payback period of about 3.6 years.	ESTWH & GFTWH & HPWH
Keinath C.M., Garimella S., Garrabrant A.M. [67]	• Experimental analysis of Coefficient of Performance of a gas-fired heat pump water heater under different water and ambient temperature test conditions. • Performance was successfully predicted whereby the system uses a 227-liter storage tank. • Stand-by losses response was investigated.	GFHPWH
Kepplinger P., Huber G., Petrasch J. [68]	• Optimized linear model developed under one-way communicated incentives. • Up to 12% savings were observed when compared to normal operation.	ESTWH
Kepplinger P. and Huber G.,	• Experimental field testing of autonomous demand side management method of electric storage tank water heaters.	ESTWH

Petrasch J. [69]	• Results show that thermal mixing is improved in the triangular style 2 enclosure.	
Li K., Li T., Tao H., Pan Y., Zhang J. [70]	• Heat and flow transfer performance of SWH with elliptical collector arrangement were numerically investigated. • Results show that velocity measurements were not equal, while temperature distributions of the tube segments remained similar.	SWH
Li S., Li S., Zhang X. [71]	• Dual source heat pump water heater designed and performance was simulated with different refrigerants. • R744 refrigerant satisfied both energy saving and environmental requirements.	HPWH
Liu Z., Fan P., Wang Q., Chi Y., Zhao Z., Chi Y. [72]	• Development of an air source heat pump water heater in conjunction with a compressor casing thermal storage. • Hot water with a volume of 10 litres at a temperature of 30 °C was gained at the standard heating time of 2.5 hours.	HPWH
Michael J.J. and Iniyan S. [73]	• Thermal performance investigated experimentally of nanofluid (CuO/H_2O) prepared from $Cu(CH_3COO)_2$ on passive based indirect flat plate SWH. • Increased efficiency was noted with an increased laminar flow to turbulent flow, performance was increased when using	SWH

	nanofluid in thermosiphon circulation test condition.	
Milani D. and Abbas A. [74]	• Examination of the heat capture rate of a diffuse flat reflector fixed to the back of an evacuated tube collector system. • Overall increase of 85.53% of annual energy savings was noted.	SWH
Moreau A. [75]	• Triple reduction of the grid's peak demand when applying control algorithm. • Minimizes pick-up demand during the initial stages of the on cycle of a resistive element whilst ensuring the consumers hot water supply.	ESTWH
Murali G., Mayilsamy K. [76]	• Evaluation of performance of a SWH with multiple inlet locations under discharge. • Results indicates that hot water availability has been maintained for longer periods of time.	SWH
Paull L., Li H., Chang L. [77]	• Multi-objective energy management model of an electric storage tank water heater was evaluated. • Accurate prediction of peak demand usage, peak shaving can be maximized with little effect to user's thermal comfort level.	ESTWH
Peng J., Li H., Zhang C.L. [78]	• Development and validation of a Quasi-steady-state model of a HPWH with an electronic expansion valve, a shortened tube orifice and thin internal diameter tube as expansion devices.	HPWH

	• Results indicate that shortened tube orifice was an appropriate fit to the heat pump water heater with the most benefits.	
Qu M. and Chen J. [79]	• Dual source HPWH was analysed with emphasis on one of the sources which was the solar PVT water heater. • Efficient operation was noted.	Hybrid PVT/HPWH
Saravanan A. and Senthkumaar J.S. [80]	• Experimental analysis comparing Nusselt numbers of V-trough SWH with helix shaped tape, square cut helix tape, V-cut helix tape in identical operational conditions. • Comparisons show that V-cut helix has a Nussalt number of 9.13% higher than helix, and V-cut has a Nusselt number of 3.08% higher than square cut.	SWH
Sathyamurthy R. and Harris Samuel D.G [81]	• Baffled parabolic trough solar collector water heater was designed to improve hot water output. • The percentage increase in outlet temperature is directly proportional to the amount of incoming solar irradiance.	PTC
Scarpa F., Tagliafico L.A., Bianco V. [82]	• Optimal operation conditions and appropriate design parameters with minimisation of non-renewable energy usage for hybrid gas/solar heat pump water heater discussed. • Suitable approach taken in line with regulation and design requirements.	Hybrid GFWH/SWH/HPWH

Shan F., Cao L., Fang G. [83]	• Modelling and evaluation of a PVT water heating system. • Results showed that reduced series-connected PVT arrangements, low inlet water temperature at increased flow rate resulted in higher efficiency.	PV/TWH
Sheng X.H. [84]	• Experimental evaluation on a SWH in conjunction with phase-change energy storage. • Comparison of performance between phase-change energy storage collector and evacuated tube direct heating system. • Phase-change SWH performs less efficiently than the evacuated tube system under exposure for same collector area.	Hybrid SWH/ESTWH
Sichialu S.M. Xia X. Zhang J. [85]	• Optimized switching strategy for a multi-source (grid connection and photovoltaic) heat pump water heater. • Short payback period for PV module was noted, while a 41.5% energy savings was observed, however in winter periods, the heat pump could not supply enough thermal energy to meet the demand.	HPWH
Sichialu and Xia S.M. X. [86]	• Optimized switching strategy for a multi-source (grid connection, photovoltaic and battery source) heat pump water heater. • A 52.5% energy savings was observed.	HPWH

Sichialu and Xia [87] S.M. X.	• Optimized switching strategy for a multi-source (diesel generator, photovoltaic and battery source) heat pump water heater. • A 68.09% energy savings was observed.	HPWH
Sichilalu Mathaba Xia [88] S., T., X.	• HPWH supplied by multiple sources (wind generation, photovoltaic and grid connection) optimization control modelling. • Cost saving of approximately 70.74% on daily basis.	HPWH
Sichilalu Tazvinga Xia [89] S., H., X.	• Optimized energy usage of a multi energy source (wind, fuel cell, photovoltaic, electrical grid input) heat pump water heater model. • A maximum cost saving of 33.8% was reached in simulation, acceptable heat pump hot water temperature level was reached and energy saving of 27.68% was obtained.	HPWH
Singh Lazarus Souliotis [90] R., I.J., M.	• Review of several solar collector systems with phase change materials and heat retaining properties. • Heat loss reduction strategies for colder periods, thermal performance and respective design characteristics were reviewed.	SWH
Tang Cheng Wu Li Yu [91] R., Y., M., Z., Y.	• Flat plate passive circulation solar collectors with and without solar selective absorbers were tested in order to obtain data about ability to withstand freezing temperatures. • Non-solar selective absorber type collectors may suffer from damage due to temperatures	SWH

	below 0 °C, while solar selective absorbers have a reduced chance of damage due to freezing temperatures.	
Tang R. and Cheng Y. [92]	• Experimental investigation on evacuated tube solar collector with direct heating in order to measure reverse flow and heat loss during night time. • Increased reverse flow was observed at night time, reverse flow caused mainly by collector tilt angle rather than atmospheric disturbances. Low heat losses during the night was observed.	SWH
Tanha K. and Fung A.S. [93]	• Experimental analysis on drained water heat recovery on FPC and ETC setups. • Flat plate solar collector produces approx. half the energy that an evacuated tube solar collector with the same area produced annually.	SWH
Tinti F., Barbaresi A., Torreggiani D., Brunelli D., Ferrari M. et al. [94]	• Experimental thermal response test done on geothermal source. Smart control implementation on hybrid ground/air source heat pump water heater. • Testing confirmed that increased efficiency was obtained with the hybrid heat pump system.	GTHPWH

Tsai H-L. [95]	• Model developed of a heat pump water heater being supplied by thermal and electrical energy from a PVT collector. • Model results shows increased accuracy and adequate confidence.	Hybrid PVT/HPWH
Tse K. and Chow T. [96]	• Indirectly heated, natural flow solar water heating setup with a cylindrical tube ring arrangement as heat exchanger was designed and analysed. • The new design had improved performance when compared to helical coil as heat exchanger setups.	SWH
Wang P., Li S., Liu Z. [97]	• A larger application based evacuated tube solar air heater in conjunction with a compact compound parabolic reflector with a concentric heat exchanger was developed to provide high temperature air flow for water heating purposes. • Thermal efficiency was noted to be 52% with an air temperature of 70 °C and 35% at a temperature of 150 °C. Efficiencies decline with higher air temperatures.	SWH
Wanjiru E.M., Sichilalu S.M., Xia X. [98]	• Optimized control of a heat pump and instantaneous water heaters supplied by integrated energy systems. • Optimized model shows that 7.5 kWh can be sold to the grid, while energy costs can be reduced by 19% daily.	HPWH

Willem H., Lin Y., Lekov A. [99]	• Survey of heat pump water heaters in terms of performance and system efficiency. • Increased Coefficient of Performance (COP) of 2.8 to 5.5 can be observed with new technological advances. • The survey identifies and recommends key focus areas for future work in order to boost COP numbers.	HPWH
Wilson Jr. R.P. [100]	• Conservation of energy discussion for both gas tankless water heaters and electric storage tank water heaters. • Both water heating systems can have reduced energy usage as a result when looking at global figures especially with recent advances in these respective technologies.	GFTWH and ESTWH
Xiaowu W. and Ben H. [101]	• Exergy usage and loss management and minimization for cost saving purposes for solar water heater. • High amounts of exergy losses occur in the storage tank, careful consideration in the design of the tank should be taken in order to improve exergy efficiency.	SWH
Yan C., Wang S., Ma Z., Shi W. [102]	• Development of an optimal design method regarding tank volume and collector area of a SWH system. • The storage tank size is highly dependent on the collector area, while the collector area	SWH

	optimization is not affected significantly by the tank size.	
Yang L., Yuan H., Peng J.W., Zhang C.L. [103]	• Development and validation of a domestic heat pump water heater model with the performance of off-design components in mind. • Using experimental data from literature, it was deduced that the heat pump performance was competitive in cold weather.	HPWH
Ziapour B.M. and Palideh V. [104]	• An integrated solar collector system combined with a photovoltaic cell was modelled in order to observe the change in PVT power conversion efficiency. • An increased area of the collector has a decreased system efficiency as a result.	PV/TWH
Zou B. and Dong J. [105]	• A proposed compact parabolic trough collector for heating water in colder areas was tested to verify if a viable solution to shortcomings of conventional solar collectors could be found. • The parabolic trough collector had acceptable operation in cold testing conditions with exceptional anti-freezing properties.	PTC

2.3 DISCUSSION

2.3.1 Key results and findings

After reviewing the research studies linked to domestic water heating technologies, it is evident that a wide spectrum of hybrid arrangements has emerged. These hybrid systems can consist of two or more water heating technologies. Consequently, higher energy and cost savings are observed in domestic households. Table 2.2 presents some advantages, drawbacks, approximate installation cost and life expectancy. This information gives an indication on which technologies are most suited for a specific case in South Africa.

Table 2.2: Techno-economic comparison of water heating technologies.

Technology	Specific comments applicable to the South African case	Approximate install cost (ZAR)	Average Life Expectancy (years)
Electric storage tank water heater	• Hot water always available • Large amount of non-renewable energy required to heat water • High LCC • Standby losses due to tank	2584 – 4000	5 - 10
Electric tankless water heater.	• Hot water always available • High energy consumption • Compact • No standby losses • Medium LCC	2799 – 4800	5 - 8

Solar water heater	• Hot water available only during the day • Consumes renewable energy (free) • High standby losses during night time • Low LCC	7000 – 11 598	5 - 20
Heat-pump water heater	• Hot water availability limited to warmer months • Consumes less electrical energy when compared to ESTWH and ETWH • Medium LCC • Standby losses due to tank	12000 – 18762	5 - 8
Gas fired tankless water heater	• Hot water always available • Consumes significant amount of non-renewable energy • Compact • No standby losses • High LCC	3984 – 5597	6 - 8
Geothermal water heating (springs)	• Hot water always available • Limited hot spring locations • Uses small amount of electrical energy (pump) • Low LCC	N/A (Method of hot water transport cost may vary)	N/A (Depends on pumping system)

	• Heat losses through extended pipes		
Hybrid Photovoltaic/Thermal (PVT) water heater	• Hot water only available during the day • Only small amounts of water can be (limited to cell area) • Low retro fitment cost • Low LCC • Increases power efficiency of the PV cell • Standby losses during night	10 000 + (180W panel and copper piping)	10 - 15
Hybrid heat pump gas fired water heater	• Hot water always available • Large amount of energy required. • Complicated system • High LCC • Standby losses due to tank	15984 – 24359	5 - 8
Hybrid solar electric water heater with evacuated tube collector (indirect system)	• Hot water always available • More efficient solar energy conversion than FPC HSWH • Uses renewable energy as its primary energy source • Medium LCC • Standby losses due to tank	15170 – 18 000	5 - 20

Hybrid solar electric water heater with flat plate collector (direct/indirect)	• Hot water always available • Less efficient energy conversion than FPC-HSWH • Uses renewable energy as its primary energy source • Lower LCC compared to ETC/ESTWH • Standby losses due to tank	11100 - 14710	5 - 20
Hybrid geothermal heat pump water heater	• Hot water always available • More efficient than standalone HPWH • Bulky • High Initial install cost • Medium LCC • Standby losses due to tank	12000 – 18762 (with an additional 7000 for underground heat exchanging conduits)	5 - 8

2.3.2 Impact of water heating systems on South African energy efficiency program

The idea of using hybrid water heating systems in South Africa has become increasingly popular in recent years. This is mainly due to its ability to shave off significant energy costs and high reliability [106]. Rebates and incentives from the government have played a key role in the rise of renewable energy system implementation in the country. This is not only good news for the consumer, but also for the electricity supplier, Eskom. Eskom mentions that saving 1000 kWh can reduce carbon dioxide production by 990 tons, which translates into a saving of 60 kilotons of carbon dioxide released in the air annually [107]. However, with the increasing population the demand will soon exceed the generating capacity. Eskom has had some problems in the past with meeting electrical demand.

Innovative ways of saving energy is needed more than ever to save the electrical grid from total shutdown. Furthermore, price hikes approved by NERSA have recently dampened the mood of many South Africans. Statistics show that approximately 54% of South Africa's population lives under the poverty line making it hard to withstand all the price hikes that the electricity supplier has recently announced [108].

In addition, a large number of South Africans live with the human immunodeficiency virus (HIV), which makes it easier for opportunistic diseases i.e. legionnaires disease to be contracted. Legionnaire's disease is caused by Legionella Pneumophila bacteria commonly located in water. In order to eliminate these bacteria, the water needs to be heated to at least 60 ºC once per day according to the World Health Organization (WHO) [109, 110]. The South African populous needs to be educated in the importance of hygiene and saving energy, not only to save money, but more importantly to secure a future with a pollution free environment.

2.4 SUMMARY

Conventional water heaters can consume as much as half of the total energy used by a traditional household. This high consumption of energy is mainly due to inefficient and outdated electric storage tank water heating technologies, combined with lack of energy efficient activities. Research and development on new, more energy efficient water heating technologies has been done surrounding most aspects associated with energy management and design. Furthermore, heat loss reduction and optimization studies have also brought significant changes to energy consumption and load management of these water heating systems.

This chapter presented a survey of improvements and research done on most common water heating methods. These technologies include electric water heaters, solar water heaters (passive and active systems), heat pump water heater, geothermal water heaters, photo-voltaic/thermal water heater and the gas-fired tankless water heater. An increased reliability

and the potential to lower energy costs was observed for hybrid systems if these systems are combined in such a way that they could function independently.

The feasibility, cost effectiveness and life expectancy of each technology was discussed. Drawbacks and benefits have been outlined for clear comparison between the different methods. The solar water heater (SWH) coupled with an electric storage tank water heater (ESTWH) was shown to be the most viable. This viability is based on hot water availability and cost saving being the top concern for consumers. The flat plate collector type is approximately 30% less costly to install than the evacuated tube collector. Furthermore, studies suggest that more than enough solar energy is captured to maintain a comfortable temperature level, even with a 30% less efficient heat absorbance factor compared to the ETC. In addition, the evacuated tube collector array system is more expensive to replace in the event of damage caused by hail, whereas only the glass pane over the flat plate collector need be replaced at a minimal cost for the same instance.

The impact resistance of glass covers for the FPC system have improved in recent years with the advent of superior glass hardening techniques. This in turn reduces the probability of hail damage to the collector cover. The only major drawback of the flat plate collector is lower frost resistance in colder climates. This is especially true for the direct collector systems. In retrospect, the indirect FPC coupled to an existing or new ESTWH is proposed for the South African case with the country's climate taken into consideration. The amount of solar radiation the country receives makes it an ideal water heater system for all provinces.

Low-income households can benefit from Eskom rebates to implement these systems. The ESTWH part can assist in the prevention of infection by heating water to 60 °C daily.

The consumers should be able to implement a system that suits their geographical and hot water needs with the suitable financial support from the governing body in order to reduce the use and dependency on fossil fuels.

Energy efficient systems with applicable knowledge of the advantages these systems might offer can decrease the severity of the energy crisis that South Africa is facing. This will, in turn, allow South Africans to improve their financial condition.

CHAPTER III: OPTIMAL ENERGY MANAGEMENT OF THE HYBRID SOLAR/ELECTRIC WATER HEATER AND ALGORITHM FORMULATION

3.1 INTRODUCTION

In this chapter, the mathematical modelling of the operation of the hybrid solar/electrical water heater system is discussed. The hybrid system consists of an indirect flat plate collector coupled to an existing electric storage tank water heater. The electric storage tank is located inside the residential building's roof space, while the solar collector is fitted on the roof close to the storage tank.

The model is developed and presented with the aim to minimize costs, taking into account the time-of-use tariff, while maintaining the desired water temperature inside the ESTWH.

The relevant components are discussed in Section 3.2. The optimal energy management model formulation and constraints are discussed in Section 3.3. Section 3.4 presents the summary of the chapter.

3.2 MATHEMATICAL MODEL FORMULATION

The proposed hybrid system consists of an electric storage tank water heater and an indirect flat plate solar collector in Figs. 3.1 and 3.2. The solar collector is accompanied by a circulation pump to aid in the flow of water through the system. The layout of this system is illustrated in Fig. 3.2. The mathematical models of the different components in the system in terms of heat and electrical energy is presented.

3.2.1 Dynamic model of the hybrid solar/electric water heating system

All factors with regards to the operation of the proposed hybrid water heater needs to be taken into consideration if a mathematical model is to be developed.

To start with, referring to Fig. 3.1, the cold water is supplied from the mains and enters the thermal storage tank. It can be considered that large degrees of thermal stratification occur due to natural convection. This natural convection is the process whereby cold water displaces hot rising water. Higher density cold water can therefore be assumed to be located at the bottom of the storage tank and the lower density hot water would be situated at the top. Hence, for modelling purposes, cold water is supplied by the storage tank to the collector.

The supply outlet as illustrated in Fig. 3.1 is located at the bottom of the storage tank water heater. With this in mind, it can be assumed that the temperature of the water supplied to the storage tank is equal to the temperature of the water supplied to the collector. A similar assumption can be made that the temperature of water from the solar collector outlet is equal to the temperature of the water supplied to the hot water user [111].

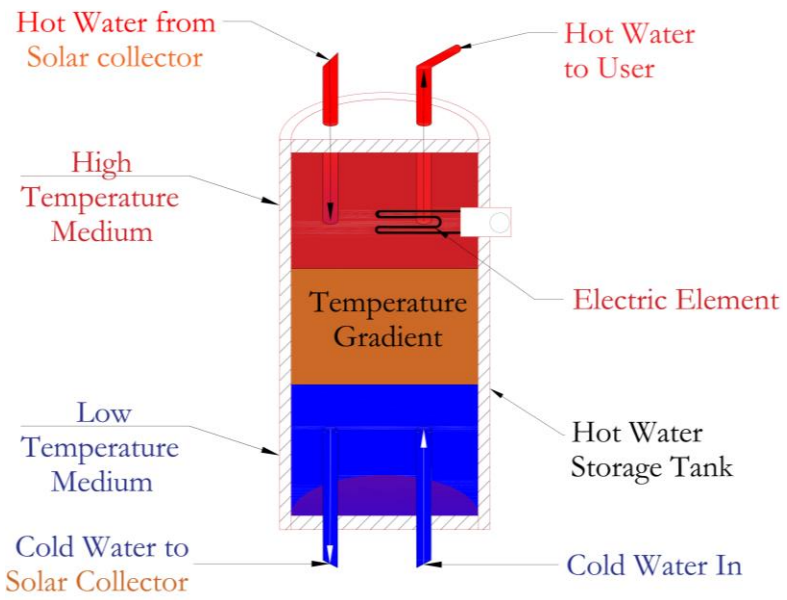

Figure 3.1: Hot water storage tank with thermal stratification

In Fig. 3.2, the complete water heating system is illustrated, which includes an indirect flat plat collector (FPC) with a heat exchanger located inside the collector. The FPC is coupled to an electric storage tank water heater with a single water heating element. The circulation pump for the collector arrangement operates automatically and can be seen as an independent system. The pump is controlled by a temperature differential control circuit. This control circuit monitors the temperature difference between the cold water inlet and hot water outlet of the collector. When the temperature difference reaches a certain value, the circulation pump is switched on. This system ensures that when solar irradiance is absent or insufficient, the pump will remain off so that cold water is not continuously being circulated through the storage tank. This is necessary to prevent a decrease of the thermal level of the water supplied to the consumer.

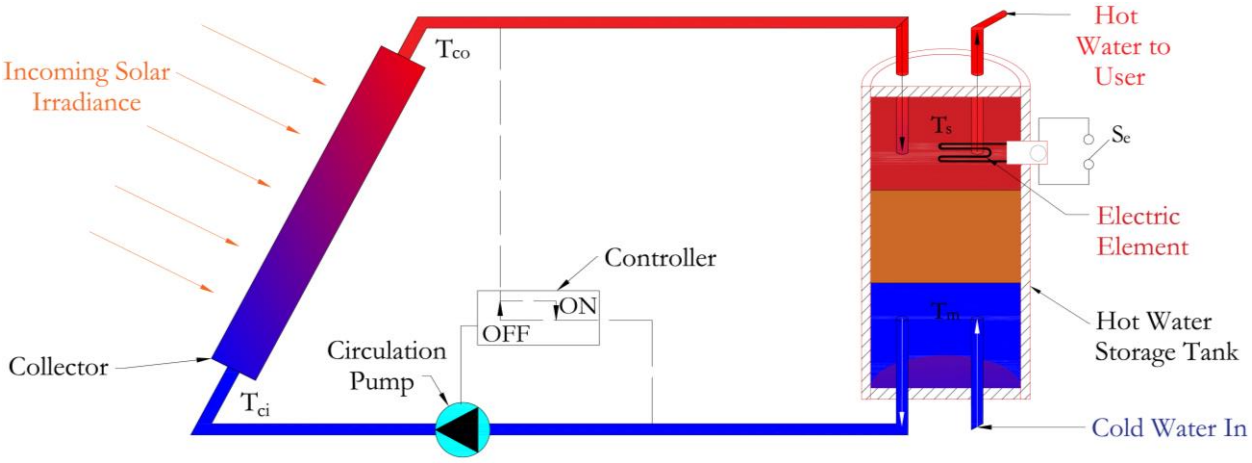

Figure 3.2: SWH/ESTWH system layout

All thermal gains and losses in the system are calculated in order to form an energy balance equation. The energy gain calculations are discussed followed by the losses in the system. In order to calculate the primary energy gain (energy gained from solar irradiance), all input variables have to be found as well as their coefficients.

The electrically supplied water heating system serves as an auxiliary heater to increase hot water availability. Therefore, if the solar energy supply is ineffective to heat water, the electric resistive element will switch on. The solar thermal energy is dependent on several factors. These factors include time of year (season), weather and time of day.

The difference in temperature between the cold and hot water supplied to and from the collector can be calculated by obtaining the heat energy gained by the collector shown in Eq. (3.1). The heat gain, therefore can be calculated in terms of the temperature differential of the water between the collector inlet and outlet as follows [112]:

$$Q_{coll} = m_c(t)c(T_{co}(t) - T_{ci}(t)) \tag{3.1}$$

Where:

Q_{coll} is the heat gained by the collector (J),

$m_c(t)$ is the variable flow rate of the water inside the collector (kg/h),

C is the heat capacity of the water inside the collector (4184 J/kg.°C),

$T_{co}(t)$ is the variable collector water output temperature (°C),

$T_{ci}(t)$ is the variable collector water input temperature (°C),

Due to large degrees of thermal stratification, $T_{ci}(t)$ is considered to be equal to the inlet water temperature ($T_m(t)$), this gives Eq. (3.2):

$$Q_{coll} = m_c(t)c(T_{co}(t) - T_m(t)) \tag{3.2}$$

Similarly, the heat gain can be calculated in terms of solar irradiance absorbed by the collector. The total hourly solar radiation absorbed by the collector can be evaluated using the isotropic diffuse model in Eq. (3.3) [113, 114].

$$G(t) = G_{DNI}\cos\theta_\beta + G_{DHI}\left[\frac{1+\cos(\beta_{coll})}{2}\right] + G_{GHI}\rho_g\left[\frac{1-\cos(\beta_{coll})}{2}\right] \tag{3.3}$$

Where:

$G(t)$ is the variable total hourly solar radiation on a tilted collector (W/m^2),

G_{DNI} is the horizontal beam radiation (W/m^2),

G_{DHI} is the horizontal diffuse radiation (W/m^2),

G_{GHI} is the horizontal global radiation (W/m^2),

θ_β is the incidence angle on a titled surface (°),

β_{coll} is the slope of the collector array (°),

ρ_g is the ground reflectance factor.

The total hourly solar irradiation can then be used in Eq. (3.4) [114, 115],

$$Q_{coll} = A_c[F_R(\tau\alpha)G(t)t_{(h)} - F_R U_L(T_{co}(t) - T_m(t))] \quad (3.4)$$

Where:

A_c is the area of the collector (m^2),

F_R is the collector heat removal factor,

$\tau\alpha$ is the transmittance absorbance product,

$G(t)$ is the variable global solar irradiance absorbed by the collector (W/m^2),

$t_{(h)}$ is the time ($3600\,s$),

U_L is the collector overall heat transfer coefficient ($W/m^2.°C$),

$T_a(t)$ is the variable ambient temperature ($°C$).

The collector heat gain equations (Eq. (3.1) and Eq. (3.4)) are equated to yield Eq. (3.5) as,

$$m_c(t)c(T_{co}(t) - T_m(t)) = A_c[F_R(\tau\alpha)G(t)t_{(h)} - F_R U_L(T_{co}(t) - T_m(t))] \quad (3.5)$$

The temperature difference between the hot water out and the cold water in $(T_{co}(t)-T_m(t))$ of the collector after heat exchanger action has taken place, can then be calculated in Eq. (3.6):

$$(T_{co}(t)-T_m(t))=\left[\frac{A_s(F_R(\tau\alpha)G(t)t_{(h)})}{m_c(t)c+A_cF_RU_L}\right] \tag{3.6}$$

The new collector heat gain can therefore be calculated as in Eq. (3.7)

So that,

$$Q_{coll}=\left[\frac{A_s(F_R(\tau\alpha)G(t)t_{(h)})m_c(t)c}{m_c(t)c+A_cF_RU_L}\right] \tag{3.7}$$

Referring to Fig. 3.2, the secondary heat gain ($Q_{EL}(t)$)can be calculated as shown in Eq. (3.8), adapted from [114]. The power supplied to the electric resistive element remains constant. Full rated power is supplied to the electric element when it is switched on and no power is supplied when it is switched off.

$$Q_{EL}(t)=P_{EL}t_{(h)}S_e(t) \tag{3.8}$$

Where:

$Q_{EL}(t)$ is the variable heat gain from the electric resistive element (J),

P_{EL} is the full rated power supplied to the element (W),

$t_{(h)}$ is the time ($3600\,s$),

$S_e(t)$ is the variable switching status of electric resistive electric element.

The energy losses due to hot water demand ($Q_D(t)$) and convectional (standby) loss ($Q_L(t)$) can be calculated using Eq. (3.9) and (3.10) respectively.

The standby losses, Q_L, represent power losses through the casing material surface conduction [114].

$$Q_L(t) = U_s t_{(h)} A_s (T_s(t) - T_a(t)) \tag{3.9}$$

Where:

U_s is the heat loss coefficient of a storage tank ($W/m^2.°C$),

A_s is the area of the storage tank (m^2),

$t_{(h)}$ is the time (3600s),

$T_s(t)$ is the variable temperature of the water inside the storage tank ($°C$),

$T_a(t)$ is the variable ambient temperature of the surrounding air ($°C$).

The hot water demand loss ($Q_D(t)$) occurs when hot water is drawn by the consumer. Consequently, every time hot water is required, the hot water demand flow rate is initiated and $T_s(t)$ drops due to cold water flowing into tank. The cold water flows into the tank in order to keep a constant volume. Losses due to the hot water demand are given in Eq. (3.10), [116].

$$Q_D(t) = cW_D(t)(T_s(t) - T_m(t)) \tag{3.10}$$

Where:

c is the heat capacity of water ($4184 J/kg/°C$),

$W_D(t)$ is the variable hot water demand flow rate (kg/h),

$T_m(t)$ is the variable temperature of the inlet water ($°C$).

The energy balance equation is described in terms of all the heat gains and losses in the system, given in Eq. (3.11).

$$M_s c \dot{T}_s = Q_{coll} + Q_{EL} - Q_L - Q_D \tag{3.11}$$

Where:

M_s is the water mass inside the storage tank (kg),

C is the heat capacity of water ($4184 J/kg/°C$),

$\dot{T}_s$ is the derivative of the temperature variation of the water inside the storage tank ($°C$).

By substituting Eq. (3.7) -(3.10) into Eq. (3.11), $M_s c_s \dot{T}_s$, can be presented in Eq. (3.12):

$$M_s c \dot{T}_s = \left[\frac{A_s(F_R(\tau\alpha)G(t)t_{(h)})m_c(t)c}{m_c(t)c + A_c F_R U_L}\right] + S_e Q_{EL} - cW_D(t)(T_s(t) - T_m(t)) - A_s U_s t_{(h)}(T_s(t) - T_a(t)) \tag{3.12}$$

For the sake of simplicity, $\left[\frac{A_s(F_R(\tau\alpha)G(t)t_{(h)})m_c(t)c}{m_c(t)c + A_c F_R U_L}\right]$ in Eq. (3.12) is replaced with $Y(t)$ in Eq. (3.13).

$$M_s c \dot{T}_s = Y(t) + S_e Q_{EL} - cW_D(t)(T_s(t) - T_m(t)) - A_s U_s t_{(h)}(T_s(t) - T_a(t)) \tag{3.13}$$

$\dot{T}_s$ is made the subject of the formula in Eq. (3.14).

$$\dot{T}_s = \frac{Y(t)}{M_s c} + \frac{S_e Q_{EL}}{M_s c} + \frac{cW_D(t) + A_s U_s t_{(h)}}{M_s c}(T_s(t)) + \frac{cW_D(t)T_m(t)}{M_s c} + \frac{A_s U_s t_{(h)} T_a(t)}{M_s c} \tag{3.14}$$

Eq. (3.14) is divided into the separate components, shown in Eq. 3.15 – 3.18, so that a state space equation is formulated. The state space equation is converted so that the temperature of the water inside the storage tank (state variable) is made the subject of the formula, denoting [116]:

$$A(t) = \frac{cW_D(t) + A_s U_s t_{(h)}}{M_s c} \tag{3.15}$$

$$B = \frac{Q_{EL}}{M_s c} \tag{3.16}$$

$$\gamma(t) = \frac{cW_D(t)T_m(t)}{M_s c} + \frac{A_s U_s t_{(h)} T_a(t)}{M_s c} + \frac{Y(t)}{M_s c} \tag{3.17}$$

$$\dot{T}_s = -A(t)T_s(t) + BS_e(t) + \gamma(t) \tag{3.18}$$

In the state space given by equations (3.14)–(3.17), the control or decision variable is $S_e(t)$, while the state variable is $\dot{T}_s$ and the disturbance variable in the system is $\gamma(t)$ shown in Eq. (3.18).

3.2.2 Discretized hot water temperature

Eq. (3.18) is a continuous function and needs to be transferred into a general discrete formulation in terms of the k^{th} hot water function. The forward Euler method was used in order to find the general discreet equation. This equation assists in the visualisation of the temperature variation inside the storage tank at any time interval:

$$T_{k+1} = T_k(1 - t_s A_k) + t_s BS_{e_k} + t_s \gamma_k \tag{3.19}$$

T_k in Eq. (3.19) is the temperature variation inside the storage tank.

Since the state variable, T_{k+1} has to be expressed in terms of its initial value, T_0 and the control variable, S_{e_k}, T_{k+1} at each interval is first derived as:

When substituting $k = 0$, then T_1 in Eq. (3.19) becomes Eq. (3.20):

$$T_1 = T_0(1 - t_s A_0) + t_s BS_{e_0} + t_s \gamma_0 \tag{3.20}$$

Similarly, when $k = 1$, then T_2 is given in Eq. (3.21):

$$T_2 = T_1(1-t_sA_1) + t_sBS_{e_1} + t_s\gamma_1 \tag{3.21}$$

Substitute T_1 in Eq. (3.20) into Eq. (3.21) so that Eq. (3.22):

$$T_2 = [T_0(1-t_sA_1) + t_sBS_{e_0} + t_s\gamma_0](1-t_sA_1) + t_sBS_{e_1} + t_s\gamma_1 \tag{3.22}$$

After expansion and factorization, T_2 will become Eq. (3.23):

$$T_2 = T_0[(1-t_sA_0)(1-t_sA_1)] + t_sB[(1-t_sA_1)S_{e_0} + S_{e_1}] + t_s[(1-t_sA_1)\gamma_0 + \gamma_1] \tag{3.23}$$

Following the same steps taken for Eq. (3.20) - (3.23) after $k=2$, T_3 will then become Eq. (3.24):

$$T_3 = [(1-t_sA_0)(1-t_sA_1)(1-t_sA_2)] + t_sB[(1-t_sA_1)(1-t_sA_2)S_{e_0} + (1-t_sA_2)S_{e_1} + S_{e_2}] + t_s[(1+t_sA_1)(1+t_sA_2)\gamma_1 + \gamma_2] \tag{3.24}$$

.

.

.

$$T_{(k+1)} = T_0\prod_{j=0}^{k}(1-t_sA_j) + t_sB\sum_{j=0}^{k}S_{e_j}\prod_{i=j+1}^{k}(1-t_sA_i) + t_s\sum_{j=0}^{k}\gamma_j\prod_{j=i+1}^{k}(1-t_sA_i) \tag{3.25}$$

Where:

T_0 and T_k are the initial and k-th water temperatures inside the tank respectively ($°C$),

t_s is the sampling time (s),

S_{e_j} is the switching status with a single binary value (1 to represent the ON status and 0 indicates an OFF status).

3.3 CONTROL OPTIMIZATION PROBLEM

3.3.1 Algorithm formulation

- Operation cost minimisation

The primary objective is to minimize the cost of energy supplied to the electric resistive element. In order to accomplish this, most of control switching-on needs to take place in off-peak periods. When switching on during off-peak periods, the cost of electrical energy will be significantly reduced. The Eskom 2017/2018 TOU tariff periods [117] are represented by Fig. 3.3.

Figure 3.3: Time-of-Use Periods [117]

The tariff circle chart on the left represents the TOU tariff periods of the low demand season, whereas the circle chart on the right denotes the periods of the high demand season.

The low demand season is from September to May, while the high demand season starts in June and ends in August. The winter season peak period starts an hour earlier than the summer season. This can be accredited to increased energy requirement to heat water to the desired temperature and the usage of other high energy consumption appliances such as space heaters.

The TOU tariff structure forms a substantial part of the primary objective function and is derived in Eq. (3.26) which is the electricity cost J_p minimization [118]. The switching function "S_{e_k}" is therefore highly dependent on the TOU tariff.

$$J_p = t_s \sum_{k=1}^{N} P_{EL} p_k S_{e_k} \tag{3.26}$$

Where:

t_s is the sampling time (hours),

p_k is the TOU tariff function (R/kWh),

P_{EL} is the rated power of the electric resistive element (kW),

S_{e_k} is the switching status function of the element.

- Thermal discomfort level minimisation

The level of thermal discomfort can be defined by the experience of the user once the temperature levels of the hot water are above or below the desired temperature. The discomfort level is reduced or minimized when the thermal level reaches the desired hot water temperature. The secondary objective therefore becomes the minimization of thermal discomfort experienced by the user. In order to know when the desired temperature needs to be reached, a user specific load profile is evaluated. The load profile is a continuous function represented by $F(t)$ and denotes the desired hot water temperature of the user. $\boldsymbol{T_s(t)}$ is the temperature of the water inside the storage tank and needs to be close or equal to the desired temperature at the time when hot water is required.

In other words, the difference between $F(t)$ and $\boldsymbol{T_s(t)}$ needs to be as small as possible at the precise time when hot water is usually drawn. Thus, the difference in temperature $(\boldsymbol{T_s(t) - F(t)})^2$ will be minimized [119].

The secondary objective function, J_s, is shown in Eq. (3.27).

$$\text{Min } J_s = \int_{t_0}^{t_f} (T_s(t) - F(t))^2 dt \tag{3.27}$$

Where :

t_0 is the initial sampling interval at $T_s(t) = T_s(t_0)$ (initial temperature)

t_f is the final sampling interval at $T_s(t) = T_s(t_f)$ (final temperature)

- Fixed-final state condition

In order to simulate continuous operation and repeated implementation of the optimal energy control strategy for the hybrid system, the thermal energy stored in the storage tank at the end of the control horizon should be equal to the thermal energy at the beginning of the control horizon. Therefore, the sum of all the energy gained should be equal to all the energy lost in the system for the respective control horizon. This is represented in Eq. (3.28). The final temperature ($T(t_f)$) in the last sampling interval should thus be equal to the initial temperature ($T(t_0)$) of the water inside the storage tank at the initial sampling interval of the control horizon.

$$\sum_{k=1}^{N} (Q_{s_k}) = 0 \tag{3.28}$$

This can be achieved by minimizing the difference between the actual final temperature and the desired final temperature, which is equal to the initial temperature of the water inside the storage tank. The same method used to minimize the discomfort level of the user can be applied for this instance, as shown in Eq. (3.29). In this case, the difference between the final and initial temperature is minimized, so that Eq. (3.29) forms part of the final objective function.

$$J_t = \int_{t_0}^{t_f} (T(t_f) - T(t_0))^2 \tag{3.29}$$

- Operation cost and discomfort level minimization

In order to minimize the operational cost of the solar water heater while maintaining the thermal comfort level of the user, the primary, secondary and tertiary objective functions need to be added as in Eq. (3.30).

$$\text{Min } \boldsymbol{J} = \boldsymbol{J}_p + \boldsymbol{J}_s + \boldsymbol{J}_t \tag{3.30}$$

The aggregate objective function needs to be represented in discreet-time domain. Eqs. (3.27) and (3.29) is converted from continuous-time domain to discreet-time domain and substituted into Eq. (3.30), Eq. (3.26) does not need to be converted and is substituted without alteration, so that one gets Eq. (3.31):

$$\text{Min J} = w_1(t_s \sum_{k=1}^{N} P_{EL_k} p_k S_{e_k}) + w_2(ts \sum_{k=1}^{N} (T_k - F_k)^2 + ts \sum_{k=1}^{N} (T_N - T_0)^2) \tag{3.31}$$

Where:

w_1 is the weighting factor for energy cost,

w_2 is the weighting factor for comfort level,

J is the aggregated objective function to be minimized.

- Constraint on the state of temperature inside the storage tank

The desired temperature when evaluating the load profile should be between 55 °C and 65 °C at 06:30 in the morning and at 20:00 in the evening, while from 07:00 to 20:00, the

temperature should be maintained at 60 °C. The temperature can fluctuate without any constraints in the remaining hours of the day. For repeated operation, the final temperature in the control horizon should be equal to the initial temperature. Eq. (3.32) shows the temperature requirements throughout a 24-hour control horizon.

$$F(t)=\begin{cases} T_s(t), t\in[00h00, 06h00)\cup[20h30, 24h00) \\ 60, t\in[06h30]\cup[20h00] \\ T_0(t_0), t\in[24h00] \end{cases} \tag{3.32}$$

Where:

$F(t)$ is the desired temperature function,

And, $T_s(t)=T_0\prod_{j=0}^{k}(1-t_sA_j)+t_sB\sum_{j=0}^{k}S_{e_j}\prod_{i=j+1}^{k}(1-t_sA_i)+t_s\sum_{j=0}^{k}\gamma_j\prod_{j=i+1}^{k}(1-t_sA_i)$ (3.33)

The switching function, S_{e_k}, which is the function which describes how the electric element will switch on or off, either full rated power or no power is delivered, respectively. This means that the switching status can only be a single binary value as illustrated in Eq. (3.34). The constraint on the temperature inside the storage tank is presented in Eq. (3.35):

$$S_{e_j}\in\{0, 1\} \tag{3.34}$$

$$T_{\min}\le T_k\ge T_{\max} \tag{3.35}$$

3.3.2 Proposed optimization solver and algorithm

The objective function as shown in Eq. (3.31) is a non-linear function with an integer binary control variable that needs to be solved in order to obtain the optimal switching status of electric resistive element. This type of problem can be solved by the universal SCIP (Solving

Constraint Integer Programs) solver in Matlab optimization toolbox. SCIP has also been reported to be one of the fastest solvers in the Matlab interface OPTI-Toolbox [120].

The MINLP form needs to be satisfied so that SCIP can operate properly. The form MINLP form is shown in Eq. (3.36); the objective function is minimized by default and is subjected to the constraints shown. The mathematical model needs to be rearranged to fit the SCIP constraints in order to solve the optimization problem. The end result is an optimal switching status function constrained to take on a binary value [121].

$$
\begin{aligned}
&\text{Min}_x \ f(x) \\
&\text{subject to: } Ax \le b \\
&\qquad A_{eq}x = b_{eq} \\
&\qquad lb \le x \le ub \\
&\qquad c(x) \le d \\
&\qquad c_{eq}(x) = d_{eq} \\
&\qquad x_i \in \mathbb{Z} \\
&\qquad x_j \in \{0,1\}
\end{aligned}
\tag{3.36}
$$

Where:

$f(x)$ is the objective function,

$Ax \le b$ is the linear inequality constraint,

$A_{eq}x = b_{eq}$ is the linear equality constraint,

$lb \le x \le ub$ is the decision variable bounds,

$c(x) \le d$ is the nonlinear inequality constraint,

$c_{eq}(x) = d_{eq}$ is the nonlinear equality constraints,

x_i is an integer number decision variable,

x_j is a binary number decision variable.

The objective function is consequently replaced with $f(x)$. The decision variable shown in Eq. (3.34) is a binary value, which means only a 1 or a 0 can be taken as the switching status. The lower and upper boundaries are therefore shown in Eq. (3.37) and Eq. (3.38) respectively:

$$lb^T = [0...0_N] \tag{3.37}$$

$$ub^T = [1...1_N] \tag{3.38}$$

The control variable that needs to be optimized is therefore constrained as shown in Eq. (3.39)

$$lb \leq x \leq ub \tag{3.39}$$

3.4 SUMMARY

In this chapter, the objective function, control, state variables and disturbances were identified and mathematically expressed in the developed model. For any solar/electric water heating setup with different design variables as well as operating conditions (solar radiation, ambient temperature, inlet water temperature, hot water consumption, etc.), the developed model's decision variables can be optimized using any suitable advanced algorithm able to solve such a problem. The SCIP solver in the Matlab interface OPTI-Toolbox has been chosen to solve this problem.

The constraints on the operation have been set and outlined according to the hot water users' specific thermal comfort level while attaining the maximum savings possible. This is achieved by shifting the load profile maximum energy usage times to time intervals where energy is charged at off-peak tariffs increasing savings in cost.

CHAPTER IV: SIMULATION RESULTS AND DISCUSSION

4.1 INTRODUCTION

In this Chapter, the optimal operation control model of the hybrid energy system is simulated using SCIP solver in Matlab OPTI-Toolbox. The objective of the present simulation is to demonstrate the effectiveness of the optimal control strategy of the hybrid system.

The minimization of the daily operation cost and the level of discomfort experienced by the consumer is shown in this chapter as well as a baseline comparison. A load profile and all other appropriate data for summer season as well as winter season were obtained and shown.

4.2 DATA DESCRIPTION

This section describes a case study from which the environmental data, hot water consumption profile and system component sizes are presented. The data is used as input to the developed optimization strategy for the proposed hybrid system.

In section 4.2.1 the data is illustrated at 1-minute averaged intervals. The sampling time is taken to be 15 minutes with the resulting total sampling interval and control horizon as well as other relevant parameters discussed in section 4.2.2.

The data is converted to 15-minute averaged intervals in order to simulate a baseline water heating system and the optimally controlled HSWH discussed in sections 4.2.3 and 4.2.4, respectively. Section 4.2.5 compares these two systems with the aim to draw a conclusion.

4.2.1 Case study

The case represents a traditional medium density house with three occupants located in Bloemfontein, Free-state, South Africa. The daily hot water demand flow rate, solar irradiance, inlet water temperature and ambient temperature taken on a 15-minute basis from the selected site, are shown in Fig. 4.1 to Fig. 4.6. The same winter and summer numerical data is tabulated in Appendix A1 and A2, respectively.

Data for diffuse horizontal, diffuse normal, global horizontal irradiance and air ambient temperature of a typical winter day in June and a summer day in January are plotted in Figs. 4.1, 4.2 and Figs. 4.3, 4.4 respectively. The data was collected from the weather station located at the University of the Free-State (latitude: -29.11074, longitude: 26.18503 and elevation: 1491 m) in Bloemfontein [122].

Referring to Fig. 4.1 and Fig. 4.2, it should be noted that most summer days in Bloemfontein are overcast or cloudy, unlike most winter days when clear skies are apparent. Furthermore, it can clearly be observed that the solar irradiance representing the two seasons are different in magnitude, with the summer irradiance having a larger magnitude than the winter irradiance.

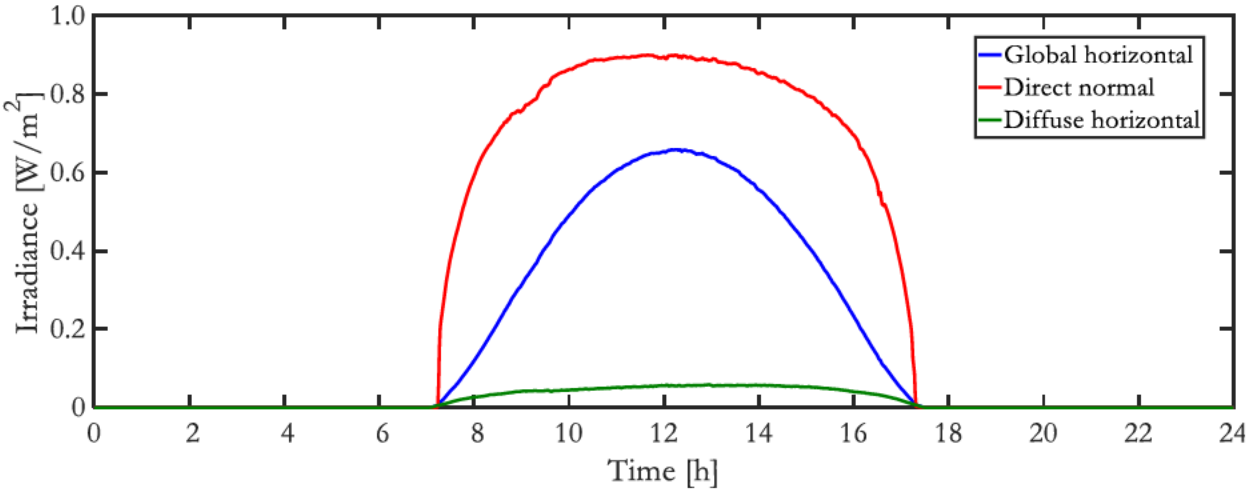

Figure 4.1: Winter solar irradiance

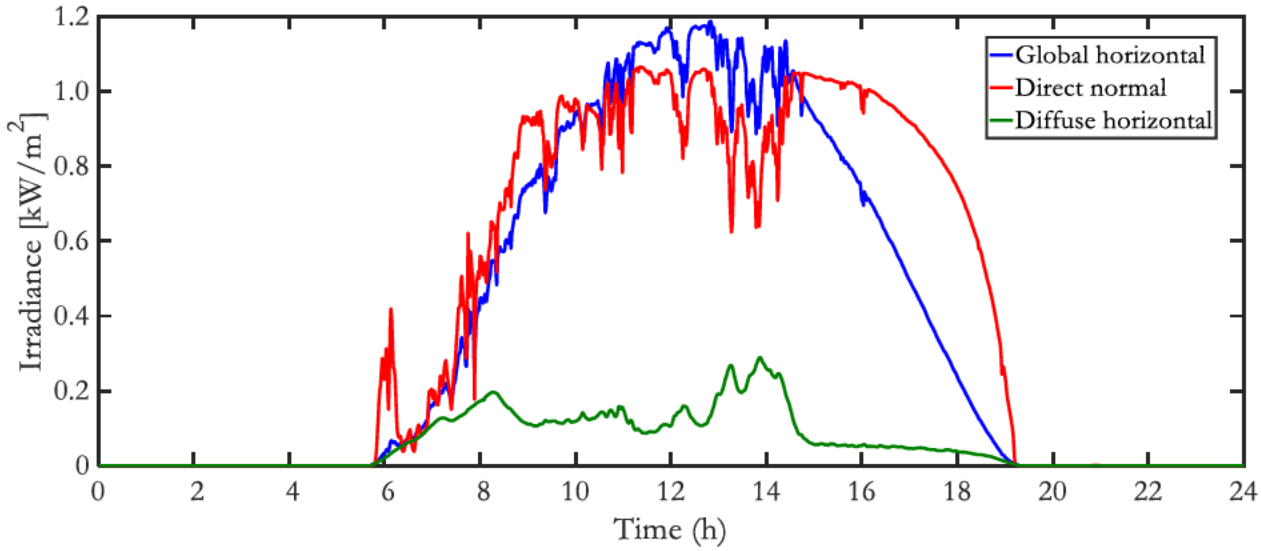

Figure 4.2: Summer solar irradiance

The ambient and water inlet temperature represented in Figs. 4.3 and 4.4 for the winter and summer season are shown, respectively. The ambient temperature deviates significantly with time when compared to the inlet water temperature. No minute or hour averaged data for inlet water temperature exists for the case study area. This means that the inlet water temperature needs to be based on assumptions. The median water temperatures taken once per season, retrieved from [123], were used for the case study. The median inlet water temperatures of winter and summer was taken as 13.3 °C and 23.1 °C, respectively. Only small changes in temperature can be assumed for the inlet water, the approximations were made with heat capacity and density of water and air in mind combined with the fact that most of the city's water conduits are buried underground. Fluctuations in ground temperature are much lower when compared to air temperature. This in turn reduces the influence of ambient air temperature on the inlet water temperature. The water temperatures are therefore assumed to be near constant with slight delayed deviations that follows the change in air temperature.

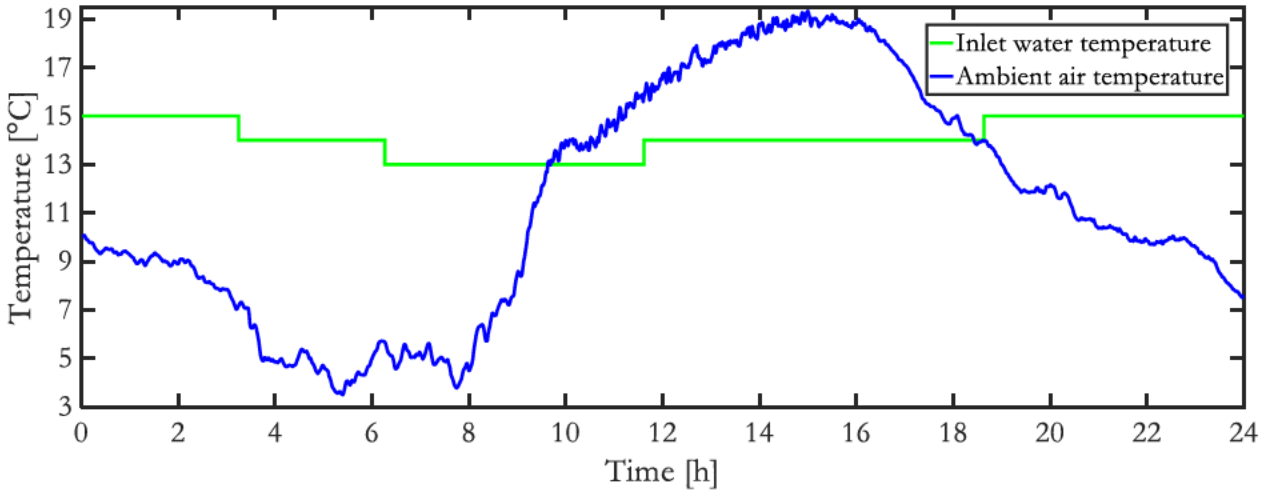

Figure 4.3: Winter ambient and inlet water temperature

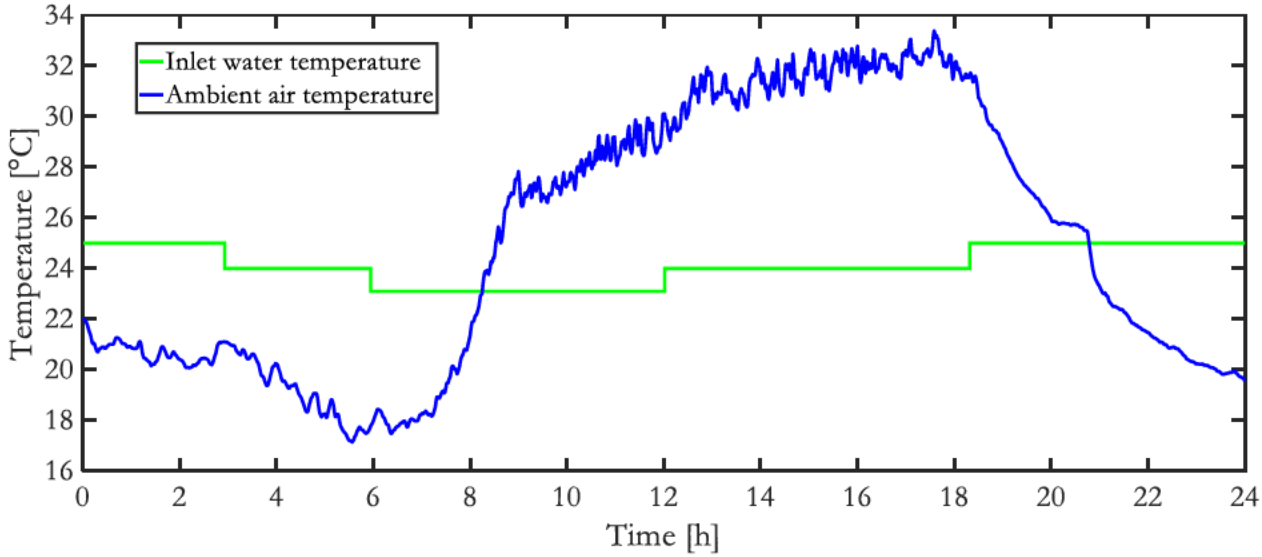

Figure 4.4: Summer ambient and inlet water temperature

A 24-hour detailed average summer hot water consumption profile was obtained and is shown in Fig. 4.5, while the winter profile was adapted from [124] with the summer hot water consumption as base profile. In summer, the desired temperature was obtained by adjusting the hot and cold water taps. The flow rate per minute of the hot water, after the cold water tap was closed, was measured to be 3.23 litres per minute. The shower time of the first occupant was measured to be 7 minutes, while the second and third occupants had shower

times of 9 and 10 minutes, respectively. The times during the day at which the showers of the first 2 occupants took place was between 06:30 and 07:30. At 11:00, a dishwasher/washing machine draws hot water to complete one washing cycle. The third occupant as per the normal daily routine showered at 20:00.

As described by [124] the winter hot water consumption of a medium density household in South-Africa is approximately 1.7 times higher than the consumption in the summer. This is mainly due to the large temperature differential between the inlet water and the hot water supplied from the water heater in the winter season. As a result, additional hot water is required to compensate for the differential. Consequently, the hot water consumption in winter was estimated to be higher by a factor of 1.7., this estimated winter demand profile is shown in Fig. 4.6.

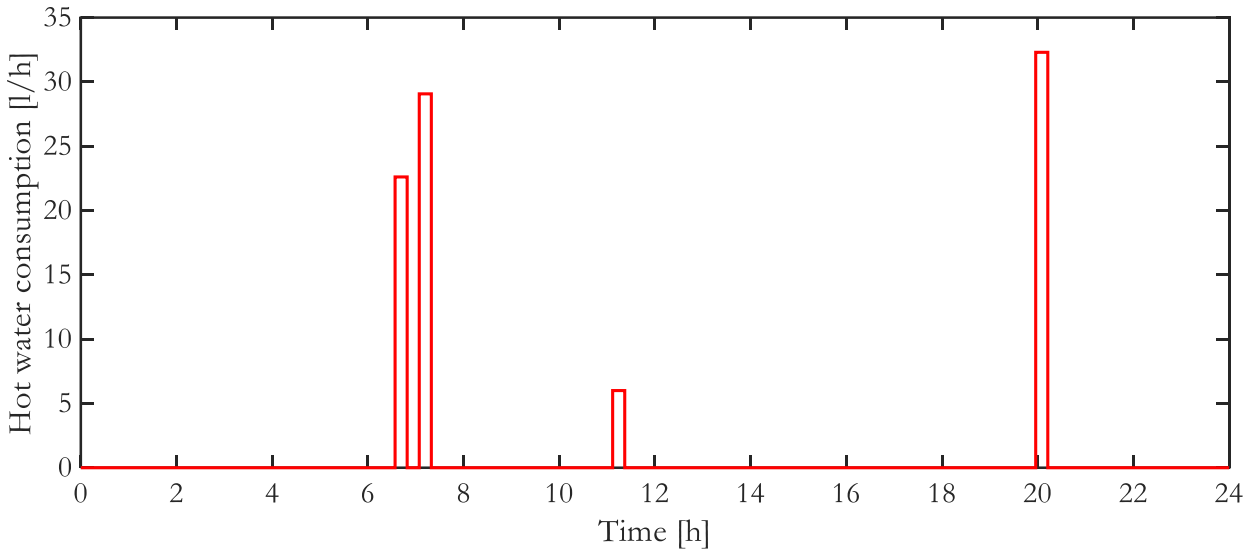

Figure 4.5: Summer hot water demand i.e. flow rate

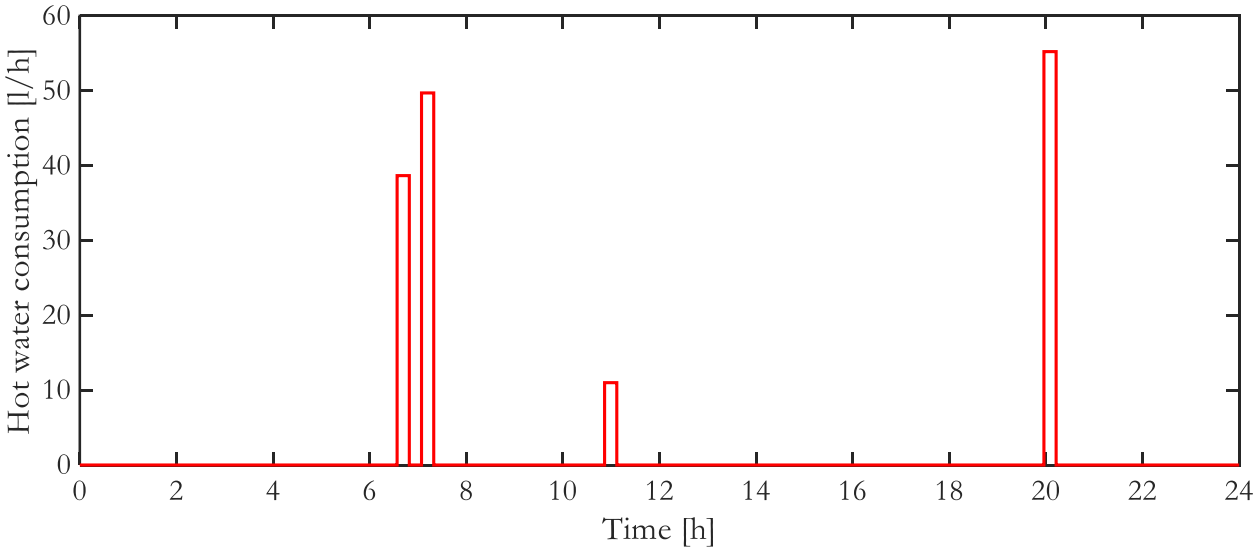

Figure 4.6: Winter hot water demand i.e. flow rate

4.2.2 Component size and simulation model parameters

As specified in the study objective (Chapter I, section 1.4), the aim of the current work is principally on the optimal energy management of the hybrid water heating system. A baseline model in section 4.2.3 is adapted from the hybrid water heating system model in section 4.2.4 to simulate thermostat operation without solar irradiance as input. Rather the only energy input to the system will be the energy supplied from the electric resistive element. The baseline model is hence simulated with the same component sizes and input data as the hybrid system without the influence of the collector. The component sizes and parameters of the baseline and hybrid system are shown in Table 4.1. Retrieved from [111,115,125-129] and adapted for South African case.

In chapter 2, section 2.1.3, the optimal tilt angle of the collector is taken to be 30°. Most certified collector installers in the region usually use this angle as a rule of thumb. The solar angles of incidence were calculated for the days on which the data was taken. The angles obtained were 67.6° for winter (June 2017) and 109° for the summer (January 2017).

The storage tank size was taken as 150 litres, this choice in capacity was based on the requirements of the 3 occupants in the case study. The 150 litre ESTWH is accompanied by a 3-kW electric resistive element.

Table 4.1: Component sizes and parameters of the hybrid solar electric water heater

Parameter	Description	Value
A_{coll}	Effective absorbance area of the collector (m^2)	2
A_s	Storage tank area (m^2)	1.1
β_{coll}	Tilted angle of the collector array (°)	30
C	Heat capacity of water (J/kg.°C)	4184
F_R	Heat removal factor (-)	0.6646
$m_c(t)$	Collector flow rate ($kg/s.\ m^2$)	0.011
M	Storage tank capacity (kg)	150
P_{EL}	Rated power of electric resistive element (W)	3000
Q_{EL}	Energy delivered to resistive element (MJ/h)	10.8
ρ_g	Ground reflectance (-)	0.2
T_d	Desired hot water temperature (°C)	60
$T_{s,\max}$	Default thermostat switch-off temperature (°C)	65
T_{tstat}	Thermostat switch-on temperature (°C)	60
$\theta_{\beta,s}$	Summer incidence angle on tilted surface (°)	109
$\theta_{\beta,w}$	Winter Incidence angle on titled surface (°)	67.6
$\tau\alpha$	Transmittance absorbance product (-)	1.12
U_L	Collector overall heat transfer coefficient ($W/m^2.°C$)	7.28
U_s	Heat loss coefficient of storage tank (W/m^2)	0.3

The TOU tariff structure and pricing layout is illustrated in Table 4.2, the tariff is enforced by Centlec (electricity distribution and managing company for the Bloemfontein and

surrounding area). From the table, the high demand season with the most costly electricity prices falls in winter period which is from June to August, while the low demand season is between September and May. Additionally, the low and high demand season's peak, off-peak and standard periods start and end at different hours during the day. The highest electricity price at R3.23, is effective in the peak period of the high demand season, while the lowest is R1.20 during the off-peak period of the low demand season. This means that there is a difference of 269% from the lowest electricity price to the highest for the same year [130,131].

Table 4.2: Homeflex single phase TOU tariff structure and pricing

Season	Months	Period	Time	Rate (ZAR)
High Demand (Winter)	June - August	Off-peak	00:00-06:00, 22:00-24:00	1.7875
		Standard	09:00-17:00, 19:00-22:00	1.8643
		Peak	06:00-09:00, 17:00-19:00	3.2351
Low Demand (Summer)	September - May	Off-peak	00:00-06:00, 22:00-24:00	1.2063
		Standard	06:00-07:00, 10:00-18:00, 20:00-22:00	1.3269
		Peak	07:00-10:00, 18:00-20:00	1.7108

The simulation parameters are shown in Table 4.3. For increased accuracy of the results, a sampling interval of 15 minutes was taken over a control horizon of 24 hours. Therefore, the number of samples in the control horizon will be 96.

Table 4.3: Simulation parameters

Parameter	Description	Value
t_s	Sampling time (minutes)	15
N	Samples over the control horizon (-)	96
Hours	Total hours in control horizon (hours)	24

4.2.3 Baseline

In order to validate if the optimal switching model reduces energy costs to the consumer, a baseline needs to be established. The baseline model is an electric storage tank water heater (ESTWH) without a solar collector. The temperature is regulated by means of a thermostat, where the default temperature is set at 65 °C. The thermostat will maintain an approximate temperature of 65 °C throughout the day by automatically switching the electric resistive element on and off at the times when it is required. The thermostat has a temperature range of 5 °C. This means that the element will switch on to increase the thermal level, when the temperature drops to the lower thermostat switch on temperature which in this case is 60 °C.

Most electric storage tank water heaters in South Africa use the bi-metal thermostat system, this system is known to deviate from the actual set temperatures by an average of 3 °C. The simulation of the thermostat operation should hence stay within the 3 °C range so that the accuracy of the baseline operation is maintained [132].

Two separate cases are simulated to represent the winter and summer months. The switching function of the thermostat and the associated change in water temperature inside the storage tank is shown in section 4.2.3.1 for winter and section 4.2.3.2 for summer.

4.2.3.1 Baseline: Winter case

In Fig. 4.7, the switching function of the thermostat is shown. For the specific hot water consumption profile, inlet water temperature and ambient air temperature described in section 4.2.1, the switching of the electric element is shown to take place during the peak and standard periods of the TOU tariff structure. Fig 4.8 illustrates the resultant change in temperature of the water inside the storage tank due to the switching in Fig. 4.7. After the first two occupants have finished their showers at 07:45, the temperature drops below the thermostat switch-on temperature so that water can be heated to 65 °C. The dishwasher/washing machine draws water at 11:00, however, the associated temperature drop is not enough to permit the electric resistive element to switch on. The temperature drops after 20:00 due to the last hot water

demand and the thermostat delivers power to the resistive element once more. The preferred thermal level, is shown to be between 55°C and 65°C illustrated in orange, while hot and cold is shown in red and blue, respectively. With the thermostat setting at 65°C, the water temperature remains within the desired temperature even when hot water is not required. This increases the cost of electricity significantly validating the need for an optimal control approach.

When comparing the switching function to the water temperature inside the storage tank, it can be observed that the switching mainly occurs directly after the times when hot water is drawn by the occupants. This can mainly be attributed to temperature falling below the thermostat switch on temperature due to the withdrawal of hot water and the incoming cold inlet water temperature to maintain the constant volume. Due to the 15-minute sampling time, difficulty in equalizing the final and initial temperatures were experienced when the thermostat operation was simulated in Fig. 4.8.

The difference in temperature between the initial and final sampling intervals is approximately 1.5 °C. Calculations dictates that a sampling time of 5 minutes should be used to remove this temperature differential. However, the small difference in temperature can be neglected as it will not have any adverse effects on the cost saving calculations.

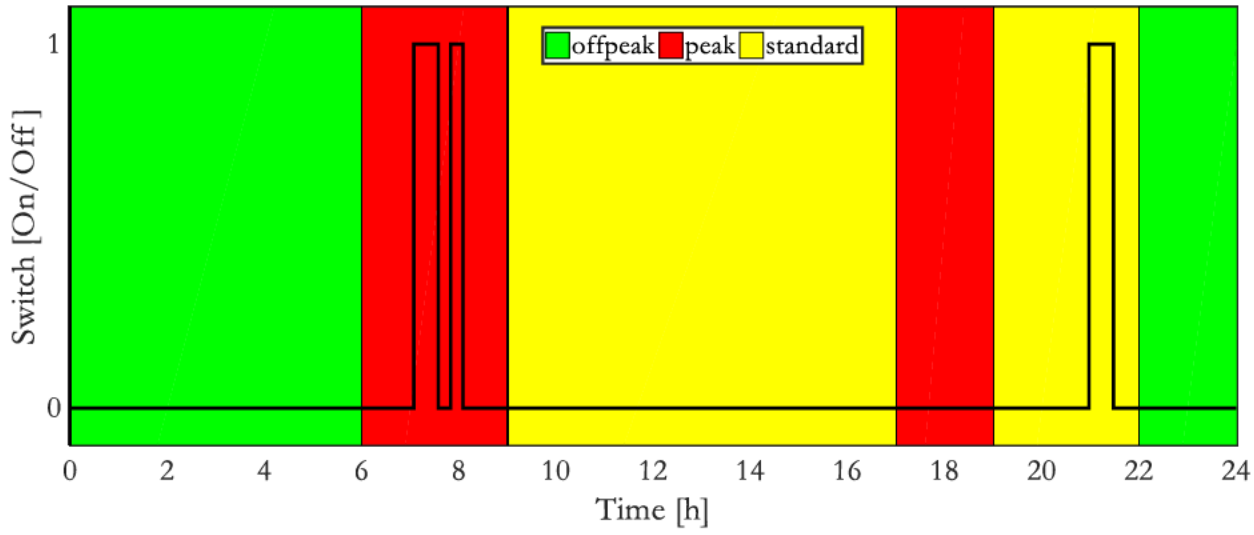

Figure 4.7: Switching function of the ESTWH

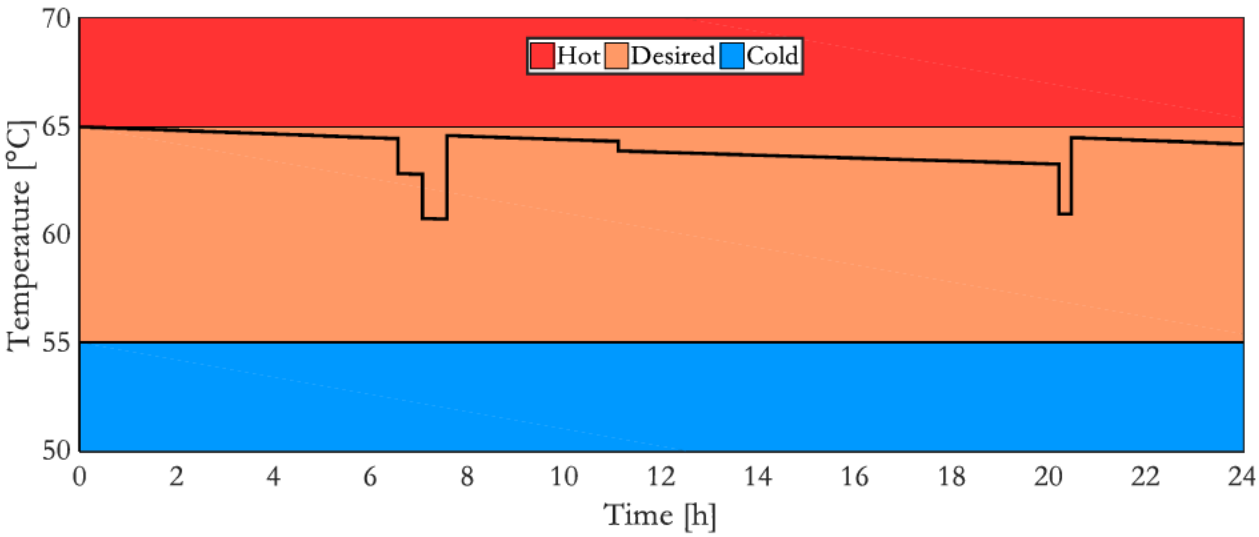

Figure 4.8: Storage tank water temperature of the ESTWH

4.2.3.2 Baseline: Summer case

In Fig. 4.9, the switching function of the thermostat is shown. The summer input data from section 4.2.1 is used for this simulation, similar to the winter baseline case discussed in section 4.3.2.1. The switching of the electric element is shown to take place during the peak and standard periods of the TOU tariff structure. Fig 4.10 illustrates the resultant change in temperature of the water inside the storage tank due to the switching in Fig. 4.9.

The summer baseline system follows the same trend as the discussed winter baseline. In this case, the duration of the switch-on time is less compared to the winter case.

The desired temperature as with the winter case is shown to be between 55 °C and 65 °C. When comparing the storage tank temperature of the winter case with the summer case temperature of the water inside the storage tank, a smaller drop can be observed at the times of hot water consumption. This is due to the directly proportional relationship that the hot water consumption profile has with the temperature of the water inside the storage tank.

The fixed final state condition of the summer baseline case is maintained better than the winter case where only a small temperature differential between the initial and final sampling intervals can be observed.

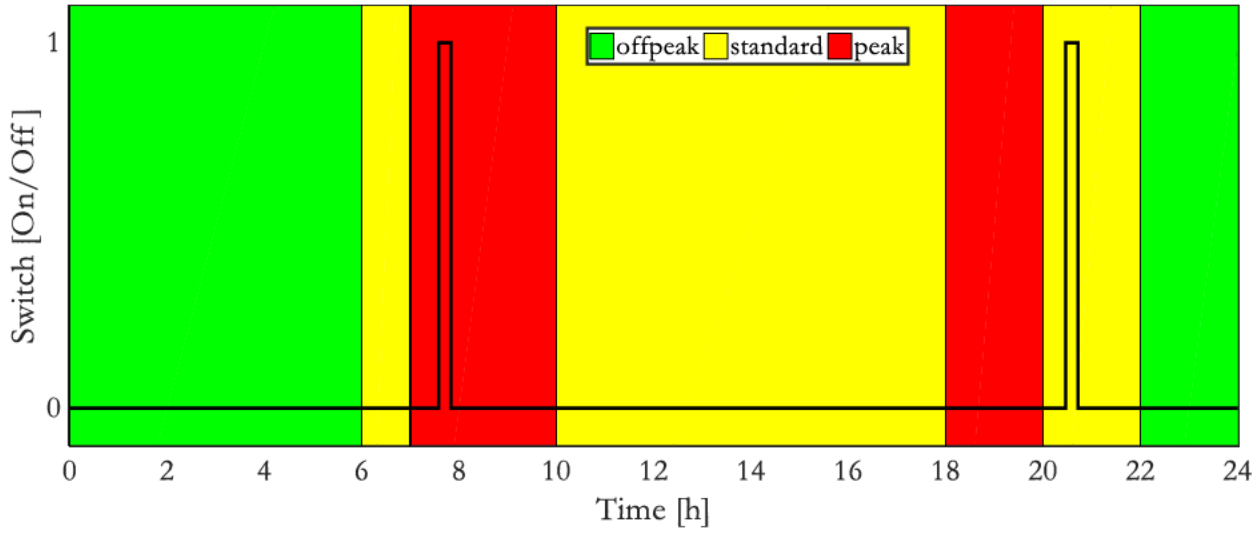

Figure 4.9: Switching function of the ESTWH

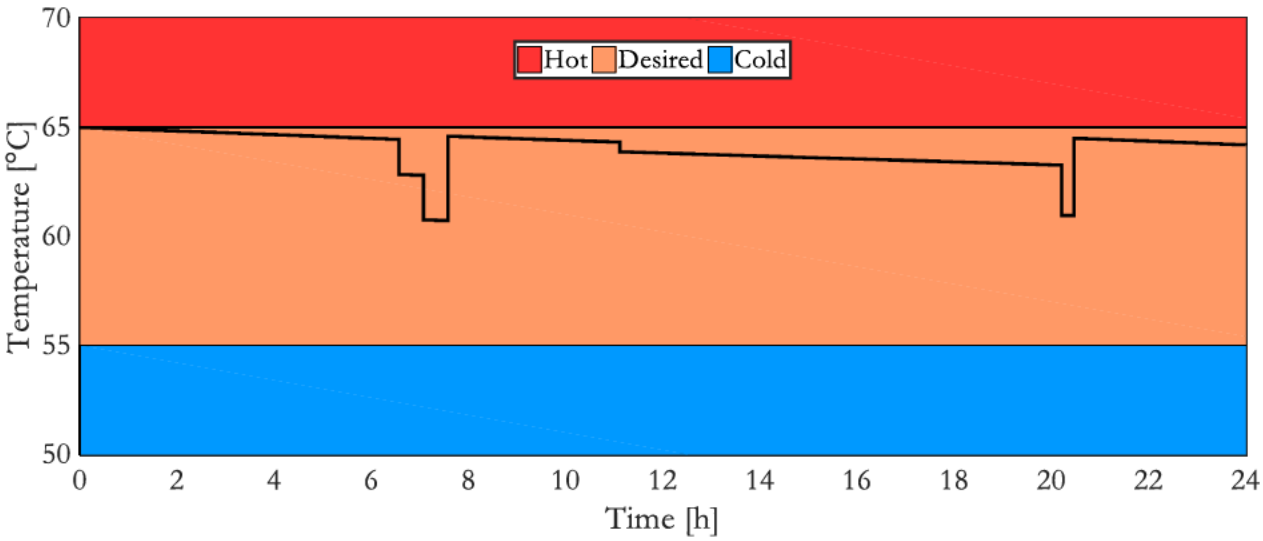

Figure 4.10: Storage tank water temperature of the ESTWH

4.2.4 Optimal scheduling of the proposed hybrid solar water heater

In this section, the operation of the proposed hybrid system with optimal scheduling is described. The hybrid system's optimal switching function and corresponding water temperature inside the storage tank is illustrated in section 4.2.4.1 for the winter case and 4.2.4.2 for the summer case. The same input data in section 4.2.1 is used to simulate the operation of the hybrid system with the optimal scheduling approach.

4.2.4.1 Optimal scheduling of the HSWH: Winter case

The optimal switching function of the HSWH is shown in Fig. 4.11 and the resultant temperature of the water inside the storage tank is shown in Fig. 4.12. In order to reach the desired temperature at the instant when a hot water demand occurs, switching needs to take place prior to when this demand occurs as shown in Fig. 4.11.

Most of the switching occurs during the off-peak periods, once in the morning at 04:30 and once at night at 10:15. The heating element is switched on for 15 minutes so that the water temperature can reach the desired temperature at 06:30 and the water temperature decreases from 04:30 to 06:30 until it reaches a temperature above the desired level. The decrease in temperature is caused by stand by losses. At 06:30, the first occupant draws hot water, a sharp decrease of temperature is observed, while at 07:00, the water is still within the desired thermal comfort level so that switching is not required to increase the thermal level.

The temperature of the water in the storage tank at 07:30 when the second occupant has ended his shower is shown to drop slightly below the comfortable level. This thermal level at 54 °C can still be seen as acceptable if one of the first two occupants decide to take a longer shower. Solar radiation starts to increase the thermal level of the water inside the storage tank at the same time-step. The temperature rises until 11:00 where it suddenly drops due to the hot water consumed by the dishwasher or washing machine. At 11:30, the water temperature slowly rises due to the solar irradiance supplied to the collector. At 20:00, the third occupant showers and the temperature drops due to the inflow of cold water in the storage tank while hot water is drawn, after the third occupant's hot water consumption routine, the temperature remains within the desired temperature range. However, no hot water demand is expected after 21:00, meaning that no switching is required.

The element switches on for the last time at 22:15 during the off-peak period in order to maintain final fixed state conditions.

The temperature (58 °C) at the final sampling interval is equal to the initial temperature so that the cycle can be repeated for the next day.

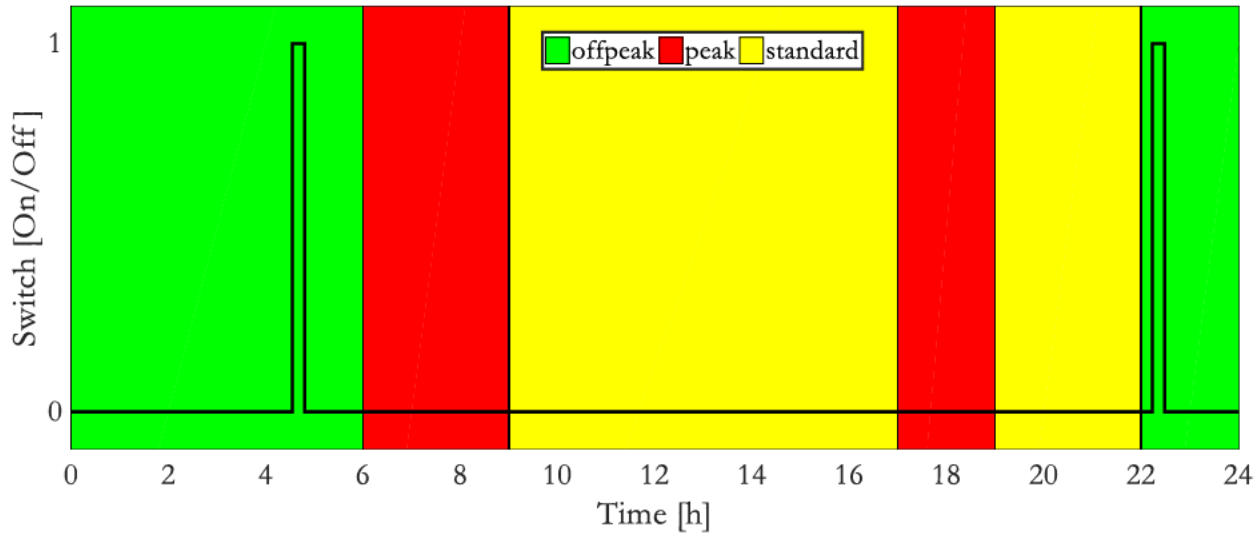

Figure 4.11: Optimal switching function of the HSWH

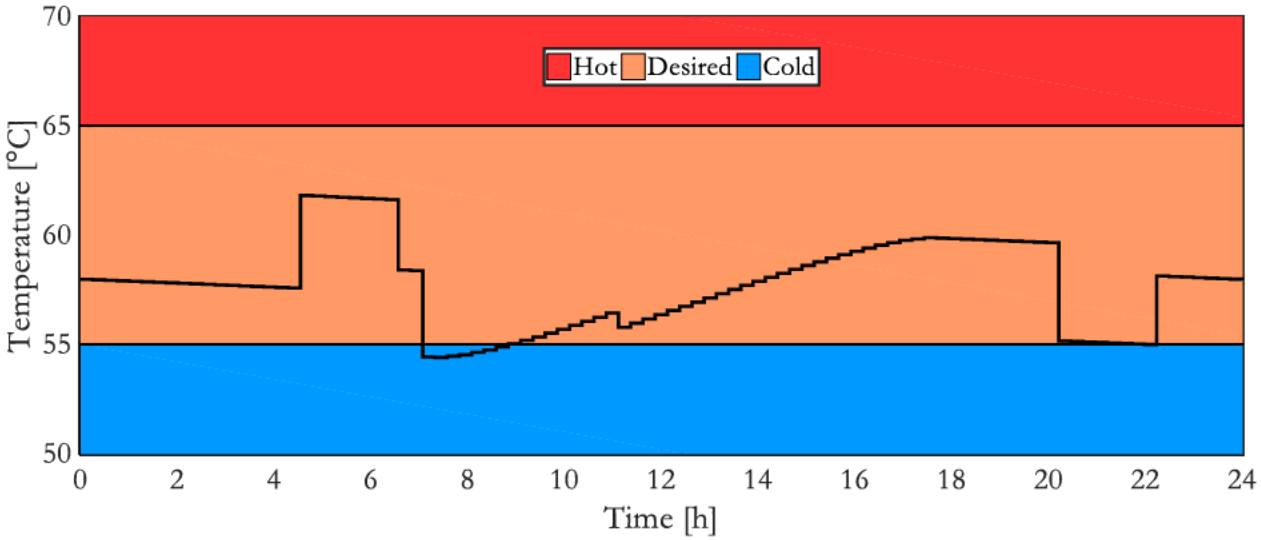

Figure 4.12: Optimal storage tank water temperature of the HSWH

4.2.4.2 Optimal scheduling of the HSWH: Summer case

Referring to Fig 4.13 and 4.14, the switching function shows that switching only takes place once at 05:30 for 15 minutes in order to prepare for the first occupant's hot water demand. The switching function remains at zero throughout the rest of the control horizon. The lack of switching during the summer period can be accredited to low hot water demand and higher ambient and inlet water temperatures compared to the winter season. However, the angle at which the solar radiation (beam radiation) penetrates the collector in the summer season is higher than that of winter. This means that the total effective solar irradiance absorbed by the collector is less. The combined effect of all these factors gives rise to a storage tank water temperature that remains within the comfortable thermal level with minimal switching required as shown in Fig. 4.13.

At 07:30 when the first two occupants have finished their daily hot water consumption routine, the temperature briefly falls but stays within the desired range. Afterwards the heat from the sun increases the temperature. The dishwasher/washing machine demand at 11:00 causes a small reduction in temperature, while it is once again recovered by solar energy up until 20:00, when the third occupant draws hot water. At 20:15, after the last demand of the day has taken place, the temperature drops down to 58.3 °C, where it decreases further due to standby losses. At 24:00 the temperature reaches approximately 58 °C which is equal to the initial temperature in the control horizon to maintain fixed final state conditions.

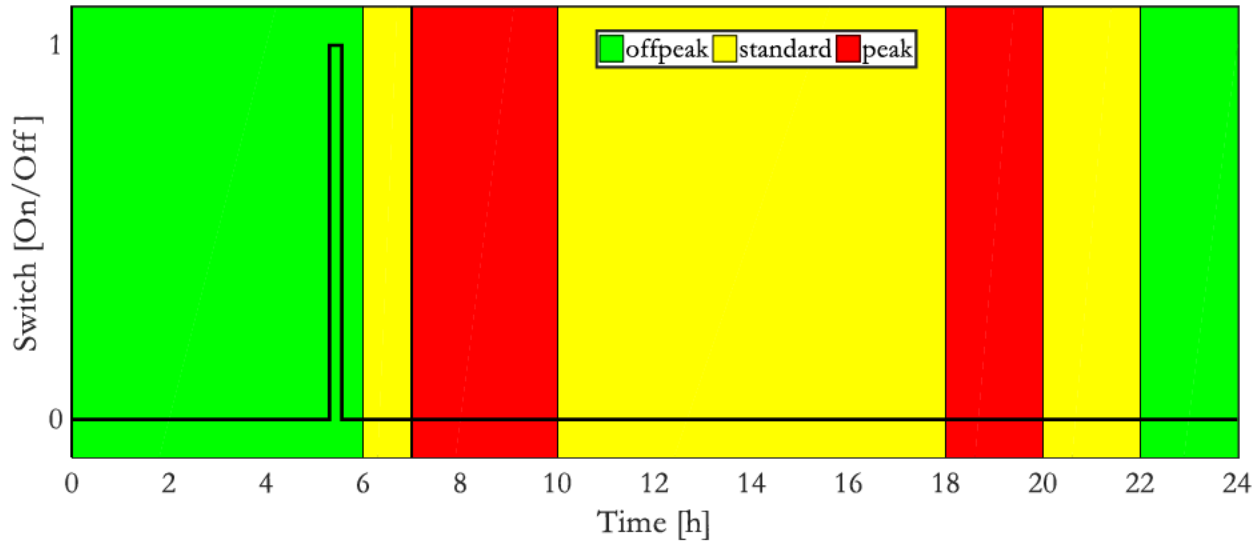

Figure 4.13: Optimal switching function of the HWHS

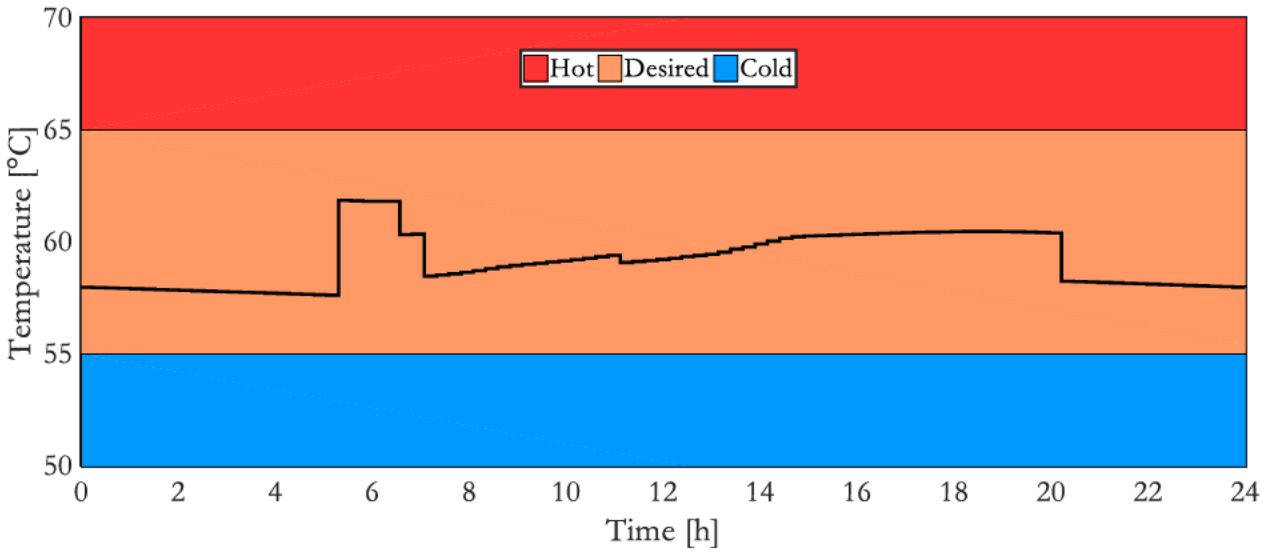

Figure 4.14: Storage tank water temperature of the HWHS

4.2.5 Comparison between the baseline and optimal scheduling of the HSWH

For both the baseline and the optimized hybrid system, the temperature of the water inside the storage tank exceeds 60°C at least twice a day for the winter as well as the summer case. As discussed in Section 1.1, this reduces the risk of contracting Legionair's disease caused by the Legionella pnuemphilla bacteria.

It is evident that switching the resistive element on during off-peak periods, rather than peak or standard periods, the desired thermal level of the hot water consumer can still be maintained. The fact that the temperature remained within the preferred range for the winter case, when hot water consumption is higher in comparison, substantiates the need for an optimal control strategy.

All optimal control scenarios shown in section 4.2.4 have been solved with equal weighting factors so that equal priority is given to cost and discomfort minimization. For the optimal scheduling scenario, it can be observed that all switching takes place during off-peak periods. This means that if higher priority was given to cost minimization, the cost savings would not increase. However, if priority was given to discomfort level minimization, higher energy costs could result.

4.3 SUMMARY

In this Chapter, the hybrid system's optimal operation control model has been simulated using SCIP solver in Matlab OPTI-Toolbox. Realistic and actual historic data was used and the developed model has been successfully used to represent the operation of a baseline as well as an optimal control strategy of the proposed system. The daily non-linear load, non-linear renewable resources as well as the storage tank temperature dynamic was evaluated in terms of the impact on the hybrid system's daily operation cost compared to a baseline.

The optimal energy management model has also been used to:

- Obtain the minimized operation costs achieved by using a certified hybrid SWH/ESTWH combination.

- Analyse the impact of the solar irradiance on the storage tank temperature dynamic during the two seasons represented by the TOU tariff implemented by the electricity supplier.
- Reveal the importance of taking into account the differences in seasonal load profiles and variations in the renewable energy resource, water inlet temperature as well as ambient temperatures while calculating the daily and annual operation cost of the hybrid system.

The developed model, as well as the solver (SCIP) used in this work, required low computational power to solve with high accuracy, while the added benefit of fast processing and simulation was experienced. The processing specifications of the computer used to solve the optimal control problem included an Intel Core i7 -7700HQ (Processor) and 16 GB of DDR4 RAM. The time taken to solve the optimal control problem for the summer and winter cases were 2.35 seconds and 21.08 seconds respectively.

CHAPTER V: ECONOMIC ANALYSIS

5.1 INTRODUCTION

In order to evaluate the cost effectiveness of the hybrid system in terms of money spent, several economic performance indicators exist. These indicators can include the simple payback period (SPP), life cycle cost (LCC), benefits-to-cost ratio (BCR) and initial rate of return (IRR). The SSP is the easiest to understand due to its simplified cost calculation, however, limitations exist in the sense that it does not take into account future inflation that might affect the total cost over the lifetime of a project. Another drawback of the SPP is that it does not account cash flows beyond the payback period (PBP), as the project lifetime is not taken into consideration. This reduces the accuracy of the economic analysis and leaves investors with an approximate cost or profit prediction. With this in mind, methods such as the BCR, LCC and IRR offer a more precise cost analysis when compared to SSP due to the fact that inflation and project lifetime are taken into account [133]. Therefore, for increased accuracy, a total life cycle cost evaluation is done followed by a break-even point (BEP) analysis in terms of the baseline and proposed hybrid system. The life cycle costs will then be compared to calculate the savings over a specific project lifetime. The project lifetime for this case study was chosen to be 20-years.

5.2 INITIAL INSTALL COST OF THE PROPOSED HYBRID SYSTEM

The initial investment cost of a hybrid SWH/ESTWH system is shown in Table 5.1. The ESTWH and SWH combination was chosen, due to the manufacturer being approved by the Eskom rebate programme. Furthermore, the manufacturers' products all comply with Eskom and South African Bureau of Standards (SABS) criteria. The rebate reduces the total investment cost by approximately 40%. The Flat plate collector listed is frost resistant, so that it is suitable for Bloemfontein's freezing temperatures in winter. In addition, the flat plate was

chosen over the evacuated tube system due to the major cost difference as mentioned in Chapter II, section 2.4. The prices in Table 5.1 obtained from [134-136] are average component prices for the year 2017.

Table 5.1: Bill of quantity of HSWH

Component description	Quantity	Net price (ZAR)
150L GAP Eco Electric Storage tank water heater	1	2560.40
150L GAP 2.1m^2 Flat Plate Collector	1	4586.80
Geyserwise Max controller	1	1222.08
Air release valve	1	277.00
Circulation pump	1	1425
22mm thermostatic mixing valve (55°C)	1	624.15
Labour	-	1500
Eskom rebate	-	-4677.00
Total initial investment cost	-	7518.43

5.3 CUMULATIVE COST COMPARISON

Calculating the cumulative costs incurred over a specific project lifetime, in this case 20-years, some factors need to be taken into consideration. Described in section 5.2, the initial cost of implementation cannot be seen as cumulative, due to the fact that the cost implementation is a once off amount incurred only at the inception of the project. With this in mind, the annual costs incurred, which includes replacement costs and operation & maintenance (O & M) costs after each year since the starting point of the project can directly be added to the initial implementation cost in order to obtain the total cumulative cost over the project's lifetime.

Salvage costs at the end of the project lifetime are also included, however, similar to the case of the initial cost of implementation, this cost can be seen as once off. Moreover, the salvage cost can be deducted from the total life cycle cost and seen as a cost benefit rather than a loss.

5.3.1 Cumulative energy cost

In order to calculate the daily cumulative energy cost, the primary objective function can be adapted from chapter III so that Eq. (5.1) can be used in this instance:

$$C_{daily-EC} = t_s . P_{EL} \sum_{k=1}^{N} (C_{TOU_k} . S_{e_k}) \tag{5.1}$$

Where;

t_s is the sampling time,

P_{EL} is the rated power of the electric resistive element (3 kW),

C_{TOU_k} is the time-based cost of electricity at each kth interval defined in chapter IV, section 4.2.2, Table 4.2 in ZAR/kWh,

S_{e_k} is the switching status of the electric resistive element.

With this, the daily cumulative daily cost values (ZAR) were obtained and illustrated in section 5.3.1.1. - 5.3.1.2. and compared in section 5.3.1.3. for the summer and winter cases, respectively. In section 5.3.1.4., the annual cumulative costs were calculated using the total daily energy cost values obtained in terms of the low and high demand seasons defined by Eskom.

5.3.1.1 Winter cumulative energy cost comparison

The cumulative cost of the winter period is shown in Fig. 5.1. The switching functions in section 4.2.3. and 4.2.4. refers, as can be observed from the curves, every time switching occurs, the cost of switching in the specific TOU tariff period increases the total daily cost. At the end of the control horizon at 24:00, the difference in total cost can be observed. The cumulative curves in Fig. 5.1 shows a directly proportional relationship between the baseline and optimal control strategy. The optimally scheduled hybrid system switches on during the off-peak period, while the baseline switching-on time is delayed by 2 hours and 30 minutes. Observation reveals that the cumulative cost of switching the baseline system on for 15 minutes at this time is nearly equal to the total cumulative cost of the optimally controlled system. The baseline heater is effectively switched on for 45 minutes during the peak period in order to maintain the thermostat temperature. This process is repeated in the evening with the only differences being that the system is switched on for a shorter time during the off peak period. When comparing the operational cost curves at the end of the control horizon, it can be deduced that the baseline's total net energy costs is approximately 4 times higher than that of the optimally scheduled hybrid system.

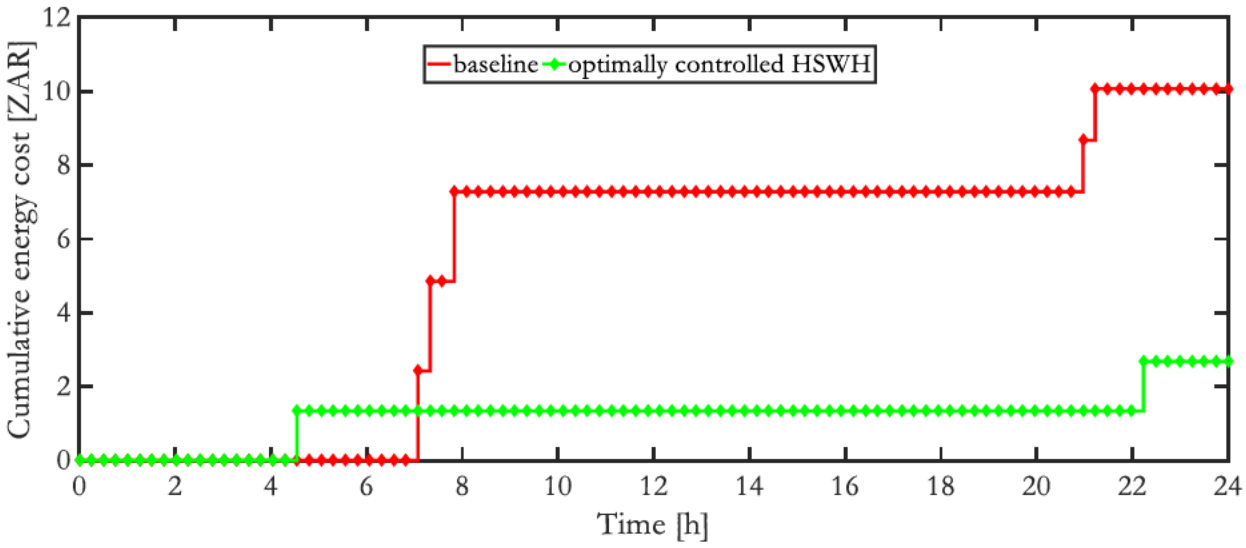

Figure 5.1: Winter cumulative energy cost

5.3.1.2 Summer cumulative energy cost comparison

The cumulative cost of the summer period is shown in Fig. 5.2. Similar to the winter cumulative cost curve in Fig. 5.1, the summer switching function of the baseline system follows the optimal switching curve with a 2 hour and 15 minute delay, the energy cost difference of this delay can be seen from the figure. After the first switch-on interval of the optimally controlled system, the curve remains constant so that the cumulative cost remains close to R1.00 for the rest of the control horizon. This is a result of the element being on for 15 minutes during the off-peak period. The baseline heater and optimally controlled hybrid system switch on for 15 minutes in the morning. The cost of switching the baseline on during the peak period in the morning is higher than the total cumulative costs of the optimally scheduled system. The difference in cumulative energy cost at the end of the control horizon represents the daily energy cost savings as in the winter case. The baseline energy cost compared to the optimal controlled system, shows an energy cost higher by a factor of 2.5. This is significantly lower than for the winter case and presents the notion that the optimal system is more effective during the winter season.

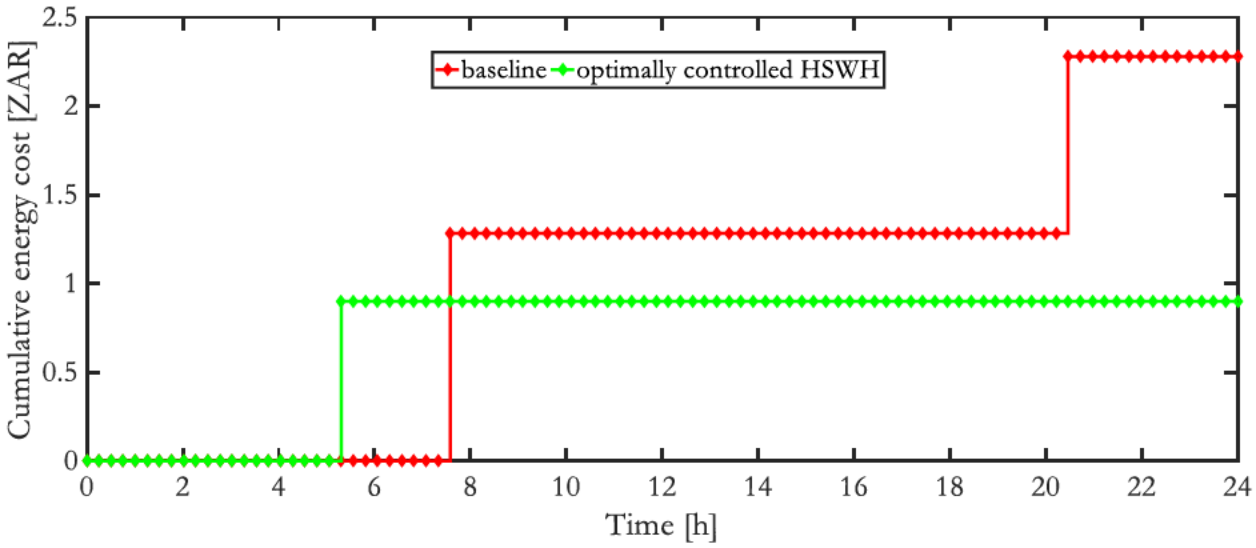

Figure 5.2: Summer cumulative energy cost

5.3.1.3 Daily energy consumption and savings

The cumulative costs and energy consumed after each simulation of the baseline and optimal control strategies are shown and compared in Table 5.2. A 60% saving of the energy in the winter season is observed, while a 50% saving during summer is noted. With switching taking place (optimal control strategy) in the low-cost regions of the TOU tariff function, a saving of 75.2% in cost can be observed for winter season while in summer a total savings in electricity cost of 60.5% made. The results of this comparison highlights the importance of avoiding the use of electricity during high demand periods.

Table 5.2 Daily energy consumption and savings

Strategy / Season	Baseline (ESTWH)		Optimal control (SWH/ESTWH)		Daily Savings (ZAR)	Daily Savings (%)	
	Energy (kWh)	Cost (ZAR)	Energy (kWh)	Cost (ZAR)	Cost	Energy	Cost
Winter	3.75	10.08	1.5	2.68	7.40	60	75.2
Summer	1.5	2.28	0.75	0.90	1.38	50	60.5

5.3.1.4 Annual energy consumption and savings

The total cost saving is calculated over the period of one year by using the data in Table 5.2. According to Eskom's tariff structure, the winter season is a total of 92 days, whereas the summer duration is 273 days. The product of the number of days in the season and the cost saving for the respective season can equate to the total seasonal savings. When adding the savings of the two seasons, an approximate annual saving in electricity cost can be obtained. Using this method, the savings in 2017 were calculated and shown in Table 5.3.

Table 5.3 Annual energy consumption and savings

Strategy / Season	Baseline (ESTWH)		Optimal control (SWH/ESTWH)		Annual Savings (ZAR)	Annual Savings (%)	
	Energy (kWh)	Cost (ZAR)	Energy (kWh)	Cost (ZAR)	Cost	Energy	Cost
Winter	345	927.36	138	246.56	680.8	60	75.2
Summer	409.5	622.44	204.75	245.70	376.74	50	60.5
Total	754.5	1549.80	342.75	492.26	1057.54	52.52	64.21

5.4 LIFE CYCLE COST ANALYSIS

In order to reduce the margin of error, a project lifetime of 20 years was chosen for the hybrid system. The 20 year lifetime was chosen based on the guaranteed collector lifetime being 10 years, however several reports have shown the lifetime reaching over 30 years. Hence the average number of years between guaranteed and actual reported lifespan was chosen.

The salvage costs were taken as 20% of the initial cost of implementation for both the baseline and the hybrid water heating system, this accounts for replacement upgrades to more efficient systems in the future.

The replacement cost is calculated using Eq. (5.2). With the average inflation rate shown in Fig. 5.3., the future costs of components can be predicted by assuming that the average inflation rate will be equal to the interest rate [133].

$$C_{rep} = \sum_{k=1}^{N_{rep}} C_{cap}.k(1+n.r) \tag{5.2}$$

Where;

C_{cap} is the initial capital cost for each component (given in Table 5.3),

N_{rep} is the number of component replacements of the 20-year lifetime,

n is the lifespan for a specific component (years),

r is the average inflation rate shown as 5.49% in Fig. 5.3.

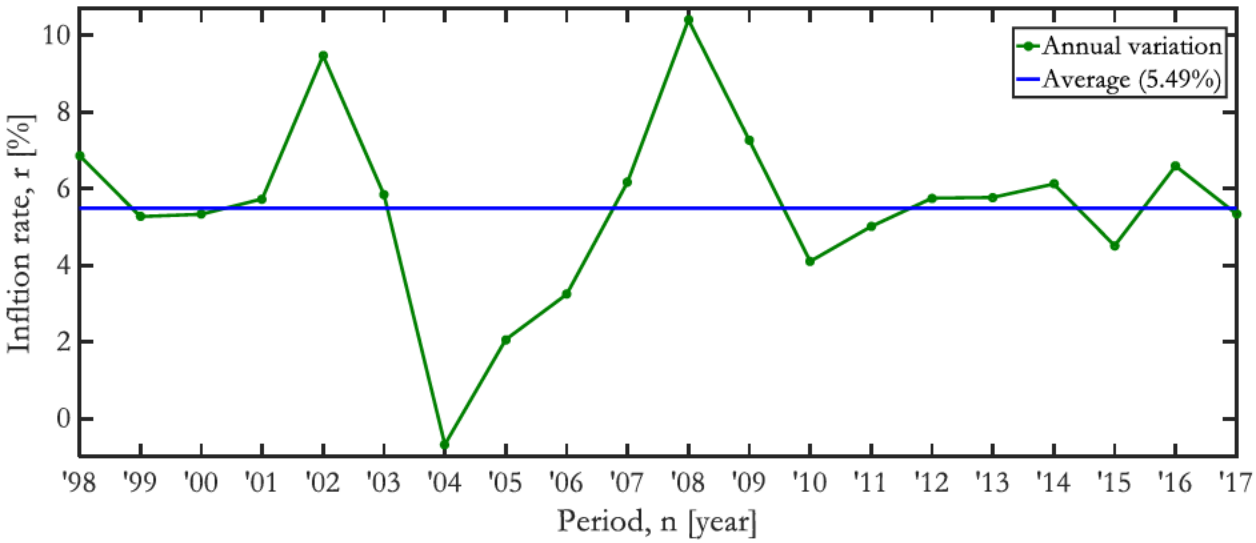

Figure 5.3: Inflation rate of South Africa from 1998 to 2017 (Adapted from Ref. [137])

5.4.1 Baseline (ESTWH) life cycle cost analysis

The total replacement costs (C_{rep}) over the 20-year lifespan for the baseline (ESTWH) are shown in Table 5.4, the ESTWH has only one component, therefore the total lifecycle replacement costs ($C_{rep-BTC}$) is equal to the replacement costs of the ESTWH as denoted in Eq. 5.3.

$$C_{rep-BTC} = C_{rep-ESTWH} \tag{5.3}$$

Eq. 5.2 is used to calculate the total replacement cost ($C_{rep-ESTWH}$) over the project lifespan and the results are noted in Table 5.4.

Table 5.4: Total replacement cost for the ESTWH

Parameters	Value
150L GAP ESTWH lifetime (years)	7
$N_{rep-ESTWH}$	2
$C_{rep-ESTWH}$	8072.68
$C_{rep-BTC}$	8072.68

The cumulative electricity costs incurred over a 20-year lifespan for the baseline system is shown in Appendix B. The cumulative cost of energy for the first year was taken from Table 5.3. The cost at the end of year 20 equates to the total cumulative electricity cost (C_{EC}), with an increase of 10% annually taken into account, shown in Eq. 5.4.

$$C_{EC} = \sum_{k=1}^{20} C_{initial-EC}.k(1+a) \tag{5.4}$$

Where;

$C_{inititail-EC}$ is the cumulative cost of energy at the end of year one (ZAR),

k represents the year at which the cumulative cost should be calculated (years),

a is the annual increase of 10%.

The operation and maintenance costs at the end of each year (i) of the ESTWH can be taken as 1% of the initial implementation cost, so that Eq. (5.5) will be:

$$C_{OM} = \sum_{k=1}^{20} C_{initial-OM}.k(1+r) \tag{5.5}$$

The initial cost of implementation ($C_{initial}$), equal to R2560.40 shown in Table 5.1 is the cost of the ESTWH.

A salvage cost ($C_{salvage}$) is 20% of the initial implementation cost ($C_{initial}$) of the ESTWH, can be calculated using Eq. 5.6.

$$C_{salvage} = 0.2 \cdot C_{initial} \tag{5.6}$$

The addition of Eqs. (5.2-5.5) and the subtraction of the salvage cost ($C_{salvage}$) will be equal to the total life cycle cost for the ESTWH in Eq. (5.7):

$$LCC_{ESTWH} = C_{initial} + C_{rep-BTC} + C_{EC} + C_{OM} - C_{salvage} \tag{5.7}$$

The total lifecycle cost value LCC_{EST-WH} (ZAR) using Eq. (5.7), is shown in Table 5.5. Over a 20-year project lifetime, a total amount of approximately R 99 777.47 will be spent in the case of the ESTWH.

Table 5.5: Total life cycle cost for the ESTWH

Cumulative Cost	Value (ZAR)
$C_{initial}$	2560.40
$C_{rep-BTC}$	8072.68
C_{OM}	891.68
C_{EC}	88 764.79
$C_{salvage}$	512.08
LCC_{ESTWH}	99 777.47

5.4.2 Hybrid system with optimal scheduling life cycle cost analysis

Table 5.6: Total replacement cost for the SWH/ESTWH

Parameters	Value
Hybrid system lifetime, n (years)	20
150L GAP FPC lifetime (years)	20
N_{rep-SC} (-)	0
C_{rep-SC} (ZAR)	0
150L GAP ESTWH lifetime (years)	7
$N_{rep-ESTWH}$ (-)	2
$C_{rep-ESTWH}$ (ZAR)	8072.68
Geyserwize Max controller lifetime (years)	7
$N_{rep-CONT}$ (-)	2
$C_{rep-CONT}$ (ZAR)	3853.10
Air release valve (years)	20
$N_{rep-ARV}$ (-)	0
$C_{rep-ARV}$ (ZAR)	0
Circulation pump (years)	12
N_{rep-CP} (-)	1
C_{rep-CP} (ZAR)	2363.79
22mm thermostatic mixing valve lifetime (years)	20
$N_{rep-TMV}$ (-)	0
$C_{rep-TMV}$ (ZAR)	0
C_{rep-TC} (ZAR)	14289.56

In the case of the hybrid system, several more components exist with different life expectancies so that the total replacement costs (C_{rep}), calculated using Eq. 5.2, over the 20-year project lifespan for all the hybrid system's components shown in Table 5.6 is added in order to get the total lifecycle replacement costs (C_{rep-TC}) denoted in Eq. (5.8).

$$C_{rep-TC} = C_{rep-SC} + C_{rep-ESTWH} + C_{rep-CONT} + C_{rep-ARV} + C_{rep-CP} + C_{rep-TMV} \quad (5.8)$$

The same method for cumulative electricity cost with an annual 10% increment was calculated for the hybrid system using Eq. (5.4) as well as for the salvage cost and the cumulative operation and maintenance costs for the HSWS in Eq. (5.5) and (5.6), respectively. Eq. (5.9) shows the calculation of the life cycle cost for the HSWS.

$$LCC_{HSWH} = C_{initial} + C_{rep-TC} + C_{OM} + C_{EC} - C_{salvage} \quad (5.9)$$

Table 5.7: Total life cycle cost for the HSWH with optimal scheduling

Cumulative Cost	Value (ZAR)
$C_{initial}$	7518.43
C_{rep-TC}	14 289.56
C_{OM}	2618.61
C_{EC}	28 194.19
$C_{salvage}$	1503.69
LCC_{HSWH}	51 117.10

The total lifecycle cost value LCC_{HSWH} (ZAR) using Eq. (5.9), with the data shown in Table 5.7 is calculated. Over a 20-year project lifetime, a total amount of approximately R51 117.10 will be spent in the case of the SWH with an optimal energy management scheme implemented.

5.4.3 Break-even point (BEP)

The break-even point is determined when the total implementation and operating costs of two systems incurred are equal. In this case, the baseline water heater is compared to the proposed hybrid system with the optimal energy management scheme in terms of the total cumulative annual energy cost in the project lifetime of 20 years.

The cumulative cost curves which includes the initial investment cost and the total annual costs incurred over this period for the baseline and optimal hybrid system is plotted on the same axis. The intersect point of these two curves shows the point in time (years) at which the two systems breaks even.

From Table 5.1, the initial total cost of implementation of the hybrid and the standalone ESTWH is R7518.43 and R2560.40 respectively. These values are therefore starting points of the two curves in Fig. 5.3. After the first year has passed the total annual cost of energy is added to the initial investment cost, which is the total present cost of energy shown in Table 5.2. This equates to the total cumulative cost for the first year after implementation. For the second year after implementation, a 10% increase in the price of electricity is taken into account to calculate the annual energy costs, this amount is again added to the previous total cumulative cost of the first year. The same method is followed for years 3 to 10 in Fig. 5.3. In this curve, the replacement costs and lifetimes of all the components are taken into account for increased accuracy of cumulative cost representation. From Fig. 5.3, a clear observation can be made that the break-even point occurs early in the project lifetime. In 3.5 years, the costs incurred are equal at R 10 360 and the differences in total money spent at the end of the project lifetime also presents an important economic performance indicator and is discussed in section 5.3.4.

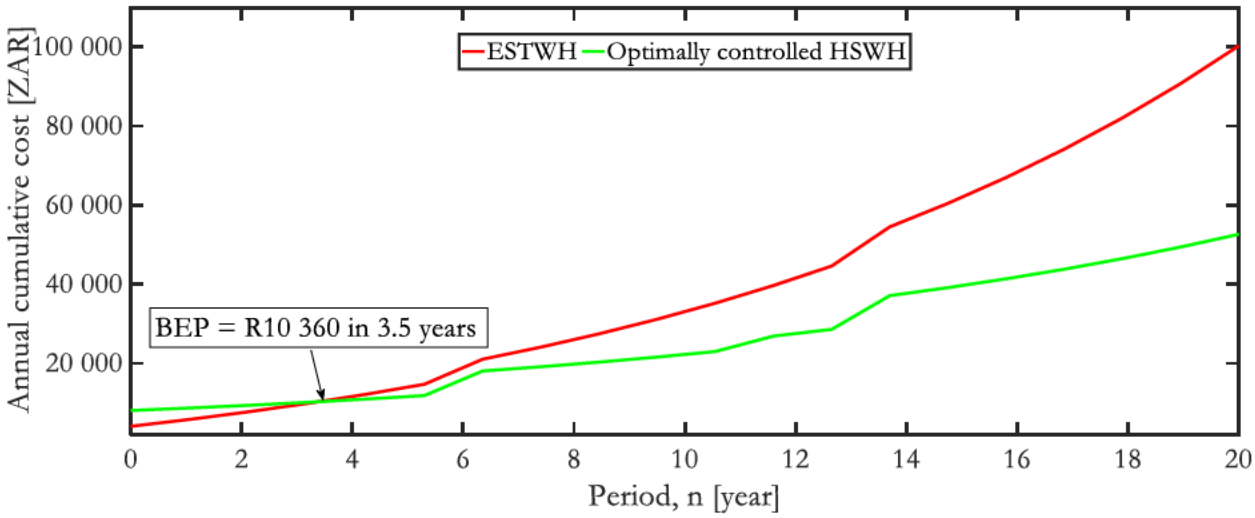

Figure 5.3: Break-even point

5.4.4 Life cycle cost comparison

The life cycle costs for the traditional electric storage tank water heater as well as for the hybrid system with optimal energy management scheme is compared in Table 5.8. The break-even point analysis shows the time it will take for cumulative cost equalization. The difference in LCC is calculated in order note the savings in cost at the end of the project lifetime.

Table 5.8: Life cycle cost comparison

LCC	Value (ZAR)
LCC_{ESTWH} (ZAR)	99 777.47
LCC_{HSWH} (ZAR)	51 117.10
Total savings over 20 years (ZAR)	48 660.37

From Table 5.8, the conclusion can be made that in the long run (over the 20-year project lifetime of the system), an approximate saving of R48 660.37 can be made if the HSWH with optimal energy management system was implemented. This translates into a saving of 49%.

The detailed life cycle cost breakdown is shown in Appendix B, illustrating the cumulative costs after each year.

5.5 SUMMARY

In this chapter, the cost effectiveness of the hybrid solar/electric water heating system was evaluated. The differences in cumulative energy consumption and costs were noted so that the annual energy usage and cost savings comparisons could be made.

A break-even point analysis was done in order to calculate when the proposed system would have an equivalent cumulative cost compared to the baseline system. The analysis showed that after 3.5 years, the cumulative costs were lower for the proposed system as opposed to the baseline. It was observed that after the break-even point, the difference in cumulative costs significantly increased with the baseline cost following an exponential trend.

The break-even point analysis was followed by a thorough life cycle cost evaluation so that the savings over a project lifetime of 20 years could be calculated. The LCC comparison of the proposed system with respect to the baseline presented a R48 660.37 saving in cost over the project lifetime. In order to put this in perspective, a saving of 49% in cost was calculated. Therefore, the LCC analysis substantiates the hypothesis in Chapter I section 1.6 that the traditional water heating system (baseline), has a lower initial investment cost, however in the long term it will incur much higher costs compared to the proposed system.

The LCC calculations for both systems included a relatively low interest rate, which in the real terms, can increase the costs of replacements of components if it were to be higher than the average calculated 5.49%. Furthermore, a 10 % increase in electricity cost can also be seen as a conservative assumption due to the fact that past increments in cost was much higher in comparison. With this in mind, it can be said that the calculated 49% saving in cost can be observed as the minimum saving that could be achieved with the proposed system.

CHAPTER VI: CONCLUSION

6.1 FINAL CONCLUSIONS

This Chapter serves as a conclusion on the research done on the optimal operation control and simulation of a hybrid energy system consisting of a solar collector array, electric storage tank water heater and all associated components.

This work developed an optimal control strategy model wherein the operation was simulated using the exogenous variables that would represent a typical winter and summer day in Bloemfontein. The winter and summer periods as defined by the TOU tariff structure implemented by the electricity supplier of South Africa, was from June to August (winter) and September to May (summer).

The major concern addressed in this research was the substantial energy consumption and the associated costs of operation of the most commonly used water heaters (the electric storage tank water heater) in South Africa. This research was based on the assumption that an optimal control strategy implemented on a hybrid solar electric water heater can reduce the energy costs when compared to traditional methods used for the heating of water. The aim, therefore, was to develop an optimization tool to minimize the daily operation costs of the hybrid system.

In order to define the operation of the hybrid system mathematically, the model of the hybrid system has been developed and described in Chapter III. The emphasis was on the minimization of energy cost, discomfort and the differential between the initial and final thermal energy states of the storage tank. While in the same chapter, the appropriate solver was chosen and described.

In Chapter IV, all the component sizes and parameters of the hybrid solar electric water heater, the detailed time-based pricing structure applicable for the case study, simulation parameters, variable input and load data was presented. A baseline was established which represented the operation of a thermostat temperature controlled ESTWH. The baseline as well as the optimal control model has been simulated and the results obtained were presented.

The presented results illustrate a considerable annual energy saving of 52.52%, while maintaining the desired temperature when compared to the baseline model. The potential annual cost savings in energy was shown to be 64.21%.

Chapter V presented an economic analysis based on the cost savings obtained in Chapter IV. The bill of quantities of the hybrid water heater with all the relevant components were included with the aim to determine the life cycle cost and break-even point. The analysis revealed that the hybrid system was economically feasible with a potential cost saving of 49% and a break-even point of 3.5 years.

The inconsistencies in daily operation cost realised for the two respective seasons, highlight the potential of the suggested optimization strategy to reduce energy consumption for the hybrid system as opposed to the ESTWH only scenario. These results furthermore prove that it is imperative to take into consideration the seasonal variations of the input variables, when calculating the daily operation cost of the system.

6.2 SUGGESTIONS FOR FURTHER RESEARCH

This dissertation has been presented as part of an ongoing research project at the Central University of Technology, the next step might include real time closed loop modelling and implementation of the system. This dissertation is not the conclusion on optimal control of a HSWH, several questions remain. This study focused on the case of Bloemfontein, the research could be adapted to fit different geographical locations with different input parameters, which might in turn change the configuration of the hybrid system.

The demand profile, renewable resources and environmental data used for simulation in this work have been collected on a 15-minute basis. Promising results might be obtained if minute averaged data could be used over an annual control horizon with the aim of evaluating the performance of the developed model in terms of results accuracy. The drawback of such an approach, while it is apparent that SCIP solver is one of the fastest solvers available in the Matlab interface OPTI toobox, is that the simulation time of such an undertaking could last significantly longer.

REFERENCES

[1] Qase, N, 2015. State of Renewable Energy in South Africa. 1st ed. Matimba House, 192 Visagie Str, Pretoria, South Africa: Department of Energy.

[2] Gets, A. 2013. Powering the Future: Renewable Energy Roll-out in South Africa. Prepared for Greenpeace Africa by AGAMA Energy (Pty) Ltd Cape Town, South Africa

[3] Eskom 2015/2016, Schedule of Standard Prices for Eskom Tariffs. (Accessed 12 February 2016). Available at:

http://www.eskom.co.za/CustomerCare/TariffsAndCharges/WhatsNew/Documents/Eskom%20Schedule%20of%20Std%20Prices%202015_16%20excl%20Transflex.pdf

[4] Delport GJ. The Geyser Gadgets that work / do not work. Paper presented at the 13th Domestic Use of Electrical Energy Conference, Cape Town, 29 - 31 March 2005. Paper included in the conference proceedings, page 139 - 144.

[5] Strickhouser, AE, 2007. Legionella pneumophila in Domestic Hot Water Systems: Evaluation of Detection Methods and Environmental Factors Affecting Survival. Master of Science in Environmental Engineering . Blacksburg, Virginia: Virginia Polytechnic Institute and State University.

[6] Quinn, C, 2013. Legionnaires' Disease Outbreak at a Long-Term Care Facility Caused by a Cooling Tower Using an Automated Disinfection System—Ohio, 2013. Advancement of the Science, 78, 5.

[7] Moodaly, A, 2008. The Modelling of solar radiation quantities and intensities in a two dimentional compound parabolic collector. Magister Ingeneriae. Johannesburg, South Africa: University of Johannesburg.

[8] Coetzee, RP, 2009. The development of a methodology to measure & verify the impact of a national solar water heating program. Magister lngeneriae . Potchefstroom, South Africa: North-West University. pp13

[9] Lutz, James D., Gary Klein, David Springer, and Bion D. Howard. "Residential hot water distribution systems: Roundtable session." Lawrence Berkeley National Laboratory (2002).

[10] Delport, G. J. "The Geyser Gadgets that work/do not work." In Proceedings of the 13th Domestic Use of Energy Conference, pp. 139-144. 2005.

[11] Sowmy, Daniel Setrak, and Racine TA Prado. "Assessment of energy efficiency in electric storage water heaters." Energy and Buildings 40, no. 12 (2008): 2128-2132.

[12] Milward, R., and J. Prijyanonda. "Electric tankless water heating: competitive assessment." Global Energy Partners, LLC, Lafayette, CA (2005): 1285-5.

[13] cres.sun.ac.za, "SolarGIS GHI South Africa" 2017, [Online]. Available at:

www.crses.sun.ac.za/files/research/publications/SolarGIS_GHI_South_Africa_width15cm_300dpi.png [Accessed: 02- November- 2017]

[14] Le Roux, Willem Gabriel. "Optimum tilt and azimuth angles for fixed solar collectors in South Africa using measured data." Renewable Energy 96 (2016): 603-612.

[15] Zhao, Dongliang, Christine Elizabeth Martini, Siyu Jiang, Yaoguang Ma, Yao Zhai, Gang Tan, Xiaobo Yin, and Ronggui Yang. "Development of a single-phase thermosiphon for cold collection and storage of radiative cooling." Applied Energy205 (2017): 1260-1269.

[16] Joubert, E. C., S. Hess, and J. L. Van Niekerk. "Large-scale solar water heating in South Africa: Status, barriers and recommendations." Renewable Energy 97 (2016): 809-822.

[17] Jamar, A. M. Z. A. A., Z. A. A. Majid, W. H. Azmi, M. Norhafana, and A. A. Razak. "A review of water heating system for solar energy applications." International Communications in Heat and Mass Transfer 76 (2016): 178-187.

[18] Roberts, D. E. "A figure of merit for selective absorbers in flat plate solar water heaters." Solar Energy 98 (2013): 503-510.

[19] Ayompe, L. M., and Aidan Duffy. "Thermal performance analysis of a solar water heating system with heat pipe evacuated tube collector using data from a field trial." Solar Energy 90 (2013): 17-28.

[20] Mohammed, Ibrahim Ladan. "Design and development of a parabolic dish solar water heater." International Journal of Engineering Research and Applications 2, no. 1 (2012).

[21] Eickhoff, Martin. "Parabolic trough collector." U.S. Patent 7,240,675, issued July 10, 2007.

[22] Bari, Saiful. "Optimum orientation of domestic solar water heaters for the low latitude countries." Energy Conversion and Management 42, no. 10 (2001): 1205-1214.

[23] Kakaza, M., and K. A. Folly. "Effect of solar water heating system in reducing household energy consumption." IFAC-PapersOnLine48, no. 30 (2015): 468-472.

[24] Hepbasli, Arif, and Yildiz Kalinci. "A review of heat pump water heating systems." Renewable and Sustainable Energy Reviews13, no. 6 (2009): 1211-1229.

[25] Bourke, Grant, Pradeep Bansal, and Robert Raine. "Performance of gas tankless (instantaneous) water heaters under various international standards." Applied Energy 131 (2014): 468-478.

[26] Boros, Jozef, Qian Zhang, Yoshiki Semba, and Subbu Thenappan. "High efficiency gas-fired water heater." U.S. Patent 9,004,018, issued April 14, 2015.

[27] Waddicor, David A., Elena Fuentes, Marc Azar, and Jaume Salom. "Partial load efficiency degradation of a water-to-water heat pump under fixed set-point control." Applied Thermal Engineering 106 (2016): 275-285.

[28] Park, Hansaem, Ki Hwan Nam, Gi Hyun Jang, and Min Soo Kim. "Performance investigation of heat pump–gas fired water heater hybrid system and its economic feasibility study." Energy and Buildings 80 (2014): 480-489.

[29] Tshibalo, A. E., J. Olivier, and P. K. Nyabeze. "South Africa Geothermal Country Update (2010-2014)." (2015).

[30] Han, Chanjuan, and Xiong Bill Yu. "Sensitivity analysis of a vertical geothermal heat pump system." Applied Energy 170 (2016): 148-160.

[31] N. Naili, M Hazami "Assessment of surface geothermal energy for air conditioning in northern Tunisia: Direct test and deployment of ground source heat pump system" Energy and Buildings (111) (2016), pp. 207-217

[32] Su, Di, Yuting Jia, Xiang Huang, Guruprasad Alva, Yaojie Tang, and Guiyin Fang. "Dynamic performance analysis of photovoltaic–thermal solar collector with dual channels for different fluids." Energy Conversion and Management 120 (2016): 13-24.

[33] Huang, B. J., T. H. Lin, W. C. Hung, and F. S. Sun. "Performance evaluation of solar photovoltaic/thermal systems." Solar energy70, no. 5 (2001): 443-448.

[34] Chow, Tin Tai. "A review on photovoltaic/thermal hybrid solar technology." Applied energy 87, no. 2 (2010): 365-379.

[35] Abas, N., N. Khan, A. Haider, and M. S. Saleem. "A thermosyphon solar water heating system for sub-zero temperature areas." Cold Regions Science and Technology 143 (2017): 81-92.

[36] Aguilar, F. J., S. Aledo, and P. V. Quiles. "Experimental study of the solar photovoltaic contribution for the domestic hot water production with heat pumps in dwellings." Applied Thermal Engineering 101 (2016): 379-389.

[37] Ferrer, Philippe Alberto Friedrich. "Average economic performance of solar water heaters for low density dwellings across South Africa." Renewable and Sustainable Energy Reviews 76 (2017): 507-515.

[38] Atikol, U., and L. B. Y. Aldabbagh. "The impact of two-stage discharging on the exergoeconomic performance of a storage-type domestic water-heater." Energy 83 (2015): 379-386.

[39] Bagarella, G., R. Lazzarin, and M. Noro. "Annual simulation, energy and economic analysis of hybrid heat pump systems for residential buildings." Applied Thermal Engineering 99 (2016): 485-494.

[40] Benrejeb, Raouf, Olfa Helal, and Bechir Chaouachi. "Optical and thermal performances improvement of an ICS solar water heater system." Solar Energy 112 (2015): 108-119.

[41] Benrejeb, Raouf, Olfa Helal, and Béchir Chaouachi. "Optimization of the geometrical characteristics of an ICS solar water heater system using the two-level experience planning." Applied Thermal Engineering 103 (2016): 1427-1440.

[42] Benrejeb, Raouf, Olfa Helal, and Bechir Chaouachi. "Study of the effect of truncation on the optical and thermal performances of an ICS solar water heater system." Solar Energy 132 (2016): 84-95.

[43] Bleicher, Alena, and Matthias Gross. "Geothermal heat pumps and the vagaries of subterranean geology: Energy independence at a household level as a real-world experiment." Renewable and Sustainable Energy Reviews 64 (2016): 279-288.

[44] Bourke, Grant, and Pradeep Bansal. "New test method for gas boosters with domestic solar water heaters." Solar Energy 86, no. 1 (2012): 78-86.

[45] Bourke, Grant, Pradeep Bansal, and Robert Raine. "Performance of gas tankless (instantaneous) water heaters under various international standards." Applied Energy 131 (2014): 468-478.

[46] Bovand, M., Saman Rashidi, and J. A. Esfahani. "Heat transfer enhancement and pressure drop penalty in porous solar heaters: Numerical simulations." Solar Energy 123 (2016): 145-159.

[47] Browne, Maria C., Brian Norton, and Sarah J. McCormack. "Heat retention of a photovoltaic/thermal collector with PCM." Solar Energy 133 (2016): 533-548.

[48] Calise, Francesco, Massimo Dentice d'Accadia, Rafal Damian Figaj, and Laura Vanoli. "A novel solar-assisted heat pump driven by photovoltaic/thermal collectors: Dynamic simulation and thermoeconomic optimization." Energy 95 (2016): 346-366.

[49] Carnevale, E., L. Lombardi, and L. Zanchi. "Life Cycle Assessment of solar energy systems: Comparison of photovoltaic and water thermal heater at domestic scale." Energy 77 (2014): 434-446.

[50] Das, Debayan, and Tanmay Basak. "Role of distributed/discrete solar heaters during natural convection in the square and triangular cavities: CFD and heatline simulations." Solar Energy135 (2016): 130-153.

[51] Del Col, Davide, Marco Azzolin, Giacomo Benassi, and Mauro Mantovan. "Energy efficiency in a ground source heat pump with variable speed drives." Energy and Buildings 91 (2015): 105-114.

[52] W Deng, Weishi, and Jianlin Yu. "Simulation analysis on dynamic performance of a combined solar/air dual source heat pump water heater." Energy Conversion and Management 120 (2016): 378-387.

[53] Deng, Yuechao, Yaohua Zhao, Zhenhua Quan, and Tingting Zhu. "Experimental study of the thermal performance for the novel flat plate solar water heater with micro heat pipe array absorber." Energy Procedia 70 (2015): 41-48.

[54] Der, Joseph P., Larry W. Kostiuk, and André G. McDonald. "Analysis of the performance of a tankless water heating combo system: Simultaneous space heating and domestic hot water operation." Energy and Buildings 135 (2017): 50-61.

[55] Devanarayanan, K., and K. Kalidasa Murugavel. "Integrated collector storage solar water heater with compound parabolic concentrator–development and progress." Renewable and Sustainable Energy Reviews 39 (2014): 51-64.

[56] Gong, J., and K. Sumathy. "Active solar water heating systems." Advances in Solar Heating and Cooling 15 (2016): 203.

[57] Zou, Deqiu, Xianfeng Ma, Xiaoshi Liu, Pengjun Zheng, Baiming Cai, Jianfeng Huang, Jiangrong Guo, and Mo Liu. "Experimental research of an air-source heat pump water heater using water-PCM for heat storage." Applied Energy 206 (2017): 784-792.

[58] Hafez, A. Z., A. M. Attia, H. S. Eltwab, A. O. ElKousy, A. A. Afifi, A. G. AbdElhamid, A. N. AbdElqader et al. "Design analysis of solar parabolic trough thermal collectors." Renewable and Sustainable Energy Reviews 82 (2018): 1215-1260.

[59] A. Hepbasli, Y. Kalinci "A review of heat pump water heating systems" Renewable and Sustainable Energy Reviews (13) (6-7) (2009), pp. 1211-1229

[60] Higgins, Andrew, Cheryl McNamara, and Greg Foliente. "Modelling future uptake of solar photo-voltaics and water heaters under different government incentives." Technological Forecasting and Social Change 83 (2014): 142-155.

[61] Huang, B. J., J. H. Wang, J. H. Wu, and P. E. Yang. "A fast response heat pump water heater using thermostat made from shape memory alloy." Applied Thermal Engineering 29, no. 1 (2009): 56-63.

[62] Ibrahim, Oussama, Farouk Fardoun, Rafic Younes, and Hasna Louahlia-Gualous. "Optimal management proposal for hybrid water heating system." Energy and Buildings 75 (2014): 342-357.

[63] Ibrahim, Oussama, Farouk Fardoun, Rafic Younes, and Hasna Louahlia-Gualous. "Review of water-heating systems: General selection approach based on energy and environmental aspects." Building and Environment 72 (2014): 259-286.

[64] Johnson, Geoffrey, and Ian Beausoleil-Morrison. "The calibration and validation of a model for predicting the performance of gas-fired tankless water heaters in domestic hot water applications." Applied Energy 177 (2016): 740-750.

[65] Kato, Takeyoshi, and Yasuo Suzuoki. "Autonomous scheduling of heat-pump water heaters for mitigating voltage rise caused by photovoltaic power generation systems." Applied Thermal Engineering 71, no. 2 (2014): 652-657.

[66] Keinath, Christopher M., and Srinivas Garimella. "An energy and cost comparison of residential water heating technologies." Energy 128 (2017): 626-633.

[67] Keinath, Christopher Mahlo. "Direct-fired heat pump for multi-pass water heating using microchannel heat and mass exchangers." PhD diss., Georgia Institute of Technology, 2015.

[68] Kepplinger, Peter, Gerhard Huber, and Jörg Petrasch. "Autonomous optimal control for demand side management with resistive domestic hot water heaters using linear optimization." Energy and Buildings 100 (2015): 50-55.

[69] Kepplinger, Peter, Gerhard Huber, and Jörg Petrasch. "Field testing of demand side management via autonomous optimal control of a domestic hot water heater." Energy and Buildings 127 (2016): 730-735.

[70] Li, Kaichun, Tong Li, Hanzhong Tao, Yuanxue Pan, and Jingshan Zhang. "Numerical investigation of flow and heat transfer performance of solar water heater with elliptical collector tube." Energy Procedia 70 (2015): 285-292.

[71] Li, Shanshan, Shuhong Li, and Xiaosong Zhang. "Comparison analysis of different refrigerants in solar-air hybrid heat source heat pump water heater." International Journal of Refrigeration 57 (2015): 138-146.

[72] Liu, Zhongbao, Pengyan Fan, Qinghua Wang, Ying Chi, Zhongqian Zhao, and Yuanying Chi. "Air source heat pump with water heater based on a bypass-cycle defrosting system using compressor casing thermal storage." Applied Thermal Engineering (2017).

[73] Michael, Jee Joe, and S. Iniyan. "Performance of copper oxide/water nanofluid in a flat plate solar water heater under natural and forced circulations." Energy Conversion and Management 95 (2015): 160-169.

[74] Milani, Dia, and Ali Abbas. "Multiscale modeling and performance analysis of evacuated tube collectors for solar water heaters using diffuse flat reflector." Renewable Energy 86 (2016): 360-374.

[75] Moreau, Alain. "Control strategy for domestic water heaters during peak periods and its impact on the demand for electricity." Energy Procedia 12 (2011): 1074-1082.

[76] Murali, G., and K. Mayilsamy. "Effect of Latent Thermal Energy storage and inlet locations on enhancement of stratification in a solar water heater under discharging mode." Applied Thermal Engineering 106 (2016): 354-360.

[77] Paull, Liam, Howard Li, and Liuchen Chang. "A novel domestic electric water heater model for a multi-objective demand side management program." Electric Power Systems Research 80, no. 12 (2010): 1446-1451.

[78] Peng, Jing-Wei, Hui Li, and Chun-Lu Zhang. "Performance comparison of air-source heat pump water heater with different expansion devices." Applied Thermal Engineering 99 (2016): 1190-1200.

[79] Qu, Minglu, Jianbo Chen, Linjie Nie, Fengshu Li, Qian Yu, and Tan Wang. "Experimental study on the operating characteristics of a novel photovoltaic/thermal integrated dual-source heat pump water heating system." Applied Thermal Engineering 94 (2016): 819-826.

[80] Saravanan, A., J. S. Senthilkumaar, and S. Jaisankar. "Performance assessment in V-trough solar water heater fitted with square and V-cut twisted tape inserts." Applied Thermal Engineering 102 (2016): 476-486.

[81] R Sathyamurthy, D. G. Harris Samuel "Theoretical analysis of inclined solar still with baffle plates for improving the fresh water yield" Process Safety and Environmental Protection (101) (2016), pp 93-107

[82] Scarpa, Federico, Luca A. Tagliafico, and Vincenzo Bianco. "A novel steady-state approach for the analysis of gas-burner supplemented direct expansion solar assisted heat pumps." Solar Energy 96 (2013): 227-238.

[83] Shan, Feng, Lei Cao, and Guiyin Fang. "Dynamic performances modeling of a photovoltaic–thermal collector with water heating in buildings." Energy and Buildings 66 (2013): 485-494.

[84] Xue, H. Sheng. "Experimental investigation of a domestic solar water heater with solar collector coupled phase-change energy storage." Renewable Energy 86 (2016): 257-261.

[85] Sichilalu, S., X. Xia, and J. Zhang. "Optimal scheduling strategy for a grid-connected photovoltaic system for heat pump water heaters." Energy Procedia 61 (2014): 1511-1514.

[86] Sichilalu, Sam M., and Xiaohua Xia. "Optimal power dispatch of a grid tied-battery-photovoltaic system supplying heat pump water heaters." Energy Conversion and Management 102 (2015): 81-91.

[87] Sichilalu, S. M., and X. Xia. "Optimal power control of grid tied PV-battery-diesel system powering heat pump water heaters." Energy Procedia 75 (2015): 1514-1521.

[88] Sichilalu, Sam, Tebello Mathaba, and Xiaohua Xia. "Optimal control of a wind–PV-hybrid powered heat pump water heater." Applied energy 185 (2017): 1173-1184.

[89] Sichilalu, Sam, Henerica Tazvinga, and Xiaohua Xia. "Optimal control of a fuel cell/wind/PV/grid hybrid system with thermal heat pump load." Solar Energy 135 (2016): 59-69.

[90] Singh, Ramkishore, Ian J. Lazarus, and Manolis Souliotis. "Recent developments in integrated collector storage (ICS) solar water heaters: A review." Renewable and Sustainable Energy Reviews54 (2016): 270-298.

[91] Tang, Runsheng, Yanbin Cheng, Maogang Wu, Zhimin Li, and Yamei Yu. "Experimental and modeling studies on thermosiphon domestic solar water heaters with flat-plate collectors at clear nights." Energy Conversion and Management 51, no. 12 (2010): 2548-2556.

[92] Tang, Runsheng, and Yuqin Yang. "Nocturnal reverse flow in water-in-glass evacuated tube solar water heaters." Energy Conversion and Management 80 (2014): 173-177.

[93] Tanha, Kamyar, Alan S. Fung, and Rakesh Kumar. "Performance of two domestic solar water heaters with drain water heat recovery units: Simulation and experimental investigation." Applied Thermal Engineering 90 (2015): 444-459.

[94] Tinti, Francesco, Alberto Barbaresi, Daniele Torreggiani, Davide Brunelli, Marco Ferrari, Andrea Verdecchia, Emanuele Bedeschi, Patrizia Tassinari, and Roberto Bruno.

"Evaluation of efficiency of hybrid geothermal basket/air heat pump on a case study winery based on experimental data." Energy and Buildings 151 (2017): 365-380.

[95] Tsai, Huan-Liang. "Modeling and validation of refrigerant-based PVT-assisted heat pump water heating (PVTA–HPWH) system." Solar Energy 122 (2015): 36-47.

[96] Tse, Ka-Kui, and Tin-Tai Chow. "Dynamic model and experimental validation of an indirect thermosyphon solar water heater coupled with a parallel circular tube rings type heat exchange coil." Solar Energy 114 (2015): 114-133.

[97] Wang, Ping-Yang, Shuang-Fei Li, and Zhen-Hua Liu. "Collecting performance of an evacuated tubular solar high-temperature air heater with concentric tube heat exchanger." Energy Conversion and Management 106 (2015): 1166-1173.

[98] Wanjiru, Evan M., Sam M. Sichilalu, and Xiaohua Xia. "Optimal Operation of Integrated Heat Pump-instant Water Heaters with Renewable Energy." Energy Procedia 105 (2017): 2151-2156.

[99] Willem, H., Y. Lin, and A. Lekov. "Review of energy efficiency and system performance of residential heat pump water heaters." Energy and Buildings (2017).

[100] Wilson, R. P. "Energy conservation options for residential water heaters." Energy 3, no. 2 (1978): 149-172.

[101] Xiaowu, Wang, and Hua Ben. "Exergy analysis of domestic-scale solar water heaters." Renewable and Sustainable Energy Reviews9, no. 6 (2005): 638-645.

[102] Yan, Chengchu, Shengwei Wang, Zhenjun Ma, and Wenxing Shi. "A simplified method for optimal design of solar water heating systems based on life-cycle energy analysis." Renewable Energy74 (2015): 271-278.

[103] Yang, Liang, Han Yuan, Jing-Wei Peng, and Chun-Lu Zhang. "Performance modeling of air cycle heat pump water heater in cold climate." Renewable Energy 87 (2016): 1067-1075.

[104] Ziapour, Behrooz M., Vahid Palideh, and Ali Mohammadnia. "Study of an improved integrated collector-storage solar water heater combined with the photovoltaic cells." Energy Conversion and Management 86 (2014): 587-594.

[105] Zou, Bin, Jiankai Dong, Yang Yao, and Yiqiang Jiang. "An experimental investigation on a small-sized parabolic trough solar collector for water heating in cold areas." Applied Energy 163 (2016): 396-407.

[106] P.J.C. Nel, M.J. Booysen "Energy perceptions in South Africa: An analysis of behaviour and understanding of electric water heaters" Energy of Sustainable Development (32) (2016), pp. 62-70.

[107] Eskom.co.za, 'COP 17 – Solar water heating Rebate Program', 2016, [Online]. Available: http://www.eskom.co.za/AboutElectricity/FactsFigures/Documents/The_Solar_Water_Heating_SWH_Programme.pdf [Accessed: 01- October- 2017]

[108] statssa.gov.za, 'South Africa: Poverty on the rise in South Africa' 2017, [Online]. Available: http://www.statssa.gov.za/?p=10334 [Accessed: 02- November- 2017]

[109] Celia Quinn MPH, M. D., M. D. Alicia Demirjian MMSc, M. D. Louise Francois Watkins MPH, P. H. N. Sara Tomczyk MSc, Ellen Brown, Alvaro Benitez, Laurel E. Garrison et al. "Legionnaires' Disease Outbreak at a Long-Term Care Facility Caused by a Cooling Tower Using an Automated Disinfection System-Ohio, 2013." Journal of environmental health 78, no. 5 (2015): 8.

[110] A.E. Strickhouser, 2007. Legionella pneumophila in Domestic Hot Water Systems: Evaluation of Detection Methods and Environmental Factors Affecting Survival. Master of Science in Environmental Engineering.

[111] Ntsaluba, Sula, Bing Zhu, and Xiaohua Xia. "Optimal flow control of a forced circulation solar water heating system with energy storage units and connecting pipes." Renewable Energy 89 (2016): 108-124.

[112] Ko, Myeong Jin. "A novel design method for optimizing an indirect forced circulation solar water heating system based on life cycle cost using a genetic algorithm." Energies 8, no. 10 (2015): 11592-11617.

[113] Duffie, John A., and William A. Beckman. "Solar engineering of thermal processes." (1980).

[114] Giglmayr, Sebastian, Alan C. Brent, Paul Gauché, and Hubert Fechner. "Utility-scale PV power and energy supply outlook for South Africa in 2015." Renewable Energy 83 (2015): 779-785.

[115] Atia, Doaa M., Faten H. Fahmy, Ninet M. Ahmed, and Hassen T. Dorrah. "Optimal sizing of a solar water heating system based on a genetic algorithm for an aquaculture system." Mathematical and Computer Modelling 55, no. 3 (2012): 1436-1449.

[116] Sichilalu, Sam, Tebello Mathaba, and Xiaohua Xia. "Optimal control of a wind–PV-hybrid powered heat pump water heater." Applied energy (2015).

[117] EE Publishers. (2017). Energy management systems save money - EE Publishers. [online] Available at:

http://www.ee.co.za/article/energy-management-systems-save-money.html [Accessed 8 Dec. 2017].

[118] Wanjiru, Evan M., Sam M. Sichilalu, and Xiaohua Xia. "Model predictive control of heat pump water heater-instantaneous shower powered with integrated renewable-grid energy systems." Applied Energy (2017).

[119] Zhang, Jiangfeng, and Xiaohua Xia. "Best switching time of hot water cylinder-switched optimal control approach." In AFRICON 2007, pp. 1-7. IEEE, 2007.

[120] Wanjiru, Evan M., and Xiaohua Xia. "Energy-water optimization model incorporating rooftop water harvesting for lawn irrigation." Applied Energy 160 (2015): 521-53

[121] Anon, (2017). [online] Available at:

https://www.inverseproblem.co.nz/OPTI/index.php/Probs/MINLP [Accessed 8 Dec. 2017].

[122] Sauran.net. (2017). Station Details - Southern African Universities Radiometric Network. [online] Available at:

http://www.sauran.net/ShowStation.aspx?station=7 [Accessed 8 Dec. 2017].

[123] Ratikane, Mosepeli. "Quality of drinking water sources in the Bloemfontein area of the Mangaung Metropolitan Municipality." PhD diss., Bloemfontein: Central University of Technology, Free State, 2013.

[124] Meyer, J. P., and M. Tshimankinda. "Domestic hot-water consumption in South African apartments." Energy 23, no. 1 (1998): 61-66.

[125] Ko, Myeong Jin. "Multi-Objective Optimization Design for Indirect Forced-Circulation Solar Water Heating System Using NSGA-II." Energies 8, no. 11 (2015): 13137-13161.

[126] Eskom Rebates For Solar Water Heating Systems | GeoSolar | Geo Group", Geogroup.co.za, 2017. [Online]. Available at: http://www.geogroup.co.za/solar-heating/solar-water-heating-systems/eskom-solar-heating-rebates [Accessed: 08- Dec- 2017].

[127] 150L GAP ECO ELECTRIC GEYSERS", Solar Advice, 2017. [Online]. Available: https://solaradvice.co.za/product/150l-gap-eco-electric-geyser/ [Accessed: 08- Dec- 2017].

[128] Sun & moon times today, Bloemfontein, South Africa", Timeanddate.com, 2017. [Online]. Available:

https://www.timeanddate.com/astronomy/south-africa/bloemfontein [Accessed: 08- Dec- 2017].

[129] Solar Radiation on a Tilted Surface | PVEducation", Pveducation.org, 2017. [Online]. Available:

http://www.pveducation.org/pvcdrom/properties-sunlight/solar-radiation-tilted-surface [Accessed: 08- Dec- 2017].

[130] Eskom.co.za, 2017. [Online]. Available:

http://www.eskom.co.za/CustomerCare/TariffsAndCharges/Documents/Tariff%20book%202018-2018.pdf [Accessed: 08- Dec- 2017].

[131] Cms.centlec.co.za, 2017. [Online]. Available:

http://cms.centlec.co.za/documents/CENTLEC%20Southern%20Free%20State%20Tariff%20Approval%20Letter%20201718.pdf [Accessed: 08- Dec- 2017].

[132] Harris, A., M. Kilfoil, and E. A. Uken. "Domestic energy savings with geyser blankets." (2007).

[133] Numbi, B. P., and S. J. Malinga. "Optimal energy cost and economic analysis of a residential grid-interactive solar PV system-case of eThekwini municipality in South Africa." Applied Energy 186 (2017): 28-45.

[134] Geogroup.co.za. (2017). Eskom Rebates For Solar Water Heating Systems | GeoSolar | Geo Group. [online] Available at: http://www.geogroup.co.za/solar-heating/solar-water-heating-systems/eskom-solar-heating-rebates [Accessed 21 Dec. 2017].

[135] Garden, H., Equipment, T., Hardware, D. and Geysers, G. (2017). Gap 150l Eco Electric Geysers | R2245.97 | DIY Hardware | PriceCheck SA. [online] Pricecheck.co.za. Available at:

https://www.pricecheck.co.za/offers/89825039/Gap+150l+Eco+Electric+Geysers [Accessed 21 Dec. 2017].

[136] G. Unit, "1 Price For Geyserwise Max | PriceCheck South Africa", Pricecheck.co.za, 2017. [Online]. Available:

https://www.pricecheck.co.za/search?search=geyserwise+max [Accessed: 21- Dec- 2017].

[137] T. Media, "Historic inflation South Africa – historic CPI inflation South Africa", Inflation.eu, 2017. [Online]. Available:

http://www.inflation.eu/inflation-rates/south-africa/historic-inflation/cpi-inflation-south-africa.aspx [Accessed: 08- Dec- 2017].

APPENDICES

APPENDIX A: EXOGENOUS DATA (30-MINUTE AVERAGED)

Appendix A1: Winter data

Time	Global horizontal irradiance [W/ m²]	Direct normal irradiance [W/ m²]	Diffuse horizontal irradiance [W/ m²]	Ambient air temperature [°C]	Inlet water temperature [°C]	Hot water consumption [l]
00:00	0	0	0	10,04	15	0
00:30	0	0	0	9,55	15	0
01:00	0	0	0	9,24	15	0
01:30	0	0	0	9,35	15	0
02:00	0	0	0	8,94	15	0
02:30	0	0	0	8,37	15	0
03:00	0	0	0	7,839	14	0
03:30	0	0	0	6,25	14	0
04:00	0	0	0	4,865	14	0
04:30	0	0	0	5,235	14	0
05:00	0	0	0	4,613	14	0
05:30	0	0	0	4,057	14	0
06:00	0	0	0	4,971	13	0
06:30	0	0	0	4,562	13	38,6631
07:00	0	0	0	5,201	13	49,7097
07:30	40,256	371,23	13,043	4,872	13	0
08:00	117,074	587,572	26,4254	4,489	13	0
08:30	213,085	699,653	34,157	6,863	13	0
09:00	310,381	756,024	41,139	8,47	13	0
09:30	405,021	819,074	42,8894	12,06	13	0

10:00	488,506	862,797	44,398	13,99	13	0
10:30	555,914	885,494	47,3752	13,79	13	0
11:00	604,2	892,604	50,9291	14,84	13	11
11:30	637,29	898,219	52,1292	15,76	13	0
12:00	653,092	895,211	55,4938	16,7	14	0
12:30	654,919	892,637	56,6212	17	14	0
13:00	637,945	885,528	57,1116	17,34	14	0
13:30	607,54	878,326	56,3196	18,02	14	0
14:00	555,746	852,151	56,6822	18,8	14	0
14:30	494,613	832,137	54,5361	18,9	14	0
15:00	419,061	799,034	52,4899	19,33	14	0
15:30	331,196	754,944	47,6943	19,19	14	0
16:00	234,224	695,949	40,5004	18,81	14	0
16:30	133,297	572,395	33,1852	18,07	14	0
17:00	49,1995	360,129	18,3454	17,11	14	0
17:30	0,402176	0	0,127412	15,46	14	0
18:00	0	0	0	14,91	14	0
18:30	0	0	0	13,86	15	0
19:00	0	0	0	13	15	0
19:30	0	0	0	11,89	15	0
20:00	0	0	0	12,16	15	55,23
20:30	0	0	0	10,93	15	0
21:00	0	0	0	10,35	15	0
21:30	0	0	0	10,13	15	0
22:00	0	0	0	9,86	15	0
22:30	0	0	0	9,98	15	0
23:00	0	0	0	9,58	15	0
23:30	0	0	0	8,51	15	0

Appendix A2: Summer data

Time	Global horizontal irradiance [W/ m^2]	Direct normal irradiance [W/ m^2]	Diffuse horizontal irradiance [W/ m^2]	Ambient air temperature [°C]	Inlet water temperature [°C]	Hot water consumption [l]
00:00	0	0	0	21,96	25	0
00:30	0	0	0	20,94	25	0
01:00	0	0	0	20,86	25	0
01:30	0	0	0	20,32	25	0
02:00	0	0	0	20,39	25	0
02:30	0	0	0	20,46	25	0
03:00	0	0	0	21,04	24	0
03:30	0	0	0	20,62	24	0
04:00	0	0	0	20,22	24	0
04:30	0	0,013693	0	18,88	24	0
05:00	0	0	0	18,2	24	0
05:30	0	0	0	17,19	24	0
06:00	36,467	265,316	21,7287	18,05	23	0
06:30	77,6371	90,5631	62,9353	17,77	23	22,61
07:00	160,288	179,102	111,018	18,29	23	29,07
07:30	262,911	353,803	126,542	19,46	23	0
08:00	449,131	559,136	173,1	21,58	23	0
08:30	576,487	696,098	164,165	24,69	23	0
09:00	752,366	929,623	110,858	27,49	23	0
09:30	744,271	807,218	119,13	26,89	23	0
10:00	936,704	967,007	119,328	27,43	23	0
10:30	952,619	895,161	141,405	27,93	23	0
11:00	1063,29	965,543	145,561	28,34	23	6

11:30	1127,9	1054,02	88,7868	29,65	23	0
12:00	1140,56	1025,14	109,635	30,12	24	0
12:30	1174,31	1051,06	114,231	30,24	24	0
13:00	1121,5	930,602	190,022	30,5	24	0
13:30	1096,57	911,52	200,228	30,39	24	0
14:00	1056,41	848,766	257,961	31,3	24	0
14:30	1026,3	981,309	145,527	32,08	24	0
15:00	929,177	1038,33	56,0581	32,51	24	0
15:30	837,918	1024,21	53,6154	32,12	24	0
16:00	708,317	962,071	55,7567	32,32	24	0
16:30	618,933	970,799	49,6873	32,34	24	0
17:00	491,122	917,01	46,7403	32,44	24	0
17:30	359,921	843,811	42,4697	32,45	24	0
18:00	232,078	738,098	37,1542	32,13	24	0
18:30	113,173	558,434	28,8341	30,71	25	0
19:00	21,175	220,804	10,8497	28,86	25	0
19:30	0	0	0	27,17	25	0
20:00	0	0	0	25,86	25	32,3
20:30	0	0	0	25,71	25	0
21:00	0	0,410523	0	23,21	25	0
21:30	0	0	0	22,25	25	0
22:00	0	0	0	21,46	25	0
22:30	0	0	0	20,89	25	0
23:00	0	0	0	20,24	25	0
23:30	0	0	0	19,84	25	0

APPENDIX B: ANNUAL ENERGY AND CUMULATIVE COSTS (LCC)

year	ESTWH energy cost after each year (ZAR)	HSWH energy cost after each year (ZAR)	O & M ESTWH cost after each year (ZAR)	O & M HSWH cost after each year (ZAR)	ESTWH (Annual cumulative cost) (ZAR)	HSWH (Annual cumulative cost) (ZAR)
0	-	-	-	-	2 560,40	7 518,43
1	1 549,80	492,26	25,60	75,18	4 135,80	8 085,87
2	1 704,78	541,49	27,01	79,31	5 867,59	8 706,66
3	1 875,26	595,63	28,49	83,66	7771,33	9 385,96
4	2 062,78	655,20	30,05	88,25	9 864,17	10 129,41
5	2 269,06	720,72	31,70	93,10	12 164,93	10 943,23
6	2 495,97	792,79	33,44	98,21	14 694,34	11 834,23
7	2 745,57	872,07	35,28	103,60	21 019,55	18 045,98
8	3 020,12	959,28	37,22	109,29	24 076,88	19 114,55
9	3 322,13	1 055,20	39,26	115,29	27 438,27	20 285,04
10	3 654,35	1 160,72	41,41	121,62	31 134,04	21 567,38
11	4 019,78	276,80	43,69	128,30	35 197,50	22 972,47
12	4 421,76	1 404,48	46,09	135,34	39 665,35	26 876,08
13	4 863,94	1 544,92	48,62	142,77	44 577,90	28 563,77
14	5 350,33	1 699,42	51,28	150,61	54 507,84	37 103,49
15	5 885,36	1 869,36	54,10	158,88	60 447,30	39 131,72
16	6 473,90	2 056,29	57,07	167,60	66 978,27	41 355,61
17	7 121,29	2 261,92	60,20	176,80	74 159,76	43 794,33
18	7 833,42	2 488,11	63,51	186,51	82 056,69	46 468,95
19	8 616,76	2 736,92	67,00	196,75	90 740,44	49 402,62
20	9 478,44	3 010,62	70,67	207,55	100 289,55	52 620,79
Salvage	-	-	-	-	-512.08	-1503.69
LCC	-	-	-	-	**99777.47**	**51117.10**